

Variational Bayes Neural Network: Posterior Consistency, Classification Accuracy and Computational Challenges

Shrijita Bhattacharya^{*†} Zihuan Liu[†] Tapabrata Maiti[†]

Abstract

Bayesian neural network models (BNN) have re-surfed in recent years due to the advancement of scalable computations and its utility in solving complex prediction problems in a wide variety of applications. Despite the popularity and usefulness of BNN, the conventional Markov Chain Monte Carlo based implementation suffers from high computational cost, limiting the use of this powerful technique in large scale studies. The variational Bayes inference has become a viable alternative to circumvent some of the computational issues. Although the approach is popular in machine learning, its application in statistics is somewhat limited. This paper develops a variational Bayesian neural network estimation methodology and related statistical theory. The numerical algorithms and their implementational are discussed in detail. The theory for posterior consistency, a desirable property in nonparametric Bayesian statistics, is also developed. This theory provides an assessment of prediction accuracy and guidelines for characterizing the prior distributions and variational family. The loss of using a variational posterior over the true posterior has also been quantified. The development is motivated by an important biomedical engineering application, namely building predictive tools for the transition from mild cognitive impairment to Alzheimer's disease. The predictors are multi-modal and may involve complex interactive relations.

Key Words: ADNI; Black-box variational inference, Kullback-Leibler divergence; Hellinger neighborhood; Mean-field family.

^{*}Corresponding author: bhatta61@msu.edu

[†]Department of Statistics and Probability, Michigan State University

1 Introduction

Due to the universal approximation theory of stochastic functions and larger access to computational power, Bayesian Neural Networks (BNNs) are fashionable in machine learning and statistics for classification and prediction from big data. The BNNs based prediction have several advantages over standard parametric statistical models as they implicitly take into account the interactions or dependence among predictor variables and model the unknown functional relationship between the predictors and responses. For example, we consider an application of classifying Alzheimer's disease status from brain imaging, an important biomedical problem. The image features are segmented into voxels or region of interests (ROI's). Due to their physical adjacency and other biological proximities, a simple parametric model or semi-parametric models, such as logistic regression or generalized additive models may not be appropriate. Besides the dependence (spatial) among the predictors, there might be some network structures in the feature space while modeling the brain images. The BNNs can take into account these data features without any explicit assumptions about their dependence structure. Further, these studies often have additional features but in different modes such as genetic and demographic information, brings additional complexity while modeling dependence among the features. Thus, machine learning based approach, such as neural networks, becomes useful in this type of applications.

Bayesian neural networks (BNNs) have been comprehensively studied by Bishop (1997), Neal (1992), Lampinen and Vehtari (2001), and many others. More recent developments which establish the efficacy of BNNs can be found in Sun et al. (2017), Mullachery et al. (2018), Hubin et al. (2018), Liang et al. (2018), Javid et al. (2020) and the references therein. The estimation of posterior distribution is a key part of Bayesian inference and represents the information about the uncertainties for both data and parameters. However, exact analytical solution for the posterior distribution is intractable as the number of parameters is very large and the functional form of a neural network does not lend itself to exact integration Blundell et al. (2015). Several approaches have been proposed for solving posterior distribution of weights of BNNs, based on both optimization based techniques such as variational inference (VI), and sampling based approach, such as Markov Chain Monte Carlo (MCMC). MCMC techniques are typically used to obtain sampling based estimates of the posterior distribution. Indeed,

BNNs with MCMC have not seen widespread adoption due to computational cost in terms of both time and storage on a large dataset Kingma et al. (2015); Nagapetyan et al. (2017); Wan et al. (2018); Wu et al. (2019). In contrast to MCMC, VI tends to converge faster, and it has been applied to many popular Bayesian models, such as factorial models and topic models Li et al. (2018); Blei and Lafferty (2007); Blei et al. (2003). We want to take a variational approximation approach for posterior estimation in the context of neural network predictive models. The basic idea of VI is that it first defines a family of variational distributions, and then minimizes the Kullback-Leibler (KL) divergence with respect to the variational family. Many recent works have discussed the application of variational inference to Bayesian neural networks e.g., Logsdon et al. (2009), Graves (2011), Carbonetto and Stephens (2012), Blundell et al. (2015), Sun et al. (2019). Although, there is a plethora of literature implementing variational inference for neural networks, the theoretical properties of the variational posterior in BNNs remain relatively unexplored and this limits the use of this powerful computational tool beyond the machine learning community.

Some of the previous works that focused on theoretical properties of variational posterior include the frequentist consistency of variational inference in parametric models in the presence of latent variables (see Wang and Blei (2019)). Optimal risk bounds for mean-field variational Bayes for Gaussian mixture (GM) and Latent Dirichlet allocation (LDA) models have been discussed in Pati et al. (2018). The work of Yang et al. (2020) propose α -variational inference Bayes risk for GM and LDA models. A more recent work Zhang and Gao (2020) discusses the variational posterior consistency rates in Gaussian sequence models, infinite exponential families and piece-wise constant models. In order to evaluate the validity of a posterior in non-parametric models, one must establish its consistency and rates of contraction. To the best of our knowledge, for classification problems, the consistency rates of VI based Bayesian neural networks have not been explored. Additionally, there exists no previous work discussing the impact of using a VI approach on the classification accuracy of the BNN's. Both these issues have been addressed in this paper. *As a systematic development of Variational Bayes Neural networks with theoretical rigor, our contributions are summarized as follows:*

We first demonstrate that the variational posterior asymptotically gives negligible probability to shrinking Hellinger neighborhoods of the true density function provided that the rate

of growth in the number of nodes is well controlled.

Besides the theoretical validation, the challenges of implementing a VI based approach is two folds: (1) the optimization of the KL-divergence (2) the choice of the variational family. There exists several algorithms for the optimization of the KL-divergence measure, each having its own pros and cons. We implemented the black-box variational inference (BBVI) to obtain Monte Carlo estimates of the gradient of the evidence lower bound (ELBO) and used stochastic optimization to estimate the variational parameters. We reveal that the complexity involved in this optimization depends on several factors and tuning parameter selection. We then provide statistically principled guideline in couple with optimization theory for its practical implementation. For the second issue, we show that a simple mean-field variational family suffices for posterior consistency along with good numerical performance.

Further we derive the rates of consistency for the true posterior and the variational posterior. With no assumptions on the true function, we first establish that the true posterior probability of an ε - Hellinger neighborhood grows at the rate $1 - 2e^{-n\varepsilon^2/2}$ in contrast to the slower $1 - \nu, 0 < \nu < 1$ rate for the variational posterior. Next, under suitable assumptions on the approximating neural network solution of the true function, we establish that the true posterior probability of a shrinking $\varepsilon\epsilon_n$ - Hellinger neighborhood grows at the rate $1 - 2e^{-n\varepsilon^2\epsilon_n^2/2}$ in contrast to the slower $1 - \nu$ rate for the variational posterior. The reason for this difference is explained as follows: (1) first, the true posterior probability of a shrinking $\varepsilon\epsilon_n$ - Hellinger neighborhood grows at the rate $1 - 2e^{-n\varepsilon^2\epsilon_n^2/2}$ (2) second, the KL-distance between the variational posterior and the true posterior grows at a rate $o(n\epsilon_n^2)$. For (1) and (2) to simultaneously hold, for every $\nu > 0$, the variational posterior must give greater than $1 - \nu$ probability to shrinking Hellinger neighborhoods otherwise the rate of growth of the KL-distance between the true and variational posterior cannot be controlled. Indeed, for (1) to hold, one must choose the prior appropriately and for (2) to hold, one must choose the variational family appropriately. Indeed, for the optimal classification, one needs to optimally choose the pair of prior and variational family. This paper carefully characterizes the properties of a prior and variational family which allows the variational posterior to be consistent and establishes that a simple mean field family choice for both these families provides a numerically stable and a theoretically consistent solution.

We next establish the connection between posterior consistency and classification accuracy. In this direction, we first show that the classification accuracy of a consistent posterior asymptotically approaches to the classification accuracy of a Bayes classifier. With no assumption on the true function, we show that the rates of convergence of the classification accuracy is same for both variational approximation and true posterior. However, under suitable assumptions on the approximating neural network solution, we establish that the classification accuracy of variational posterior approaches to the classification accuracy of the Bayes classification at the rate $(\epsilon_n^2)^{2/3}$ in contrast to the higher rate of ϵ_n^2 for the true posterior. This interesting theoretical discovery quantifies the loss due to the use of variational posterior instead of using the true posterior density.

Finally, we discuss the usefulness of this modeling technique for prediction from a multimodal data that characterizing various aspects among the feature variables. Specifically, we provide an application in the context of Alzheimer disease classification from brain imaging, genetic variable and other clinical factors.

The rest of the paper is organized as follows: section 2 presents the statistical framework for neural networks based classification problem and section 3 provides the variational algorithm for Bayesian implementation. The theoretical properties including posterior consistency and classification consistency are provided in section 4. The detailed numerical issues in practice are explained in section 5 in the context of a real life biomedical engineering application. Section 6 concludes the article with brief remarks on research directions.

2 The Neural Networks Classifier and Likelihoods

Let Y be a binary random variable taking values 0 or 1, representing the class levels and $X \in \mathbb{R}^p$ is a feature vector drawn from a feature space with some marginal distribution P_X . We consider the following binary classification problem

$$P(Y = 1|X = x) = \sigma(\eta_0(\mathbf{x})), \quad P(Y = 0|X = x) = 1 - \sigma(\eta_0(\mathbf{x})) \quad (1)$$

where $\eta_0(\cdot) : \mathbb{R}^p \rightarrow \mathbb{R}$ is some continuous function and $\sigma(\cdot) = e^{(\cdot)}/(1 + e^{(\cdot)})$ is the sigmoid function. Thus, $P_{X,Y}$, the joint distribution of (X, Y) is a product of the conditional distribu-

tion in (1) and the marginal distribution P_X . Borrowing some notations from Cannings and Samworth (2017) and Yang and Maiti (2020), a classifier C is a Borel measurable function $C : \mathbb{R}^p \rightarrow \{0, 1\}$, with the interpretation that we assign a point $\mathbf{x} \in \mathbb{R}^p$ to class $C(\mathbf{x})$. The test error of a classifier C is given by

$$R(C) = \int_{\mathbb{R}^p \times \{0,1\}} I_{\{C(X) \neq Y\}} dP_{X,Y} \quad (2)$$

Based on (1), we define the Bayes classifier as

$$C^{\text{Bayes}}(\mathbf{x}) = \begin{cases} 1, & \sigma(\eta_0(\mathbf{x})) \geq 1/2 \\ 0, & \text{otherwise} \end{cases} \quad (3)$$

The Bayes classifier is optimal Friedman et al. (2009) since it minimizes the mis-classification error risk in (2). However, the Bayes classifier is not useful in practice, since the function $\eta_0(\mathbf{x})$ is unknown. Thus, a classifier is obtained based on a set of training observations $\{(\mathbf{x}_1, y_1), \dots, (\mathbf{x}_n, y_n)\}$, which are drawn from $P_{X,Y}$. A good classifier based on the sample should have the risk tending to the Bayes risk as the number of observations tends to infinity, without any requirement for its probability distribution. This is so called universal consistency. Multiple methods have been adopted to estimate $\eta_0(\mathbf{x})$, including logistic regression (a linear approximation), generalized additive model (GAM, a nonparametric nonlinear approximation), neural networks (a complicated structure which is dense in continuous functions) etc.

The first two methods usually work in practice with good theoretical foundation, however, they may fail to catch the complicated dependency of the feature vector \mathbf{x} in a wide range of applications including the problem that we consider in this article. The neural network structure exploits the dependency implicitly without any specific parametric structure. Consider a single layer neural network model with p predictor variables. The layer has k_n nodes, where k_n may be a diverging sequence depending on n . A diagram is shown in figure 1 for illustration.

The validity of neural network approximations is based on the universal approximation results Cybenko (1989), which states that the single layer neural network is able to approximate any continuous function with a quite small approximation error when k_n is large. Assume a Fourier representation of $\eta_0(\mathbf{x})$ and denote $\Gamma_{B,C} = \{f(\cdot) : \int_B \|\boldsymbol{\omega}\|_2 |\tilde{f}|(d\boldsymbol{\omega}) < C\}$ for some

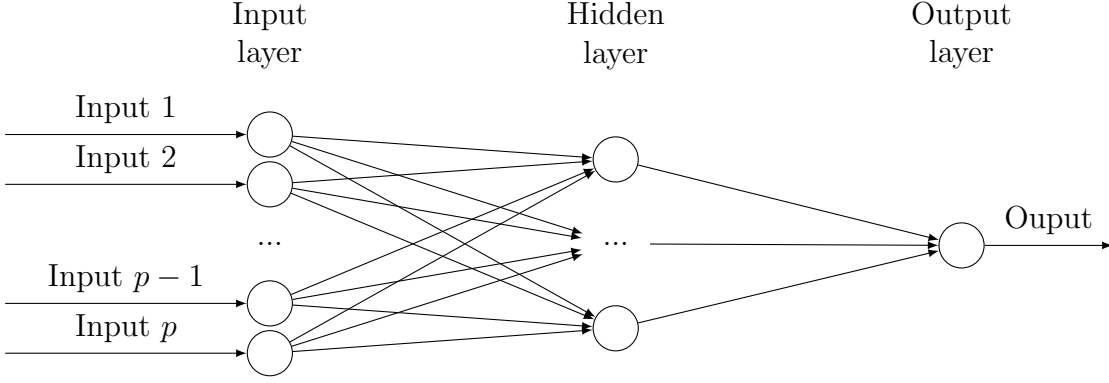


Figure 1: A diagram for the single-layer neural network model

bounded subset B of \mathbb{R}^p containing zero for some constant $C > 0$. Then, for all functions $\eta_0 \in \Gamma_{B,C}$, there exist a single layer neural network output $\eta(\mathbf{x})$ such that $\|\eta - \eta_0\|_2 = O(1/\sqrt{k_n})$ Barron (1993). This result ensures good approximation property of single layer neural network, and the convergence rate depends only on the number of nodes under mild conditions on $\eta_0(\mathbf{x})$.

For the $p \times 1$ input vector \mathbf{x} , and weight $\boldsymbol{\gamma}$, let $k_n \times 1$ vector $\boldsymbol{\xi}$ be the corresponding values in the hidden nodes, i.e.,

$$\xi_j = \gamma_{j0} + \boldsymbol{\gamma}_j^\top \mathbf{x}, \quad j = 1, \dots, k_n$$

Let $\psi(\cdot)$ be an activation function, then the output for a given set of weight $\boldsymbol{\beta}$, is calculated by

$$\beta_0 + \boldsymbol{\beta}^\top \boldsymbol{\psi}(\boldsymbol{\xi})$$

where the function $\boldsymbol{\psi}(\cdot)$ is the function $\psi(\cdot)$ being applied element-wise. Leshno et al. (1993) proved that as long as the activation function is not algebraic polynomials, the single layer neural network is dense in the continuous function space, thus can be used to approximate any given continuous function. This structure can be considered as a non-parametric model. For a given activation function $\psi(\cdot)$, a $p \times 1$ input vector maps to an output score

$$\begin{aligned} \eta_{\boldsymbol{\theta}_n}(\mathbf{x}) &= \beta_0 + \sum_{j=1}^{k_n} \beta_j \psi(\gamma_{j0} + \boldsymbol{\gamma}_j^\top \mathbf{x}) \\ &= \beta_0 + \boldsymbol{\beta}^\top \boldsymbol{\psi}(\boldsymbol{\gamma}_0 + \boldsymbol{\Gamma} \mathbf{x}) \end{aligned} \quad (4)$$

where $\boldsymbol{\gamma}_0 = [\gamma_{10}, \dots, \gamma_{k_n 0}]$ and $\boldsymbol{\Gamma} = [\boldsymbol{\gamma}_1, \dots, \boldsymbol{\gamma}_{k_n}]$ and $\boldsymbol{\theta}_n = (\beta_0, \boldsymbol{\beta}, \boldsymbol{\gamma}_0, \text{vec}(\boldsymbol{\Gamma}))$ is the set of all

the parameters. Note, $\boldsymbol{\theta}_n$ is a $K(n) \times 1$ vector where $K(n) = k_n(p + 1) + 1$. Assuming the number of covariates p to be fixed, the total number of parameters $K(n) \sim k_n$, where k_n is the number of nodes. For the purposes of this paper, we use the activation function to be the sigmoid function,

$$\psi(x) = \frac{e^x}{1 + e^x}.$$

although the results may be generalized to a wider class of activation functions. Thus, using the neural network in (4) as an approximation to the true function $\eta_0(\mathbf{x})$ in (1), the conditional probabilities of Y given $X = \mathbf{x}$ is given by

$$\begin{aligned} P(Y = 1|X = \mathbf{x}) &= \sigma(\eta_{\boldsymbol{\theta}_n}(\mathbf{x})) \\ P(Y = 0|X = \mathbf{x}) &= 1 - \sigma(\eta_{\boldsymbol{\theta}_n}(\mathbf{x})) \end{aligned} \quad (5)$$

Assuming Bernoulli probability distribution, the conditional density function of $Y|X = \mathbf{x}$ under the model is given by

$$\ell_{\boldsymbol{\theta}_n}(y, \mathbf{x}) = \exp(y\eta_{\boldsymbol{\theta}_n}(\mathbf{x}) - \log(1 + e^{\eta_{\boldsymbol{\theta}_n}(\mathbf{x})})) \quad (6)$$

Thus, the likelihood function for the data $(\mathbf{y}_n, \mathbf{X}_n) = (y_i, \mathbf{x}_i)_{i=1}^n$ under the model can be expressed as.

$$L(\boldsymbol{\theta}_n) = \prod_{i=1}^n \ell_{\boldsymbol{\theta}_n}(y_i, \mathbf{x}_i) = \exp\left(\sum_{i=1}^n [y_i\eta_{\boldsymbol{\theta}_n}(\mathbf{x}_i) - \log(1 + e^{\eta_{\boldsymbol{\theta}_n}(\mathbf{x}_i)})]\right) \quad (7)$$

In view of (1), the conditional density of $Y|X = \mathbf{x}$ under the truth

$$\ell_0(y, \mathbf{x}) = \exp(y\eta_0(\mathbf{x}) - \log(1 + e^{\eta_0(\mathbf{x})})) \quad (8)$$

Therefore, the likelihood function for the data under the truth is given by

$$L_0 = \prod_{i=1}^n \ell_0(y_i, \mathbf{x}_i) = \exp\left(\sum_{i=1}^n [y_i\eta_0(\mathbf{x}_i) - \log(1 + e^{\eta_0(\mathbf{x}_i)})]\right) \quad (9)$$

3 Bayesian Inference with Variational Algorithm

3.1 Prior Choice

For Bayesian analysis, prior distributions have to be assigned for all parameters defining the model. Although one may have a prior knowledge concerning the function represented by a neural network, it is generally difficult to translate this into a meaningful prior on neural network weights.

We assume a normal prior on each entry of Θ_n as follows:

$$p(\boldsymbol{\theta}_n) = \prod_{j=1}^{K(n)} \frac{1}{\sqrt{2\pi\zeta_{jn}^2}} e^{-\frac{1}{2\zeta_{jn}^2}(\theta_{jn}-\mu_{jn})^2} \quad (10)$$

where each Θ_{jn} requires a separate mean μ_{jn} and variance ζ_{jn}^2 . Note, we use Θ_n to denote the random variable for parameter $\boldsymbol{\theta}_n$.

Let $\boldsymbol{\zeta}_n = [\zeta_{1n}, \dots, \zeta_{K(n)n}]$ and $\boldsymbol{\zeta}_n^* = [1/\zeta_{1n}, \dots, 1/\zeta_{K(n)n}]$, we assume the following two conditions on the variance parameter

$$\begin{aligned} \text{(A1)} \quad & \|\boldsymbol{\zeta}_n\|_\infty = O(n) \\ & \|\boldsymbol{\zeta}_n^*\|_\infty = O(1) \end{aligned}$$

where $\|\cdot\|_\infty$ is the supremum norm of a vector as in definition 7.1. Note, the above assumption ensures that the variances of each Θ_n do not grow at an arbitrarily large rate in which case the consistency of both the Bayesian and variational Bayes approach would break down. Restrictions on the mean parameter $\boldsymbol{\mu}_n = [\mu_{1n}, \dots, \mu_{K(n)n}]$ directly impact the consistency rate and are more case specific. We thereby leave their thorough discussion under section 4.

The reason for choosing the above form of prior is two folds: (1) first it guarantees that the true posterior distribution of Θ_n is consistent (2) second it guarantees, under a suitable choice of the variational family, the approximated variational posterior is also consistent. The choice of prior in (10) is not unique. Indeed, one can work with a much more generic class of prior such that (1) and (2) hold. Note, each prior comes with its own associated computation complexity, implementation and theoretical justification. We choose one which does a fairly

good job under all these three criterion.

In view of (7) and (10), posterior distribution of Θ_n given $\mathbf{y}_n = [y_1, \dots, y_n]^\top$ and $\mathbf{X}_n = [\mathbf{x}_1, \dots, \mathbf{x}_n]^\top$ is

$$\pi(\boldsymbol{\theta}_n | \mathbf{y}_n, \mathbf{X}_n) = \frac{\pi(\boldsymbol{\theta}_n, \mathbf{y}_n, \mathbf{X}_n)}{\pi(\mathbf{y}_n, \mathbf{X}_n)} = \frac{L(\boldsymbol{\theta}_n)p(\boldsymbol{\theta}_n)}{\int L(\boldsymbol{\theta}_n)p(\boldsymbol{\theta}_n)d\boldsymbol{\theta}_n} \quad (11)$$

where the denominator $\pi(\mathbf{y}_n, \mathbf{X}_n)$ is free from the parameter and depends only on \mathbf{y}_n and \mathbf{X}_n .

3.2 Variational Inference

As a first step to variational inference (VI) procedure, one has to start with a variational family. Given several options, we work with one which is simple, computationally and structurally tractable, and more importantly statistically consistent. We posit a mean field Gaussian variational family of the form

$$\mathcal{Q}_n = \left\{ q(\boldsymbol{\theta}_n) : q(\boldsymbol{\theta}_n) = \prod_{j=1}^{K(n)} \frac{1}{\sqrt{2\pi s_{j_n}^2}} e^{-\frac{1}{2s_{j_n}^2}(\theta_{j_n} - m_{j_n})^2} \right\} \quad (12)$$

Note that the variational family assumes that each Θ_{j_n} is independent with mean and standard deviation equal to m_{j_n} and s_{j_n} respectively.

The variational posterior aims to reduce the KL-distance between the variational family and the true posterior Blei and Lafferty (2007); Hinton and Van Camp (1993); Zhang et al. (2017); Blundell et al. (2015). Thus, for the true posterior, $\pi(\cdot | \mathbf{y}_n, \mathbf{X}_n)$ in (11), the variational posterior is given by

$$\pi^* = \operatorname{argmin}_{q \in \mathcal{Q}_n} d_{\text{KL}}(q, \pi(\cdot | \mathbf{y}_n, \mathbf{X}_n)). \quad (13)$$

where d_{KL} , the Kullback-Leibler (KL) divergence between a variational family member $q(\boldsymbol{\theta}_n)$ and the true posterior $\pi(\boldsymbol{\theta}_n | \mathbf{y}_n, \mathbf{X}_n)$ is given by

$$d_{\text{KL}}(q, \pi(\cdot | \mathbf{y}_n, \mathbf{X}_n)) = \int \log \frac{q(\boldsymbol{\theta}_n)}{\pi(\boldsymbol{\theta}_n | \mathbf{y}_n, \mathbf{X}_n)} q(\boldsymbol{\theta}_n) d\boldsymbol{\theta}_n \quad (14)$$

From (11), note that $\pi(\boldsymbol{\theta}_n | \mathbf{y}_n, \mathbf{X}_n) = \pi(\boldsymbol{\theta}_n, \mathbf{y}_n, \mathbf{X}_n) / \pi(\mathbf{y}_n, \mathbf{X}_n)$. Thus, simplifying the KL-

divergence further, we get:

$$\begin{aligned} d_{\text{KL}}(q, \pi(\cdot|\mathbf{y}_n, \mathbf{X}_n)) &= \int [\log q(\boldsymbol{\theta}_n) - \log \pi(\boldsymbol{\theta}_n, \mathbf{y}_n, \mathbf{X}_n) + \pi(\mathbf{y}_n, \mathbf{X}_n)] q(\boldsymbol{\theta}_n) d\boldsymbol{\theta}_n \\ &= \int [\log q(\boldsymbol{\theta}_n) - \log \pi(\boldsymbol{\theta}_n, \mathbf{y}_n, \mathbf{X}_n)] q(\boldsymbol{\theta}_n) d\boldsymbol{\theta}_n + \log \pi(\mathbf{y}_n, \mathbf{X}_n) \end{aligned} \quad (15)$$

Since the last term in (15) does not depend q , optimizing (15) w.r.t. to q boils down to optimizing the first term. Indeed the first term is nothing but the negative of the evidence lower bound (ELBO) where the ELBO is given by

$$\text{ELBO}(q, \pi(\cdot, \mathbf{y}_n, \mathbf{X}_n)) = \int [\log \pi(\boldsymbol{\theta}_n, \mathbf{y}_n, \mathbf{X}_n) - \log q(\boldsymbol{\theta}_n)] q(\boldsymbol{\theta}_n) d\boldsymbol{\theta}_n \quad (16)$$

Thus in order to minimize the KL-distance, we shall instead maximize the ELBO between q and $\pi(\cdot, \mathbf{y}_n, \mathbf{X}_n)$. For the purposes of implementation, we alternatively define π^* as

$$\pi^* = \underset{q \in \mathcal{Q}_n}{\text{argmax}} \text{ELBO}(q, \pi(\cdot, \mathbf{y}_n, \mathbf{X}_n)) \quad (17)$$

In order to maximize ELBO in (16) with respect to the distribution q we index each density q in the variational family \mathcal{Q}_n by its parameters,

$$\mathcal{V}_q = (m_{1n}, \dots, m_{K(n)n}, s_{1n}^2, \dots, s_{K(n)n}^2) \quad (18)$$

where m_{jn} and s_{jn} is the mean and standard deviation of Θ_{jn} under the density q . This consequently produces an indexing of the ELBO in (16) as

$$\mathcal{L}_{\mathcal{V}_q} = \text{ELBO}(q(\cdot|\mathcal{V}_q), \pi(\cdot, \mathbf{y}_n, \mathbf{X}_n)) = \int [\log \pi(\boldsymbol{\theta}_n, \mathbf{y}_n, \mathbf{X}_n) - \log q(\boldsymbol{\theta}_n|\mathcal{V}_q)] q(\boldsymbol{\theta}_n|\mathcal{V}_q) d\boldsymbol{\theta}_n \quad (19)$$

Thus, the optimization problem in (17) reduces to optimizing $\mathcal{L}_{\mathcal{V}_q}$ w.r.t. to \mathcal{V}_q . In this direction,

we consider the derivative of $\mathcal{L}_{\mathcal{V}_q}$ w.r.t. \mathcal{V}_q . Thus,

$$\begin{aligned}\nabla_{\mathcal{V}_q}\mathcal{L}_{\mathcal{V}_q} &= \nabla_{\mathcal{V}_q} \int [\log \pi(\boldsymbol{\theta}_n, \mathbf{y}_n, \mathbf{X}_n) - \log q(\boldsymbol{\theta}_n|\mathcal{V}_q)]q(\boldsymbol{\theta}_n|\mathcal{V}_q)d\boldsymbol{\theta}_n \\ &= \int \nabla_{\mathcal{V}_q}q(\boldsymbol{\theta}_n|\mathcal{V}_q)d\boldsymbol{\theta}_n + \int [\log \pi(\boldsymbol{\theta}_n, \mathbf{y}_n, \mathbf{X}_n) - \log q(\boldsymbol{\theta}_n|\mathcal{V}_q)]\nabla_{\mathcal{V}_q}q(\boldsymbol{\theta}_n|\mathcal{V}_q)d\boldsymbol{\theta}_n \\ &= \int \nabla_{\mathcal{V}_q} \log q(\boldsymbol{\theta}_n|\mathcal{V}_q)[\log \pi(\boldsymbol{\theta}_n, \mathbf{y}_n, \mathbf{X}_n) - \log q(\boldsymbol{\theta}_n|\mathcal{V}_q)]q(\boldsymbol{\theta}_n|\mathcal{V}_q)d\boldsymbol{\theta}_n\end{aligned}\quad (20)$$

where the last equality follows since $\int \nabla_{\mathcal{V}_q}q(\boldsymbol{\theta}_n|\mathcal{V}_q)d\boldsymbol{\theta}_n = \nabla_{\mathcal{V}_q} \int q(\boldsymbol{\theta}_n|\mathcal{V}_q)d\boldsymbol{\theta}_n = \nabla_{\mathcal{V}_q}1 = 0$ and $\nabla_{\mathcal{V}_q} \log q(\boldsymbol{\theta}_n|\mathcal{V}_q)q(\boldsymbol{\theta}_n|\mathcal{V}_q) = \nabla_{\mathcal{V}_q}q(\boldsymbol{\theta}_n|\mathcal{V}_q)$. Therefore, the gradient of $\mathcal{L}_{\mathcal{V}_q}$ w.r.t. \mathcal{V}_q reduces to

$$\nabla_{\mathcal{V}_q}\mathcal{L}_{\mathcal{V}_q} = E_{q(\cdot|\mathcal{V}_q)}[\nabla_{\mathcal{V}_q} \log q(\boldsymbol{\Theta}_n|\mathcal{V}_q)[\log \pi(\boldsymbol{\Theta}_n, \mathbf{y}_n, \mathbf{X}_n) - \log q(\boldsymbol{\Theta}_n|\mathcal{V}_q)]]\quad (21)$$

The black-box variational inference (BBVI) algorithm Ranganath et al. (2013), optimizes the ELBO using gradient descent method by making use the above form of gradient. Note, the key challenge in evaluating the gradient in (21) is the computation of the expectation. Exact computation of the expectation leads to high computational complexity whereas using noisy estimates leads to high variability. In section 3.3, we elucidate how to balance the trade off between these two factors in order to ensure fast and efficient estimation of the gradient.

3.3 Black Box Variational Algorithm using score function estimator

The black box variational inference (BBVI) algorithm aims at computing the derivative in (21) in an efficient manner. The gradient (21) is difficult to evaluate for problems with complex likelihood structures arising out of neural network models. Alternatively, the above expectation is evaluated using Monte Carlo techniques—by sampling from the variational distribution and forming the corresponding Monte Carlo estimates of the gradient. These Monte Carlo estimates can be then used for stochastic optimization to fit the variational parameters (see Ranganath et al. (2013); Taghia (2018)). The Monte Carlo estimator of the quantity in (21), obtained by sampling from the variational distribution is referred to as the score-function estimator. Indeed, the score function estimator technique views the gradient of ELBO as the expectation with respect to the variational distribution using the log-derivative trick (see the derivation in (20)). This technique implicitly assumes that the Lebesgue’s dominated convergence theorem

is applicable so that one can take the gradient of the expectation in by moving the gradient inside the expectation (see Ranganath et al. (2013); Owen (2018); Taghia (2018)).

We next explain the computation of Monte Carlo estimate of the gradient in (21). In this direction, let \mathcal{V}_q denote the current value of the variational parameters. We generate S samples from the variational distribution $q(\cdot|\mathcal{V}_q)$. We then define the noisy but unbiased estimate of the gradient as

$$\widehat{\nabla} \mathcal{L}_{\mathcal{V}_q} = \frac{1}{S} \sum_{w=1}^S \nabla_{\mathcal{V}_q} \log q(\boldsymbol{\theta}_n[w]|\mathcal{V}_q) [\log \pi(\boldsymbol{\theta}_n[w], \mathbf{X}_n, \mathbf{y}_n) - \log q(\boldsymbol{\theta}_n[w]|\mathcal{V}_q)] \quad (22)$$

where $\boldsymbol{\theta}_n[1], \dots, \boldsymbol{\theta}_n[S]$ are samples generated from $q(\cdot|\mathcal{V}_q)$. Analogous to (22), a noisy but unbiased estimate of the ELBO in (16) is given by

$$\widehat{\mathcal{L}}_{\mathcal{V}_q} = \frac{1}{S} \sum_{w=1}^S [\log \pi(\boldsymbol{\theta}_n[w], \mathbf{X}_n, \mathbf{y}_n) - \log q(\boldsymbol{\theta}_n[w]|\mathcal{V}_q)] \quad (23)$$

Algorithm 1 provides the pseudocode summarizing the overall algorithm for training BBVI using score function estimator.

Algorithm 1 BBVI using score function estimator

1. Fix an initial value for variational family parameters \mathcal{V}_q^1 .
2. Fix a step size sequence $\rho_t, t = 1, \dots$.
3. Set $t = 1$.
4. Simulate S samples $\boldsymbol{\theta}_n[1], \dots, \boldsymbol{\theta}_n[S]$ from $q(\cdot|\mathcal{V}_q^t)$.

5. Compute

$$\widehat{\nabla} \mathcal{L}_{\mathcal{V}_q^t} = \frac{1}{S} \sum_{w=1}^S \nabla_{\mathcal{V}_q^t} \log q(\boldsymbol{\theta}_n[w]|\mathcal{V}_q^t) [\log \pi(\boldsymbol{\theta}_n[w], \mathbf{X}_n, \mathbf{y}_n) - \log q(\boldsymbol{\theta}_n[w]|\mathcal{V}_q^t)]$$

6. Update

$$\mathcal{V}_q^{t+1} = \mathcal{V}_q^t + \rho_t \widehat{\nabla} \mathcal{L}_{\mathcal{V}_q^t} \quad (24)$$

7. Set $t = t + 1$.

8. Repeat steps 4-7 until the convergence of $\widehat{\mathcal{L}}_{\mathcal{V}_q^t}$ where

$$\widehat{\mathcal{L}}_{\mathcal{V}_q^t} = \frac{1}{S} \sum_{w=1}^S [\log \pi(\boldsymbol{\theta}_n[w], \mathbf{X}_n, \mathbf{y}_n) - \log q(\boldsymbol{\theta}_n[w]|\mathcal{V}_q^t)]$$

Note the most crucial step in the implementation of algorithm 1 is the computation of the quantity $\nabla_{\mathcal{V}_q} \log q(\boldsymbol{\theta}_n|\mathcal{V}_q)$ for the variational parameters \mathcal{V}_q as in (18). For the choice of

q as in (12) and the variational parameters $(m_{1n}, \dots, m_{K(n)n})$, the explicit expressions for $\nabla_{\mathcal{V}_q} \log q(\boldsymbol{\theta}_n | \mathcal{V}_q)$ have been presented in appendix (A) (see section 7).

For the variational parameters $(s_{1n}, s_{2n}, \dots, s_{K(n)n})$, the updating rule in (24) may lead to negative estimates of s_{jn} , $j = 1, \dots, K(n)$. However, one must guard against this since variance terms cannot be negative. Thus, to perform the optimization, we reparametrize the variance terms as $s_{jn} = \log(1 + e^{r_{jn}})$, $j = 1, \dots, K(n)$ and update the quantities r_{jn} in each step instead of s_{jn} . Note, by chain rule,

$$\nabla_{r_{jn}} \log q(\boldsymbol{\theta}_n | \mathcal{V}_q) = \left(\frac{e^{r_{jn}}}{1 + e^{r_{jn}}} \right) \left(\nabla_{s_{jn}} \log q(\boldsymbol{\theta}_n | \mathcal{V}_q) \Big|_{s_{jn} = \log(1 + e^{r_{jn}})} \right) \quad (25)$$

where the term in the second bracket is the derivative of $\log q(\boldsymbol{\theta}_n | \mathcal{V}_q)$ with respect to (w.r.t.) s_{jn} evaluated at the point $s_{jn} = \log(1 + e^{r_{jn}})$ and the first term is the derivative of s_{jn} w.r.t. r_{jn} . The explicit expressions for derivative of $\log q(\boldsymbol{\theta}_n | \mathcal{V}_q)$ w.r.t. to both r_{jn} and s_{jn} have been presented in the appendix (A) (see section 7).

3.4 Control Variate: Stabilizing the stochastic gradient

We can use algorithm 1 to maximize the ELBO, however a major drawback is that the noisy estimator of the gradient has high variance. There are two major techniques to reduce the variance of gradients. One of them is ‘‘Rao-Blackwellization’’, where the idea is to replace the noisy estimate of gradient with its conditional expectation with respect to a subset of the variables, Ranganath et al. (2013). This method is useful when the posterior distribution is separable across subsets of variables especially while dealing with latent variables. However, a convoluted likelihood as in (7) is not separable across the components of $\boldsymbol{\Theta}_n$ and there are no latent variables in our model. We thereby refrain from using the Rao-Blackwellization approach of gradient stabilization.

The other method which also gives an efficient technique for stabilizing the gradient is called control variate (CV). Recently, control variates have been of interest for variational inference and for general optimization problems that occur in machine learning Ross (2013); Paisley et al. (2012); Ranganath et al. (2013). CV can be used to further reduce the variance of the MC approximations of the gradients. The key idea behind the variance reduction as proposed in Ross (2013) is to replace the target function, whose expectation is being approximated by

Monte Carlo, with an auxiliary function that has the same expectation but a smaller variance. As described in both Ross (2013) and Ranganath et al. (2013), to reduce the variance of the function $\xi(\phi)$, one instead considers the function $\hat{\xi}(\phi) = \xi(\phi) - a(\varphi(\phi) - E_q(\varphi(\phi)))$ where $\varphi(\phi)$ is function with finite expectation and a is a scalar. Such a choice ensures $E_q(\hat{\xi}(\phi)) = E_q(\xi(\phi))$ and $\text{Var}_q(\hat{\xi}(\phi)) = \text{Var}_q(\xi(\phi)) + a^2\text{Var}_q(\varphi(\phi)) - 2a\text{Cov}_q(\xi(\phi), \varphi(\phi))$ which is minimized at

$$a^* = \frac{\text{Cov}_q(\xi(\phi), \varphi(\phi))}{\text{Var}_q(\varphi(\phi))} \quad (26)$$

Thus, greater the correlation between ξ and φ , the greater the variance reduction. In the context of BBVI, Ranganath et al. (2013) proposed the use of $\nabla_{\mathcal{V}_q} \log q(\boldsymbol{\theta}|\mathcal{V}_q)$ as a choice for $\varphi(\phi)$. The stochastic approximation of the gradient in (22) can then modified as

$$\widehat{\nabla} \mathcal{L}_{\mathcal{V}(H)} = \frac{1}{S} \sum_{w=1}^S \nabla_{\mathcal{V}_q} \log q(\boldsymbol{\theta}_n[w]|\mathcal{V}_q) [\log \pi(\boldsymbol{\theta}_n[w], \mathbf{X}_n, \mathbf{y}_n) - \log q(\boldsymbol{\theta}_n[w]|\mathcal{V}_q) - a^*] \quad (27)$$

Since it is impossible to obtain an exact expression for a^* as in (26), one thus uses

$$\widehat{a}^* = \frac{\text{cov}(\mathbf{u}, \mathbf{v})}{\text{var}(\mathbf{v})} \quad (28)$$

where both \mathbf{u} and \mathbf{v} are $S \times 1$ vectors whose w^{th} element is given by

$$\begin{aligned} u[w] &= \nabla_{\mathcal{V}_q} \log q(\boldsymbol{\theta}_n[w]|\mathcal{V}_q) [\log \pi(\boldsymbol{\theta}_n[w], \mathbf{X}_n, \mathbf{y}_n) - \log q(\boldsymbol{\theta}_n[w]|\mathcal{V}_q)] \\ v[w] &= \nabla_{\mathcal{V}_q} \log q(\boldsymbol{\theta}_n[w]|\mathcal{V}_q) \end{aligned} \quad (29)$$

The extension of algorithm 1 with variance reduction of MC approximations due to CV is, is annotated as BBVI-CV and summarized in algorithm 2.

Similar to the implementation of algorithm 1, for the implementation of algorithm 2, we use the reparametrization of $s_{jn} = \log(1 + e^{r_{jn}})$ as explained in section 3.3. We have implemented both the algorithms in our numerical study and discussed further practical complexity.

Algorithm 2 BBVI with control variates using score function estimator

1. Fix an initial value for variational parameter \mathcal{V}_q^1 .

2. Fix a step size sequence $\rho_t, t = 1, \dots$.

3. Set $t = 1$.

4. Simulate S samples $\boldsymbol{\theta}_n[1], \dots, \boldsymbol{\theta}_n[S]$ from $q(\cdot|\mathcal{V}_q^t)$.

5. Compute

$$u^t[w] = \nabla_{\mathcal{V}_q^t} \log q(\boldsymbol{\theta}_n[w]|\mathcal{V}_q^t) [\log \pi(\boldsymbol{\theta}_n[w], \mathbf{X}_n, \mathbf{y}_n) - \log q(\boldsymbol{\theta}_n[w]|\mathcal{V}_q^t)]$$

$$v^t[w] = \nabla_{\mathcal{V}_q^t} \log q(\boldsymbol{\theta}_n[w]|\mathcal{V}_q^t)$$

and

$$\hat{\mathbf{a}}^{*t} = \frac{\text{Cov}(\mathbf{u}^t, \mathbf{v}^t)}{\text{Var}(\mathbf{v}^t)}$$

6. Compute

$$\widehat{\nabla} \mathcal{L}_{\mathcal{V}_q^t} = \frac{1}{S} \sum_{s=1}^S u^t[w] - \hat{\mathbf{a}}^{*t} v^t[w]$$

7. Update

$$\mathcal{V}_q^{t+1} = \mathcal{V}_q^t + \rho_t \widehat{\nabla} \mathcal{L}_{\mathcal{V}_q^t} \quad (30)$$

8. Set $t = t + 1$.

9. Repeat steps 4-7 until the convergence of $\widehat{\mathcal{L}}_{\mathcal{V}_q^t}$ where

$$\widehat{\mathcal{L}}_{\mathcal{V}_q^t} = \frac{1}{S} \sum_{w=1}^S [\log \pi(\boldsymbol{\theta}_n[w], \mathbf{X}_n, \mathbf{y}_n) - \log q(\boldsymbol{\theta}_n[w]|\mathcal{V}_q^t)]$$

3.5 Classification using variational posterior

Define, $\hat{\eta}(\mathbf{x})$, the variational estimator of $\eta_0(\mathbf{x})$ as

$$\hat{\eta}(\mathbf{x}) = \sigma^{-1} \left(\int \sigma(\eta_{\boldsymbol{\theta}_n}(\mathbf{x})) \pi^*(\boldsymbol{\theta}_n) d\boldsymbol{\theta}_n \right) \quad (31)$$

where π^* is the variational posterior. Analogous to (3), the classifier based on $\hat{\eta}(\mathbf{x})$ is given by

$$\hat{C}(\mathbf{x}) = \begin{cases} 1, & \sigma(\hat{\eta}(\mathbf{x})) \geq 1/2 \\ 0, & \text{otherwise} \end{cases} \quad (32)$$

Note, the formulation in (31) guarantees that we directly approximate the main quantity of interest, $\sigma(\eta_0(\mathbf{x}))$ as in (1) by its posterior mean, $\int \sigma(\eta_{\boldsymbol{\theta}_n}(\mathbf{x})) \pi^*(\boldsymbol{\theta}_n) d\boldsymbol{\theta}_n$, which is empirically

estimated as

$$\hat{\eta}^M(\mathbf{x}) = \frac{1}{M} \sum_{i=1}^M \sigma(\eta_{\boldsymbol{\theta}_n[i]}(\mathbf{x})) \quad (33)$$

where $\boldsymbol{\theta}_n[1], \dots, \boldsymbol{\theta}_n[M]$ are multiple samples from the variational posterior π^* . Since generation of multiple samples from the variational posterior is much cheaper, the order of error between (31) and (33) is negligible.

4 Theoretical Properties: Posterior and Classification Consistency

In this section, we establish that the Bayesian inference procedure proposed in section 3 enjoys theoretical guarantees in terms of consistency of the posterior estimation and classification. For a simple Gaussian mean field family as in (12), we establish that the variational posterior (13) is consistent under suitable assumptions on the prior parameters. We also discuss how the true function η_0 impacts the rate of consistency of the variational posterior. Finally, we present how the consistency rates of the variational posterior differ from those of the true posterior.

Let f_0 and $f_{\boldsymbol{\theta}_n}$ be the joint density of the observations $(y_i, \mathbf{x}_i)_{i=1}^n$ under the truth and the model respectively. Next, without loss of generality, we assume $X_i \sim U[0, 1]^p$, which implies $f_0(\mathbf{x}) = 1$ and $f_{\boldsymbol{\theta}_n}(\mathbf{x}) = 1$. This further implies that the joint distribution of $(y_i, \mathbf{x}_i)_{i=1}^n$ under the model and the truth depend on the conditional distribution of $Y|X = \mathbf{x}$. In view of (1) and (5),

$$\begin{aligned} f_{\boldsymbol{\theta}_n}(y, \mathbf{x}) &= f_{\boldsymbol{\theta}_n}(y|\mathbf{x})f_{\boldsymbol{\theta}_n}(\mathbf{x}) = \exp(y\eta_{\boldsymbol{\theta}_n}(\mathbf{x}) - \log(1 + e^{\eta_{\boldsymbol{\theta}_n}(\mathbf{x})})) = \ell_{\boldsymbol{\theta}_n}(y, \mathbf{x}) \\ f_0(y, \mathbf{x}) &= f_0(y|\mathbf{x})f_0(\mathbf{x}) = \exp(y\eta_0(\mathbf{x}) - \log(1 + e^{\eta_0(\mathbf{x})})) = \ell_0(y, \mathbf{x}) \end{aligned} \quad (34)$$

where $\ell_{\boldsymbol{\theta}_n}$ and ℓ_0 are defined in (6) and (8) respectively.

We next define the Hellinger neighborhood of the true function density function $f_0 = \ell_0$ as

$$\mathcal{U}_\varepsilon = \{\boldsymbol{\theta}_n : d_H(\ell_0, \ell_{\boldsymbol{\theta}_n}) < \varepsilon\} \quad (35)$$

where the Hellinger distance, $d_{\text{H}}(\ell_0, \ell_{\boldsymbol{\theta}_n})$ is given by

$$d_{\text{H}}(\ell_0, \ell_{\boldsymbol{\theta}_n}) = \left(\frac{1}{2} \int_{\mathbf{x} \in [0,1]^p} \sum_{y \in \{0,1\}} \left(\sqrt{\ell_0(y, \mathbf{x})} - \sqrt{\ell_{\boldsymbol{\theta}_n}(y, \mathbf{x})} \right)^2 d\mathbf{x} \right)^{1/2}.$$

We also define the Kullback-Leibler (KL) neighborhood of the true function density function $f_0 = \ell_0$ as

$$\mathcal{N}_{\varepsilon} = \{\boldsymbol{\theta}_n : d_{\text{KL}}(\ell_0, \ell_{\boldsymbol{\theta}_n}) < \varepsilon\} \quad (36)$$

where the KL distance, $d_{\text{KL}}(\ell_0, \ell_{\boldsymbol{\theta}_n})$ is given by

$$d_{\text{KL}}(\ell_0, \ell_{\boldsymbol{\theta}_n}) = \int_{\mathbf{x} \in [0,1]^p} \sum_{y \in \{0,1\}} \left(\log \frac{\ell_0(y, \mathbf{x})}{\ell_{\boldsymbol{\theta}_n}(y, \mathbf{x})} \ell_0(y, \mathbf{x}) \right) d\mathbf{x}$$

We use the notation P_0^n to denote the true distribution of $(\mathbf{y}_n, \mathbf{X}_n) = (y_i, \mathbf{x}_i)_{i=1}^n$ under the true density ℓ_0 .

4.1 Posterior consistency and its implication in practice

In the following two theorems for two class of priors, we establish the posterior consistency of π^* defined in (13). In this direction, we show that the variational posterior concentrates in ε -small Hellinger neighborhoods of the true density ℓ_0 . In theorem 4.1, we establish this result for a fixed choice of the neighborhood distance ε . In theorem 4.2, we establish the same result for shrinking neighborhood sizes of the true function ℓ_0 . For both these theorems, the number of nodes k_n are allowed to grow at a rate of n^a for some $0 < a < 1$. However, since the theorem 4.2 is more restrictive in nature, it requires certain assumptions on the approximating neural network solution to the true function η_0 (see assumption (A3) below). Note that the theorem 4.1 is a weaker convergence result, however, it is free from assumptions on the approximating neural network solution. theorem 4.2 on the other hand requires the existence of a neural network solution which converges to the true function η_0 at a fast enough rate while ensuring controlled growth of the L_2 norm of its coefficients. Additionally, the rate of growth of L_2 norm of the prior mean parameter is allowed to grow faster in theorem 4.1 compared to theorem 4.2 (see assumptions (A2) and (A4) below).

Theorem 4.1 Suppose $k_n \sim n^a$, $0 < a < 1$. Additionally,

(A2) The prior parameters in (10) satisfies assumption (A1) and

$$\|\boldsymbol{\mu}_n\|_2^2 = o(n)$$

Then,

$$\pi^*(\mathcal{U}_\varepsilon^c) \xrightarrow{P_0^n} 0$$

Here, $\|\cdot\|_2$ is the L_2 norm of a vector as in definition 7.1.

A restatement of the above theorem is for any $\nu > 0$, $\pi^*(\mathcal{U}_\varepsilon^c) < \nu$ with probability tending to 1 as $n \rightarrow \infty$. Under the conditions of theorem 4.1, it can be established that the true posterior satisfies $\pi(\mathcal{U}_\varepsilon^c | \mathbf{y}_n, \mathbf{X}_n) < 2e^{-n\varepsilon^2/2}$ with probability tending to 1 as $n \rightarrow \infty$ (see theorem 7.17 part 1. in appendix (C) of section 7). This implies that the probability of the ε -Hellinger neighborhoods of the true function ℓ_0 for the true posterior increases at the rate of $1 - 2e^{-n\varepsilon^2/2}$ in contrast to the slow rate of $1 - \nu$ for the variational posterior.

Theorem 4.2 Suppose $k_n \sim n^a$, $0 < a < 1$ and $\epsilon_n^2 \sim n^{-\delta}$, $0 < \delta < 1 - a$. Additionally,

(A3) There exists a sequence of neural network functions $\eta_{\mathbf{t}_n}$ of the form (4) satisfying

$$\begin{aligned} \|\eta_0 - \eta_{\mathbf{t}_n}\|_\infty &= o(\epsilon_n^2) \\ \|\mathbf{t}_n\|_2^2 &= o(n\epsilon_n^2) \end{aligned}$$

(A4) The prior parameters in (10) satisfies assumption (A1) and

$$\|\boldsymbol{\mu}_n\|_2^2 = o(n\epsilon_n^2)$$

Then,

$$\pi^*(\mathcal{U}_{\epsilon_n}^c) \xrightarrow{P_0^n} 0$$

Here, $\|\cdot\|_2$ is the L_2 norm of a vector and $\|\cdot\|_\infty$ is the L_∞ norm of a function as in 7.1.

A restatement of the above theorem is for any $\nu > 0$, $\pi^*(\mathcal{U}_{\epsilon_n}^c) < \nu$ with probability tending to 1 as $n \rightarrow \infty$. Under the conditions of theorem 4.2, it can be established that the true posterior satisfies $\pi(\mathcal{U}_{\epsilon_n}^c | \mathbf{y}_n, \mathbf{X}_n) < 2e^{-n\epsilon_n^2/2}$ with probability tending to 1 as $n \rightarrow \infty$ (see

theorem 7.18 part 1. in appendix (C) of section 7). This implies that the probability of the shrinking $\varepsilon\epsilon_n$ -Hellinger neighborhoods of the true function ℓ_0 for the true posterior increases at the rate of $1 - 2e^{-n\varepsilon^2\epsilon_n^2/2}$ in contrast to the slow rate of $1 - \nu$ for the variational posterior.

4.2 Discussion of the proof

We next briefly outline the main steps in the the proof of theorems 4.1 and 4.2. The details are deferred to appendix (B) in section 7. We borrow a few steps and notations from Bhattacharya and Maiti (2020). The first step of the proof is to establish that $d_{\text{KL}}(\pi^*, \pi(\cdot|\mathbf{y}_n, \mathbf{X}_n))$ is bounded below by a quantity which is determined by the rate of consistency of the true posterior. The second step towards the proof is to show $d_{\text{KL}}(\pi^*, \pi(\cdot|\mathbf{y}_n, \mathbf{X}_n))$ is bounded above at a rate which is greater than its lower bound if and only if the variation posterior is consistent. In this direction, with \mathcal{U}_ε as in (35) note that for any $\varepsilon > 0$

$$\begin{aligned}
& d_{\text{KL}}(\pi^*, \pi(\cdot|\mathbf{y}_n, \mathbf{X}_n)) \\
&= \int_{\mathcal{U}_\varepsilon} \pi^*(\boldsymbol{\theta}_n) \log \frac{\pi^*(\boldsymbol{\theta}_n)}{\pi(\boldsymbol{\theta}_n|\mathbf{y}_n, \mathbf{X}_n)} d\boldsymbol{\theta}_n + \int_{\mathcal{U}_\varepsilon^c} \pi^*(\boldsymbol{\theta}_n) \log \frac{\pi^*(\boldsymbol{\theta}_n)}{\pi(\boldsymbol{\theta}_n|\mathbf{y}_n, \mathbf{X}_n)} d\boldsymbol{\theta}_n \\
&= -\pi^*(\mathcal{U}_\varepsilon) \int_{\mathcal{U}_\varepsilon} \frac{\pi^*(\boldsymbol{\theta}_n)}{\pi^*(\mathcal{U}_\varepsilon)} \log \frac{\pi(\boldsymbol{\theta}_n|\mathbf{y}_n, \mathbf{X}_n)}{\pi^*(\boldsymbol{\theta}_n)} d\boldsymbol{\theta}_n - \pi^*(\mathcal{U}_\varepsilon^c) \int_{\mathcal{U}_\varepsilon^c} \frac{\pi^*(\boldsymbol{\theta}_n)}{\pi^*(\mathcal{U}_\varepsilon^c)} \log \frac{\pi(\boldsymbol{\theta}_n|\mathbf{y}_n, \mathbf{X}_n)}{\pi^*(\boldsymbol{\theta}_n)} d\boldsymbol{\theta}_n \\
&\geq \pi^*(\mathcal{U}_\varepsilon) \log \frac{\pi^*(\mathcal{U}_\varepsilon)}{\pi(\mathcal{U}_\varepsilon|\mathbf{y}_n, \mathbf{X}_n)} + \pi^*(\mathcal{U}_\varepsilon^c) \log \frac{\pi^*(\mathcal{U}_\varepsilon^c)}{\pi(\mathcal{U}_\varepsilon^c|\mathbf{y}_n, \mathbf{X}_n)}, \text{ by Jensen's inequality}
\end{aligned}$$

Since $\pi(\mathcal{U}_\varepsilon|\mathbf{y}_n, \mathbf{X}_n) \leq 1$, thus

$$\begin{aligned}
&\geq \pi^*(\mathcal{U}_\varepsilon) \log \pi^*(\mathcal{U}_\varepsilon) + \pi^*(\mathcal{U}_\varepsilon^c) \log \pi^*(\mathcal{U}_\varepsilon^c) - \pi^*(\mathcal{U}_\varepsilon^c) \log \pi(\mathcal{U}_\varepsilon^c|\mathbf{y}_n, \mathbf{X}_n) \\
&\geq -\pi^*(\mathcal{U}_\varepsilon^c) \log \pi(\mathcal{U}_\varepsilon^c|\mathbf{y}_n, \mathbf{X}_n) - \log 2, \quad \text{since } x \log x + (1-x) \log(1-x) \geq -\log 2 \\
&= -\pi^*(\mathcal{U}_\varepsilon^c) \left(\log \int_{\mathcal{U}_\varepsilon^c} \frac{L(\boldsymbol{\theta}_n)}{L_0} p(\boldsymbol{\theta}_n) d\boldsymbol{\theta}_n - \log \int \frac{L(\boldsymbol{\theta}_n)}{L_0} p(\boldsymbol{\theta}_n) d\boldsymbol{\theta}_n \right) - \log 2
\end{aligned}$$

Thus, with

$$A_n = \log \int_{\mathcal{U}_\varepsilon^c} \frac{L(\boldsymbol{\theta}_n)}{L_0} p(\boldsymbol{\theta}_n) d\boldsymbol{\theta}_n \quad B_n = -\log \int \frac{L(\boldsymbol{\theta}_n)}{L_0} p(\boldsymbol{\theta}_n) d\boldsymbol{\theta}_n \quad (37)$$

we get the following main step towards the proof of theorems 4.1 and 4.2.

$$\boxed{-\pi^*(\mathcal{U}_\varepsilon^c)A_n \leq d_{\text{KL}}(\pi^*, \pi(\cdot|\mathbf{y}_n, \mathbf{X}_n)) + |B_n| + \log 2} \quad (38)$$

In the above proof we have assumed $\pi^*(\mathcal{U}_\varepsilon) > 0$, $\pi^*(\mathcal{U}_\varepsilon^c) > 0$. If $\pi^*(\mathcal{U}_\varepsilon) = 0$, there is nothing to prove. If $\pi^*(\mathcal{U}_\varepsilon) = 0$, then following the steps of the proof in appendix (B) in section 7, we will get $\varepsilon^2 = o_{P_0^n}(1)$ which is a contradiction.

The exponential of the first term A_n is decomposed as

$$e^{A_n} = \int_{\mathcal{U}_\varepsilon^c \cap \mathcal{F}_n} \frac{L(\boldsymbol{\theta}_n)}{L_0} p(\boldsymbol{\theta}_n) d\boldsymbol{\theta}_n + \int_{\mathcal{U}_\varepsilon \cap \mathcal{F}_n^c} \frac{L(\boldsymbol{\theta}_n)}{L_0} p(\boldsymbol{\theta}_n) d\boldsymbol{\theta}_n$$

where $\{\mathcal{F}_n\}_{n=1}^\infty$ is a suitably chosen sequence of sieves. Indeed our choice of \mathcal{F}_n is given by

$$\mathcal{F}_n = \left\{ \boldsymbol{\theta}_n : |\theta_{jn}| \leq C_n, j = 1, \dots, K(n) \right\} \quad (39)$$

where $C_n = e^{n^b/K(n)}$ in theorem 4.1 and $C_n = e^{n^b \varepsilon_n^2/K(n)}$ in theorem 4.2 respectively. The constant b is chosen suitably to ensure Hellinger bracketing entropy (see definition 7.2) of \mathcal{F}_n is well controlled (see lemma 7.15 for more details). Secondly, the prior needs to give negligible probability outside \mathcal{F}_n^c so that term e^{A_n} is well controlled. The prior in (10) satisfies this criterion for theorem 4.1 and theorem 4.2 with assumptions (A1), (A2) and (A1), (A4) respectively.

The second quantity B_n is controlled by the rate at which the prior gives mass to shrinking KL neighborhoods of the true density ℓ_0 . In theorem 4.1, this rate is controlled as long as the prior parameter of the prior in (10) satisfies (A1) and (A2). In theorem 4.2, the same rate is controlled as long as the prior parameters satisfies (A1) and (A4) and the true function η_0 has a neural network solution which satisfies assumption (A3).

Finally, we bound $d_{\text{KL}}(\pi^*, \pi(\cdot|\mathbf{y}_n, \mathbf{X}_n))$ by $d_{\text{KL}}(q, \pi(\cdot|\mathbf{y}_n, \mathbf{X}_n))$ for a suitable $q \in \mathcal{Q}_n$ (see proposition 7.13 and proposition 7.16 for more details). From (67), note that

$$d_{KL}(q, \pi(\cdot|\mathbf{y}_n, \mathbf{X}_n)) \leq d_{\text{KL}}(q, p) + \left| \int \log \frac{L(\boldsymbol{\theta}_n)}{L_0} q(\boldsymbol{\theta}_n) d\boldsymbol{\theta}_n \right| + \left| \log \int \frac{L(\boldsymbol{\theta}_n)}{L_0} p(\boldsymbol{\theta}_n) d\boldsymbol{\theta}_n \right| \quad (40)$$

In the above expression, the last term is nothing but $|B_n|$. The second term is the most crucial

quantity of interest.

$$\left| \int \log \frac{L(\boldsymbol{\theta}_n)}{L_0} q(\boldsymbol{\theta}_n) d\boldsymbol{\theta}_n \right| \approx n \int d_{\text{KL}}(\ell_0, \ell_{\boldsymbol{\theta}_n}) q(\boldsymbol{\theta}_n) d\boldsymbol{\theta}_n.$$

For both the theorems 4.1 and 4.2, the right hand side can always be controlled by choosing $q = \text{MVN}(\mathbf{t}_n, I_{K(n)}/\sqrt{n})$ for a suitable choice of the sequence \mathbf{t}_n . For theorem 4.1, this sequence corresponds to $\eta_{\mathbf{t}_n}$, the finite neural network approximation of η_0 and for theorem 4.2, this sequence corresponds to $\eta_{\mathbf{t}_n}$, the rate controlled neural network approximation of assumption (A3). Finally, the first term in (40) is determined by both prior and q . In theorem 4.1, it is controlled as long as the prior parameter of the prior in (10) satisfies (A1), (A2). In theorem 4.2, the same rate is controlled as long as the prior parameters satisfies (A1), (A4) and the sequence \mathbf{t}_n satisfies assumption (A3) part 2.

In light of the above discussion, there are three main properties which a prior must satisfy to allow for the convergence of variational posterior. For any $\nu > 0$

1. For a sequence of sieves $\{\mathcal{F}_n\}_{n=1}^{\infty}$ with well controlled Hellinger bracketing entropy,

$$\int_{\mathcal{F}_n^c} p(\boldsymbol{\theta}_n) d\boldsymbol{\theta}_n \leq e^{-n\nu}, n \rightarrow \infty$$

2. With \mathcal{N}_ε as in (36),

$$\int_{\mathcal{N}_\varepsilon} p(\boldsymbol{\theta}_n) d\boldsymbol{\theta}_n \geq e^{-n\nu}, n \rightarrow \infty$$

3. For a q satisfying $\int d_{\text{KL}}(\ell_0, \ell_{\boldsymbol{\theta}_n}) q(\boldsymbol{\theta}_n) d\boldsymbol{\theta}_n < \varepsilon, n \rightarrow \infty$,

$$d_{\text{KL}}(q, p) \leq n\nu, n \rightarrow \infty$$

Whereas the condition 1 and 2, are standard assumptions for consistency of true posterior (see assumptions 1 and 2 in Barron et al. (1999) and theorem 2 in Lee (2000)), condition 3 is an additional requirement which makes the variational posterior consistent. Indeed, the proof presented in this section can be generalized to a much wider class of priors satisfying conditions (1)-(3).

4.3 Classification consistency

In this section, we discuss the classification accuracy of the predictions made by the variational posterior by comparing to the optimal mis-classification error. In view of (2), let $R(\hat{C})$ and $R(C^{\text{Bayes}})$ denote the classification accuracy under the variational classifier in (32) and the Bayes classifier in (3) respectively. We next establish the how the difference in classification accuracy depends on the logit links $\hat{\eta}(X)$ and $\eta_0(X)$ as defined in (31) and (1) respectively.

$$\begin{aligned}
R(\hat{C}) - R(C^{\text{Bayes}}) &= E_X E_{Y|X} [I_{\hat{C}(X) \neq Y} - I_{C^{\text{Bayes}}(X) \neq Y}] \\
&= E_X E_{Y|X} [(I_{\hat{C}(X)=0} - I_{C^{\text{Bayes}}(X)=0})\sigma(\eta_0(X)) + (I_{\hat{C}(X)=1} - I_{C^{\text{Bayes}}(X)=1})(1 - \sigma(\eta_0(X)))] \\
&= 2E_X [I_{\hat{C}(X) \neq C^{\text{Bayes}}(X)} |\sigma(\eta_0(X)) - 1/2|] \\
&= 2E_X [I_{\sigma(\hat{\eta}(X)) \geq 1/2, \sigma(\eta_0(X)) < 1/2} |\sigma(\eta_0(X)) - 1/2| + I_{\sigma(\hat{\eta}(X)) < 1/2, \sigma(\eta_0(X)) \geq 1/2} |\sigma(\eta_0(X)) - 1/2|] \\
&\leq 2E_X |\sigma(\eta_0(X)) - \sigma(\hat{\eta}(X))| \tag{41}
\end{aligned}$$

Using the above result, in corollary 4.3, we establish the classification accuracy of the variational estimate $\hat{\eta}(\mathbf{x})$ under no assumptions on the true function $\eta_0(\mathbf{x})$. In corollary 4.4, we establish the same result under assumption (A3) on the true function $\eta_0(\mathbf{x})$. Note, although theorem 4.1 requires minimal assumptions, it gives a much weaker convergence result on the classification accuracy.

Corollary 4.3 *Under the conditions of theorem 4.1,*

$$|R(\hat{C}) - R(C^{\text{Bayes}})| \xrightarrow{P_0^n} 0$$

A restatement of the above corollary is for any $\nu > 0$, $|R(\hat{C}) - R(C^{\text{Bayes}})| < \nu$ with probability tending to 1 as $n \rightarrow \infty$. Under the conditions of theorem 4.1, it can be established that the true posterior also gives classification consistency at the same rate and there is no loss in using a variational posterior approximation (see theorem 7.17 part 2. in appendix (C) of 7).

Corollary 4.4 *Under conditions of theorem 4.2, for every $0 \leq \kappa \leq 2/3$,*

$$\epsilon_n^{-\kappa} |R(\hat{C}) - R(C^{\text{Bayes}})| \xrightarrow{P_0^n} 0$$

A restatement of the above corollary is for any $\nu > 0$, $0 \leq \kappa \leq 2/3$, $|R(\hat{C}) - R(C^{\text{Bayes}})| < \nu \epsilon_n^\kappa$ with probability tending to 1 as $n \rightarrow \infty$. Under the conditions of theorem 4.2, it can be established that the true posterior satisfies $|R(\hat{C}) - R(C^{\text{Bayes}})| < \nu \epsilon_n^\kappa$ for every $\nu > 0$, $0 \leq \kappa \leq 1$ with probability tending to 1 as $n \rightarrow \infty$ (see theorem 7.18 part 2. in appendix (C) of 7). Thus, the classification consistency occurs at the rate $\epsilon_n^{2/3}$ for the variational posterior in contrast to ϵ_n for the true posterior.

5 Numerical Properties and Alzheimer’s Disease Study

The transition from mild cognitive impairment (MCI) to Alzheimer’s disease (AD) is of great interest for clinical researchers. Several studies over the past decade have shown and compared the performance of different machine learning methods on this classification task. For this classification problem, we illustrate the performance of variational Bayesian neural networks as developed under section 3 in terms of classification accuracy, numerical complexity and time of convergence. We implemented both algorithms, algorithm 1 and 2 and shall hence forth refer to them as BBVI and BBVI-CV respectively. For a comparative baseline, we also report the performance for several machine learning techniques as applicable to this task. We like to emphasize that, our primary goal here is to illustrate the computational methodology rather incremental improvement for a specific application.

Alzheimer’s disease (AD) is a progressive, age-related, neurodegenerative disease and the most common cause of dementia Zhang and Shen (2011); Zhang et al. (2012); Korolev (2014). Behaviorally, AD is commonly preceded by mild cognitive impairment (MCI), a syndrome characterized by decline in memory and other cognitive domains that exceed cognitive decrements associated with normal aging Zhang et al. (2012); Petersen et al. (2009). However, the prodromal symptoms of MCI are not prognostically deterministic: individuals with MCI tend to progress to probable AD at a rate of 8%-15% per year, and most conversions occur within 3 years of presentation Cui et al. (2011); Farlow (2009); Allison et al. (2014). Research efforts to provide new insights into the incidence of MCI-to-AD conversion have focused largely on clinically or biologically relevant features (i.e., neuroimaging markers, clinical exam data, neuropsychological test scores) and on different methods for statistical classification Young et al. (2013). We used T1-weighted MRI images from the collection of standard-

ized datasets. The description of the standardized MRI imaging from ADNI can be found in <http://adni.loni.usc.edu/methods/mri-analysis/adni-standardized-data>.

This study used a subset of the MCI subjects from ADNI-1, who had data from demographic, clinical cognitive assessments, APOE4 genotyping, and MRI measurements. In total, there are 819 individuals with a baseline diagnosis of MCI, but we only consider patients whose follow-up period was at least 36 months and no missing values. The final samples included 265 subjects which included participants who were stable in their diagnosis (MCI-S) and those who converted to a diagnosis of AD over 3 years (MCI-C). We considered a total of 18 clinical as potential predictors of MCI-to-AD progression in our classification analyses. These included scores on the Mini Mental State Examination (MMSE), Clinical Dementia Rating Sum of Boxes (CDR-SB), Alzheimer’s Disease Assessment Scale-cognitive subscale (ADAS-cog), Activities of Daily living (from the Functional Activities Questionnaire, FAQ), Trail Making tests B (TRA-BSCOR), The Rey Auditory Verbal Learning Test (RAVLT), The Digit- Symbol Coding test (DIGT). We also considered genotype for carriers of the epsilon-4 allele of the apolipoprotein E (APOE) gene Young et al. (2013) as a genetic predictor in this study. Table 3 in appendix (D) of section 7 summarizes all 18 clinical, demographic and genetic features used in this study. Structural MRI data were collected according to the ADNI acquisition protocol using T1-weighted scans (GradWarp, B1 Correction, N3, Scaled). This was followed by brain extraction for further processing Doshi et al. (2013). A new multi-atlas registration based label fusion method was applied for region of interest (ROI) segmentation Doshi et al. (2015). These data include baseline MRI scans of ADNI-1 participants. MRI scans were automatically partitioned into 145 anatomic ROIs spanning the entire brain. An additional 114 derived ROIs were calculated by combining single ROIs within a tree hierarchy, to obtain volumetric measurements from larger structures Doshi et al. (2016). In total, 259 ROIs were measured and used as potential predictors of MCI-to-dementia progression in this study. Based on the extant literature Korolev et al. (2016); Liu et al. (2020), we used 24 ROI features as theoretically significant of MCI to dementia progression (see table 4 in appendix (D) of section 7).

Note that the dependence and interactions among different modes of features (clinical, MRI) and within the modes may be different and hard to model explicitly. Thus a neural network-based modeling is intuitive from predictive modeling and machine learning perspective. Out of

the 265 patients, every time 186 are selected by simple random sample as training cases and the remaining 79 as test cases. The approximate 2:1 ratio for training and test cases is, of course, arbitrary. All the covariates (except categorical variables) were z-normalized. The outcome y_i for the i th patient is either 1 for MCI-C or 0 for MCI-S in classification study. We adopted a 10-fold cross-validation to avoid optimistically-biased estimates of model performance.

Theory guided parameter choice for statistical and computational models.

In order to implement the BBVI and BBVI-CV, we first need to make a valid choice of the prior parameters μ_{jn}, ζ_{jn} for $j = 1, \dots, K(n)$ as in (10). We use the choice of $\mu_{jn} = 0$ and $\zeta_{jn} = 1$ for our prior parameters. Indeed, this choice satisfies conditions (A1), (A2) and (A4) as assumed in the consistency proofs of theorems 4.1 and 4.2. Next, for the implementation of the BBVI and BBVI-CV, we need to make a choice on the number nodes k_n . We tried with $k_n = 2, 10, 20$ and obtained the best results at $k_n = 10$, the results of which are reported in this paper. Note that $k_n = 10$ satisfies the assumption of theorem 4.1 and 4.2 with $a = 0.44$. The next two important parameters of interest in the implementation of BBVI and BBVI-CV are the sample size S , used in computation of the Monte Carlo estimate of the gradient (22) and the learning rate ρ_t used in the updation rule (24). We next discuss the performance of algorithms 1 and 2 in light of these two parameters.

Choice of the learning rate

The stochastic optimization task is to find variational parameter vector \mathcal{V}_q which maximizes the evidence lower bound ELBO in (19) or consequently minimizes the Kullback-Leibler (KL) distance in (14). Even though the BBVI is straightforward in its general definition, the choice of learning rate ρ_t can be challenging in practice. Ideally, one would want the rate to be small in situations where the noisy estimates of the gradient have large variance and vice-versa. The elements of variational parameter can also differ in scale, and one needs to set the learning rate so that both the BBVI and BBVI-CV can accommodate even the smallest scales. So, the first issue is addressed in this paper by choosing the learning rate ρ_t such that we can obtain fast convergence rate of the ELBO to a good local maximum. The ρ_t considered in this paper are

the following: 1) constant $\rho_t = \rho$; 2) varying learning rate with $\rho_t = \frac{\rho_0}{b(t+1)^c}$, where $b > 0$ and $c > 0$. On one hand, a small constant rate generally does not allow the parameter vector to converge, a large constant rate can lead to slower convergence. Indeed, we would like a learning rate which guarantees learning algorithms converge, and converge as quickly as possible. For varying learning rate, ρ_t should satisfy the Robbins and Monro conditions: $\sum_t \rho_t = \infty$ and $\sum_t \rho_t^2 < \infty$ to make BBVI and BBVI-CV converge to a local maximum Darken and Moody (1991); Robbins and Monro (1951). In this work, we found using a fixed learning rate with $\rho_t = 0.0001$ and a varying learning rate with $\rho_0 = 1$, $b = 100$ and $c = 0.3$ works well.

Choice of the sample size S

The choice of sample size S is sensitive to the performance to model in terms of algorithmic stability and convergence time. Whereas each update with small sample size takes less time, the variability of the estimate is high. On the other hand a large sample size leads to less variable estimates but each update takes a much longer time. We would thus like to have a sample size which is just large enough so that the learning algorithms can offer best testing accuracy and faster convergence rate at the same time. We started with relatively small S for learning the robustness of machines, then we increased the sample size until we obtained the best model's performance both in terms of stability of variance of gradients and testing accuracy. Specifically, we experimented with $S = 200$, $S = 500$ and $S = 1000$.

Variance of gradient estimators

As explained in section 3.4, the maximization of the ELBO in (16) requires stabilization of the variance of the stochastic gradient in (22). Indeed there are two approaches which can effectively reduce the variance of the gradients (1) increasing the sample size S in Monte Carlo estimation of the gradient and (2) using a control variate approach which is described in section 3.4. In this direction, we try to choose the balance between these two variance reduction techniques. Figure 2 illustrates how the variance of gradient estimators changes with the number of iterations for a given S . Figure 3 illustrates the difference in variance of gradient estimators as S changes from 200 to 1000. For both these figures, the variance of gradient in (22) is estimated by considering the average of the empirical variance calculated across all its \mathcal{V}_q

components. Note that the gradients are more stable using BBVI-CV with smaller difference as we go from $S = 200$ to $S = 1000$. Further the variance under BBVI-CV is smaller compared to BBVI. This investigation suggests that applying control variates and using larger sample size reduces the variance significantly and this is expected. Thus, the optimal choice is decided by the combination which produces fast convergence and better test accuracy.

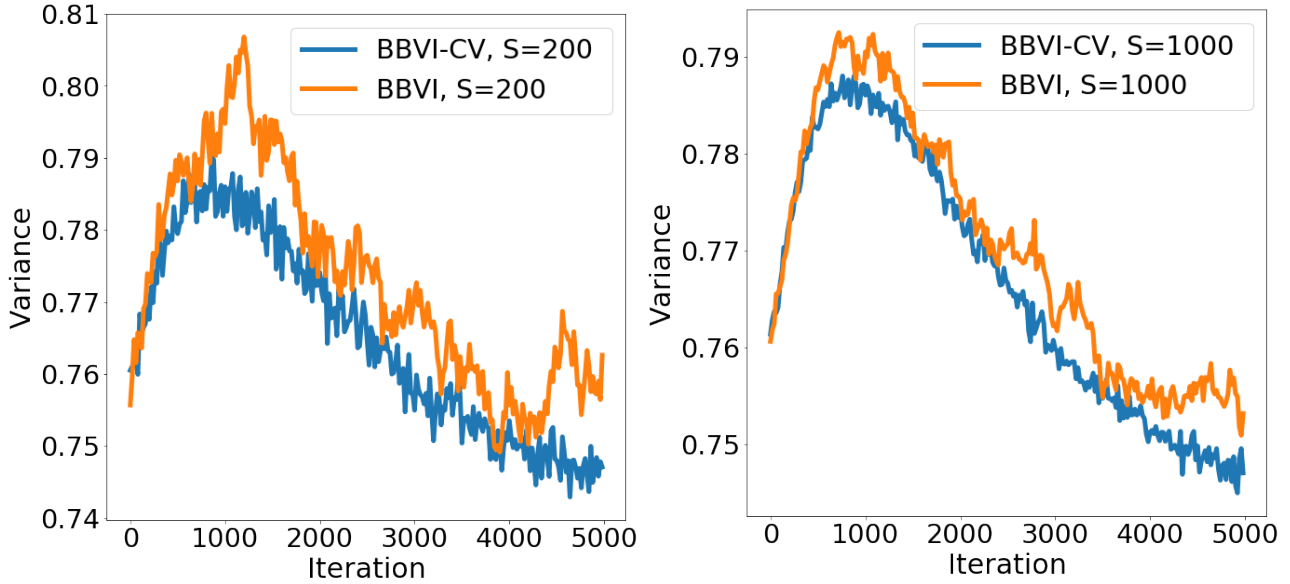


Figure 2: Variance of gradients for varying algorithms and fixed S .

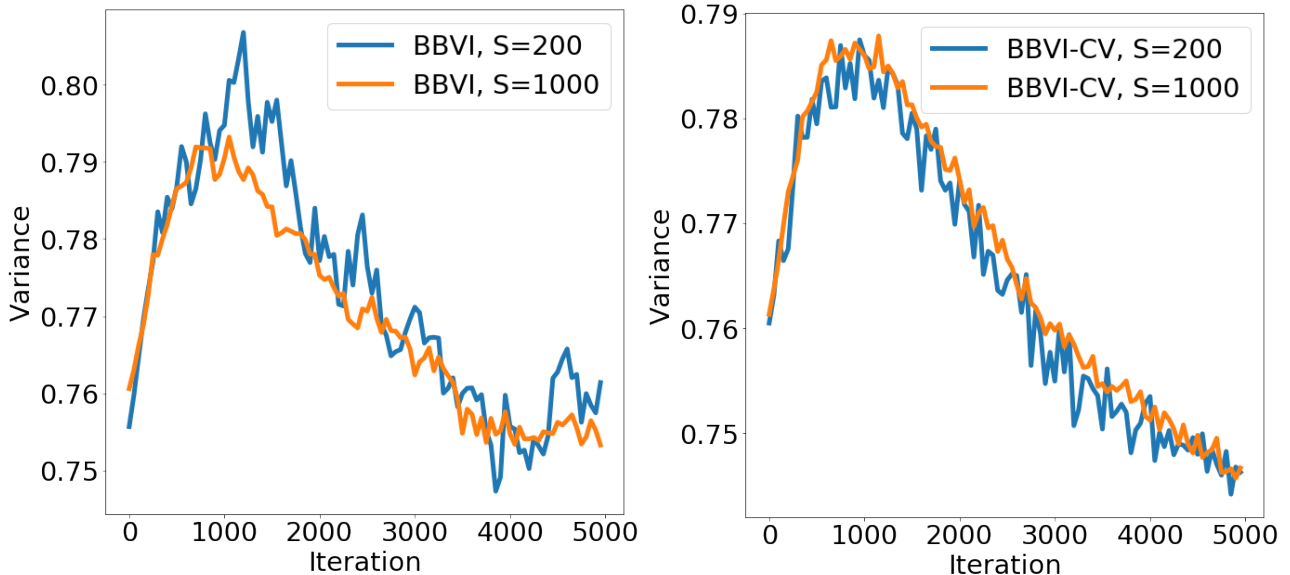


Figure 3: Variance of gradients for varying S and fixed choice of the algorithm.

Testing accuracy and convergence.

We evaluated the model’s performance for both the algorithms, BBVI and BBVI-CV under two criteria (1) testing accuracy (2) convergence time. The test accuracy of a classifier is given by

$$T(C) = \int_{\mathbb{R}^p \times \{0,1\}} I_{\{C(X,Y)=Y\}} dP_{X,Y} = 1 - R(C) \quad (42)$$

where $T(C)$ is the mis-classification error rate as described in (2). The convergence criterion is defined as the point where Monte Carlo estimate of the ELBO as in (23) converges. We report the results with several combinations of hyper-parameter in table 1 : (a) $S = 200$, $\rho_t = 0.001$; (b) $S = 500$, $\rho_t = 0.001$; (c) $S = 1000$, $\rho_t = 0.001$; (d) $S = 200$, $\rho_t(b = 100, c = 0.3)$; (e) $S = 500$, $\rho_t(b = 100, c = 0.3)$; (f) $S = 1000$, $\rho_t(b = 100, c = 0.3)$. In terms of the testing accuracy, the best model is BBVI with $S = 1000$ and a fixed learning rate. This produces average testing accuracy 75.89% with standard error 0.56%. The Table 1 also provides convergence time (second) for one complete run of BBVI and BBVI-CV for one data split on a 2.3 GHz 8-Core Intel Core i9 MacBook Pro workstation. In terms of convergence time, the best model is BBVI-CV with $S = 200$ for fixed learning rate.

Method	Sample size (S)	Testing accuracy(%)		Convergence time(s)	
		Fixed	Variate	Fixed	Variate
BBVI	200	74.46 ± 1.74	74.11 ± 1.28	1247	1860
	500	74.28 ± 0.91	74.64 ± 0.56	1359	2061
	1000	75.89 ± 0.56	75.12 ± 0.80	1652	2194
BBVI-CV	200	75.71 ± 0.61	73.93 ± 5.95	1201	1268
	500	75.35 ± 0.56	74.11 ± 5.95	1263	1255
	1000	75.00 ± 0.00	74.28 ± 6.00	1735	1466

Table 1: Performance for BBVI and BBVI-CV.

For fixed learning rate, figure 4 shows differences in ELBO values between BBVI and BBVI-CV for $S = 200$ and $S = 1000$ respectively in left and right panel. Figure 5 shows change in ELBO values for $S = 200, 500, 1000$ for BBVI and BBVI-CV respectively in left and right panel. Figure 4 suggests ELBO difference in BBVI and BBVI-CV is negligible for higher value of S . Figure 5 indicates ELBO for BBVI-CV is less sensitive to the choice of S compared to BBVI. Further, one can reach lower ELBO values much faster with BBVI-CV compared to BBVI.

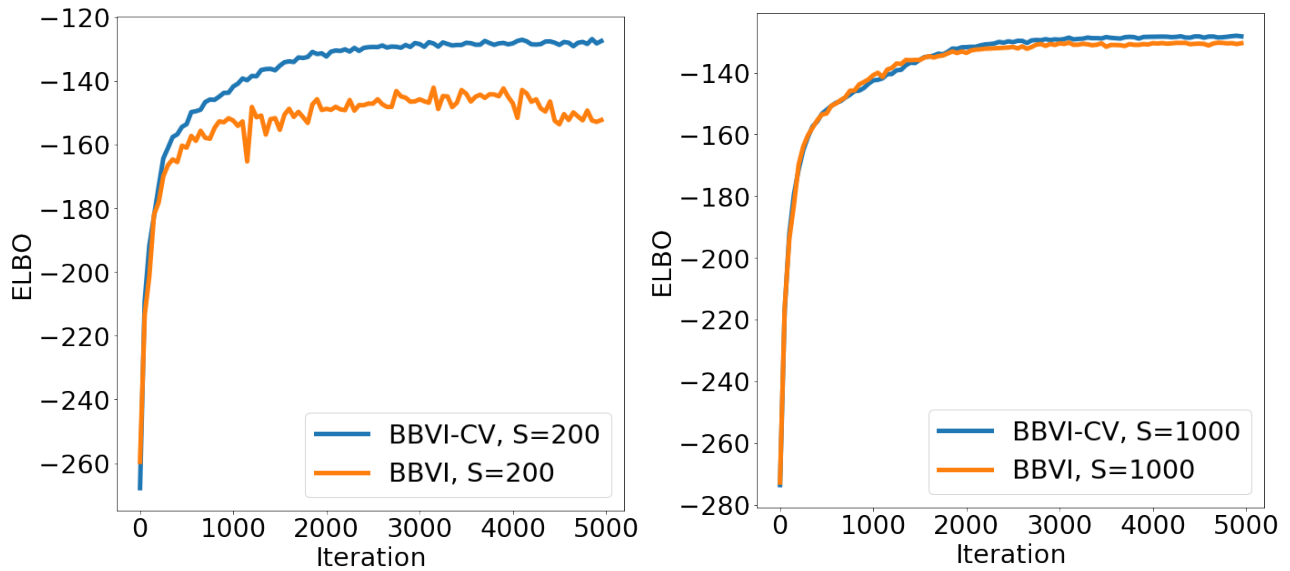


Figure 4: Convergence of the ELBO for varying algorithms and fixed S .

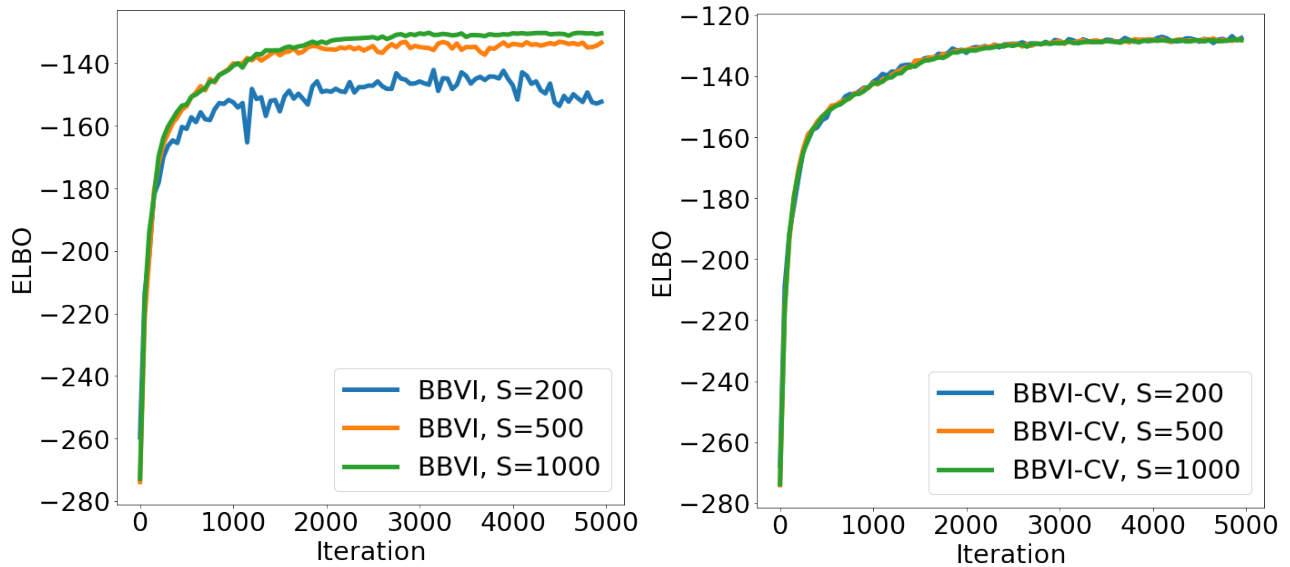


Figure 5: Convergence of ELBO for varying S and fixed choice of the algorithm.

BBVI model converges to same level of ELBO values after 4000 iterations where as BBVI-CV took less than 2000 iterations to achieve same level of ELBO values. The convergence of ELBO shares same behavior as the stabilization of the variance of the gradient. Although at large values of S , convergence of ELBO needs smaller number of iterations, each iteration itself takes much more time with large S . From table 1, we see that the overall convergence time is smaller with small values of S . However, the testing accuracy is better at larger sample sizes. The convergence time for BBVI-CV algorithm is overall smaller with comparable testing accuracy even at small values of S .

Based on all these observations, we recommend the use of BBVI-CV with $S = 200$ to allow good testing accuracy and smaller computation cost.

Numerical comparison with popular models

In this section, we numerically compare the testing accuracy of BBVI and BBVI-CV to a few benchmark models which include logistic regression (LR) and support vector machine (SVM) as developed by Pedregosa et al. (2011); McKinney (2010) and frequentist artificial neural network (ANN) Chen et al. (2015); Gurney (1997). We also compared to Bayesian neural network models which uses Stochastic Gradient MCMC Welling and Teh (2011) and variational Bayes with horse shoe prior Ghosh et al. (2019). For all the neural network models, viz, artificial neural network (ANN), Stochastic Gradient MCMC Bayesian neural network (SG-MCMC) and variational Bayesian neural network with horse shoe prior (VBNN-HS), we fix the choice of the number of nodes at $k_n = 10$ with a single hidden layer. For variational Bayes neural network with horse shoe prior, we use the default set up as available in Ghosh and Doshi-Velez (2017).

Table 2 provides the training and testing accuracy and their empirical standard errors for all different methods under consideration. Learning from the previous section, the optimal hyper-parameters for BBVI and BBVI-CV are used as $S=1000$, $\rho_t = 0.001$ and $S = 200$, $\rho_t = 0.001$, respectively. In terms of the mean and standard deviation of testing accuracy, the best models are BBVI and BBVI-CV (almost equal performance). Apparently, the VBNN-HS suffers from over-fitting issue. LR, SVM, ANN and SG-MCMC have considerably larger standard errors for testing accuracy. Note, the BBVI and BBVI-CV algorithms have been fine tuned to perform optimally. One might observe an improvement in the performance of Stochastic Gradient MCMC Bayesian neural network and variational Bayesian neural network with horse shoe prior by optimally choosing their tuning parameters. However studying that is beyond the scope of this paper as they are different methodology and the underlying statistical theories are not well established.

Classifier	Training accuracy (%)	Testing accuracy (%)
LR	82.1 ± 2.5	70.9 ± 5.5
SVM	80.32 ± 2.2	70.6 ± 5.5
ANN	82.0 ± 5.6	74.1 ± 6.8
SG-MCMC	80.8 ± 4.6	73.5 ± 5.9
BBVI	79.46 ± 1.7	75.89 ± 0.56
BBVI-CV	80.2 ± 4.9	75.71 ± 0.61
VBNN-HS	97.0 ± 0.6	71.6 ± 4.16

Table 2: Performance for different classifiers. LR: Logistic regression. SVM: Support vector machine. ANN: Frequentist artificial neural network. SG-MCMC: Stochastic gradient MCMC Bayesian neural network. VBNN-HS: Variational Bayes neural network with horseshoe prior.

6 Discussion and Conclusion

The theoretical rigour and computational detail for variational Bayes neural network classifier presented in this article is novel and unique contribution to statistical literature. Although the variational Bayes is popular in machine learning, neither the computational method nor the statistical properties are well understood for complex modeling such as neural networks. We characterize the prior distributions and the variational family for consistent Bayesian estimation. The theory also quantifies the loss due to VB numerical approximation compared to the true posterior distribution. For practical implementation, we reveal that the algorithm may not be as simple and straightforward as it sounds in computer science literature, rather it requires careful crafting on several parameters associated in various steps. Nevertheless, the computation could be quite faster compared to popular Monte Carlo Markov Chain procedure of approximating the posterior distributions.

Although this article builds the framework on a single layer neural networks model with simplistic prior structure, the detail statistical theory and computational methodology are quite involved. This investigation opens up possibility of exploring much wider class of models and priors. For example, shrinkage priors, such as double exponential and horseshoe priors can be explored for building sparse neural networks or one can experiment with various other variational families. However, their computational details and associated statistical properties are not immediate. We hope this research will accelerate further development of statistical and computational foundation for variational inference in general machine learning research.

Bibliography

- Allison, J. R., R. C. Rivers, J. C. Christodoulou, M. Vendruscolo, and C. M. Dobson (2014). A relationship between the transient structure in the monomeric state and the aggregation propensities of α -synuclein and β -synuclein. *Biochemistry* 53(46), 7170–7183.
- Barron, A., M. J. Schervish, and L. Wasserman (1999). The consistency of posterior distributions in nonparametric problems. *Ann. Statist.* 27(2), 536–561.
- Barron, A. R. (1993). Universal approximation bounds for superpositions of a sigmoidal function. *IEEE Transactions on Information theory* 39(3), 930–945.
- Bhattacharya, S. and T. Maiti (2020). Statistical foundation of variational bayes neural networks. arXiv:2006.15786.
- Bishop, C. M. (1997). Bayesian Neural Networks. *Journal of the Brazilian Computer Society* 4(1), 61–68.
- Blei, D., A. Ng, and M. Jordan (2003). Latent dirichlet allocation. *Journal of Machine Learning Research* 3, 993–1022.
- Blei, D. M. and J. D. Lafferty (2007). A correlated topic model of science. *The Annals of Applied Statistics* 1(1), 17–35.
- Blundell, C., J. Cornebise, K. Kavukcuoglu, and D. Wierstra (2015). Weight uncertainty in neural network. In *Proceedings of Machine Learning Research*, Volume 37, pp. 1613–1622. PMLR.
- Cannings, T. I. and R. J. Samworth (2017). Random-projection ensemble classification. *Journal of the Royal Statistical Society: Series B (Statistical Methodology)* 79(4), 959–1035.
- Carbonetto, P. and M. Stephens (2012). Scalable variational inference for bayesian variable selection in regression, and its accuracy in genetic association studies. *Bayesian Analysis* 7(1), 73–108.
- Chen, T., M. Li, Y. Li, M. Lin, N. Wang, M. Wang, T. Xiao, B. Xu, C. Zhang, and Z. Zhang (2015). Mxnet: A flexible and efficient machine learning library for heterogeneous distributed systems.

- Cui, Y., B. Liu, and S. Luo (2011). Identification of conversion from mild cognitive impairment to alzheimer’s disease using multivariate predictors. *PLoS ONE* 6(7). e0021896.
- Cybenko, G. (1989). Approximation by superpositions of a sigmoidal function. *Mathematics of control, signals and systems* 2(4), 303–314.
- Darken, C. and J. Moody (1991). Note on learning rate schedules for stochastic optimization. In R. P. Lippmann, J. Moody, and D. Touretzky (Eds.), *Advances in Neural Information Processing Systems*, Volume 3, pp. 832–838. Morgan-Kaufmann.
- Doshi, J., G. Erus, Y. Ou, B. Gaonkar, and C. Davatzikos (2013). Multi-atlas skull-stripping. *Acad Radiol* 12(20), 1566–76.
- Doshi, J., G. Erus, Y. Ou, S. Resnick, R. Gur, R. Gur, T. Satterthwaite, S. Furth, and C. Davatzikos (2015). Muse: Multi-atlas region segmentation utilizing ensembles of registration algorithms and parameters, and locally optimal atlas selection. *NeuroImage* 127, 186–195.
- Doshi, J., G. Erus, M. Rozycki, and C. Davatzikos (2016). Hierarchical parcellation of mri using multi-atlas labeling methods. *Alzheimer’s Disease Neuroimaging Initiative*. <http://adni.loni.usc.edu/updated-dataset-hierarchical-parcellation-of-mri-using-multi-atlas-labeling-me/>.
- Farlow, M. (2009). Treatment of mild cognitive impairment (MCI). *Current Alzheimer Research* 6(4), 362–367.
- Friedman, J., T. Hastie, and R. Tibshirani (2009). *The elements of statistical learning*. Springer series in statistics. Springer, New York.
- Ghosh, S. and F. Doshi-Velez (2017). Horseshoe priors for bayesian neural networks [Code]. <https://github.com/dtak/hs-bnn-public>.
- Ghosh, S., J. Yao, and F. Doshi-Velez (2019). Model selection in bayesian neural networks via horseshoe priors. *Journal of Machine Learning Research* (20), 1–46.
- Graves, A. (2011). Practical variational inference for neural networks. In J. Shawe-Taylor, R. Zemel, P. Bartlett, F. Pereira, and K. Q. Weinberger (Eds.), *Advances in Neural Information Processing Systems*, Volume 24, pp. 2348–2356. Curran Associates, Inc.

- Gurney, K. (1997). *An Introduction to Neural Networks*. USA: Taylor & Francis, Inc.
- Hinton, G. E. and D. Van Camp (1993). Keeping the neural networks simple by minimizing the description length of the weights. In *Proceedings of the sixth annual conference on Computational learning theory, COLT'93*, pp. 5–13. ACM press.
- Hornik, K., M. Stinchcombe, and H. White (1989). Multilayer feedforward networks are universal approximators. *Neural Networks* 2(5), 359–366.
- Hubin, A., G. Storvik, and F. Frommlet (2018). Deep bayesian regression models. arXiv:1806.02160.
- Javid, K., W. Handley, M. P. Hobson, and A. Lasenby (2020). Compromise-free bayesian neural networks. arXiv:2004.12211.
- Kingma, D. P., T. Salimans, and M. Welling (2015). Variational dropout and the local reparameterization trick. In C. Cortes, N. Lawrence, D. Lee, M. Sugiyama, and R. Garnett (Eds.), *Advances in Neural Information Processing Systems*, Volume 28, pp. 2575–2583. Curran Associates, Inc.
- Korolev, I. (2014). Alzheimer’s disease: A clinical and basic science review. *Medical Student Research Journal* 4(1), 24–33.
- Korolev, I. O., L. L. Symonds, A. C. Bozoki, and A. D. N. Initiative (2016). Predicting progression from mild cognitive impairment to alzheimer’s dementia using clinical, mri, and plasma biomarkers via probabilistic pattern classification. *PLoS ONE* 11(2). e0138866.
- Lampinen, J. and A. Vehtari (2001). Bayesian approach for neural networks—review and case studies. *Neural networks : the official journal of the International Neural Network Society* 14(3), 257–274.
- Lee, H. (2000). Consistency of posterior distributions for neural networks. *Neural Networks* 13(6), 629 – 642.
- Leshno, M., V. Y. Lin, A. Pinkus, and S. Schocken (1993). Multilayer feedforward networks with a nonpolynomial activation function can approximate any function. *Neural networks* 6(6), 861–867.

- Li, X., C. Li, J. Chi, and J. Ouyang (2018). In *Proceedings of the Twenty-Seventh International Joint Conference on Artificial Intelligence, IJCAI-18*, pp. 2404–2410. International Joint Conferences on Artificial Intelligence Organization.
- Liang, F., Q. Li, and L. Zhou (2018). Bayesian neural networks for selection of drug sensitive genes. *Journal of the American Statistical Association* 113(523), 955–972.
- Liu, Z., T. Maiti, and A. Bender (2020). A role for prior knowledge in statistical classification of the transition from mci to alzheimer’s disease. unpublished.
- Logsdon, B. A., G. E. Hoffman, and J. G. Mezey (2009). A variational bayes algorithm for fast and accurate multiple locus genome-wide association analysis. *BMC Bioinformatics* 11(1). 58.
- McKinney, W. (2010). Data structures for statistical computing in python. In S. van der Walt and J. Millman (Eds.), *Proceedings of the 9th Python in Science Conference*, pp. 56–61.
- Mullachery, V., A. Khera, and A. Husain (2018). Bayesian neural networks. arXiv:1801.07710.
- Nagapetyan, T., A. B. Duncan, L. Hasenclever, S. J. Vollmer, L. Szpruch, and K. Zygalakis (2017). The true cost of stochastic gradient langevin dynamics. arXiv:1706.02692.
- Neal, R. M. (1992). Bayesian training of backpropagation networks by the hybrid monte-carlo method. <https://www.cs.toronto.edu/~radford/ftp/bbp.pdf>.
- Owen, A. B. (2018). Monte carlo: what, why & how. <https://statweb.stanford.edu/~owen/pubtalks/01mcintro.pdf>.
- Paisley, J., D. Blei, and M. Jordan (2012). Variational bayesian inference with stochastic search. In *Proceedings of the 29th International Conference on International Conference on Machine Learning, ICML’12*, pp. 1363–1370. ACM press.
- Pati, D., A. Bhattacharya, and Y. Yang (2018). On statistical optimality of variational bayes. In A. Storkey and F. Perez-Cruz (Eds.), *Proceedings of Machine Learning Research*, Volume 84, pp. 1579–1588. PMLR.

- Pedregosa, F., G. Varoquaux, A. Gramfort, V. Michel, B. Thirion, O. Grisel, M. Blondel, P. Prettenhofer, R. Weiss, V. Dubourg, J. Vanderplas, A. Passos, D. Cournapeau, M. Brucher, M. Perrot, and E. Duchesnay (2011). Scikit-learn: Machine learning in Python. *Journal of Machine Learning Research* 12, 2825–2830.
- Petersen, R. C., R. O. Roberts, D. S. Knopman, B. F. Boeve, Y. E. Geda, R. J. Ivnik, G. E. Smith, and C. R. Jack (2009). Mild cognitive impairment: ten years later. *Archives of neurology* 66(12), 1447–1455.
- Pollard, D. (1990). Empirical processes: Theory and applications. *NSF-CBMS Regional Conference Series in Probability and Statistics* 2, i–86.
- Ranganath, R., S. Gerrish, and D. M. Blei (2013). Black box variational inference. arXiv:1401.0118.
- Robbins, H. and S. Monro (1951). A stochastic approximation method. *Annals of Mathematical Statistics* 22(3), 400–407.
- Ross, S. M. (2013). *Simulation* (Fifth ed.). Academic Press.
- Sun, S., C. Chen, and L. Carin (2017). Learning Structured Weight Uncertainty in Bayesian Neural Networks. Volume 54 of *Proceedings of Machine Learning Research*, pp. 1283–1292. PMLR.
- Sun, S., G. Zhang, J. Shi, and R. B. Grosse (2019). Functional variational bayesian neural networks. In *7th International Conference on Learning Representations, ICLR 2019*. OpenReview.net.
- Taghia, J. (2018). Lecture notes. part III: Black-box variational inference. [http://www.it.uu.se/research/systems_and_control/education/2018/pml/lectures/VILecture NotesPart3.pdf](http://www.it.uu.se/research/systems_and_control/education/2018/pml/lectures/VILecture%20NotesPart3.pdf).
- van der Vaart, A. and J. Wellner (1996). *Weak Convergence and Empirical Processes: With Applications to Statistics*. Springer Series in Statistics. Springer, New York.
- Wan, R., M. Zhong, H. Xiong, and Z. Zhu (2018). Neural control variates for variance reduction. arXiv:1806.00159.

- Wang, Y. and D. M. Blei (2019). Frequentist consistency of variational bayes. *Journal of the American Statistical Association* 114(527), 1147–1161.
- Welling, M. and Y. Teh (2011). Bayesian learning via stochastic gradient langevin dynamics. In *Proceedings of the 28th International Conference on International Conference on Machine Learning, ICML’11*, pp. 681–688. ACM press.
- Wong, W. H. and X. Shen (1995). Probability inequalities for likelihood ratios and convergence rates of sieve mles. *Annals of Statistics* 23(2), 339–362.
- Wu, A., S. Nowozin, E. Meeds, R. E. Turner, J. M. Hernández-Lobato, and A. L. Gaunt (2019). Deterministic variational inference for robust bayesian neural networks.
- Yang, K. and T. Maiti (2020). Statistical aspects of high-dimensional sparse artificial neural network models. *Machine Learning and Knowledge Extraction* 2(1), 1–19.
- Yang, Y., D. Pati, and A. Bhattacharya (2020). α -variational inference with statistical guarantees. *Annals of Statistics* 48(2), 886–905.
- Young, J., M. Modat, M. J. Cardoso, A. Mendelson, D. Cash, and S. Ourselin (2013). Accurate multimodal probabilistic prediction of conversion to alzheimer’s disease in patients with mild cognitive impairment. *NeuroImage: Clinical* 2, 735 – 745.
- Zhang, D. and D. Shen (2011). Multi-modal multi-task learning for joint prediction of clinical scores in alzheimer’s disease. In T. Liu, D. Shen, L. Ibanez, and X. Tao (Eds.), *Multimodal Brain Image Analysis*, Berlin, Heidelberg, pp. 60–67. Springer Berlin Heidelberg.
- Zhang, D., D. Shen, and A. D. N. Initiative (2012). Predicting future clinical changes of mci patients using longitudinal and multimodal biomarkers. *PLoS ONE* 7(3). e0033182.
- Zhang, F. and C. Gao (2020). Convergence rates of variational posterior distributions. *Annals of Statistics* 48(4), 2180–2207.
- Zhang, G., S. Sun, D. Duvenaud, and R. Grosse (2017). Noisy natural gradient as variational inference. arXiv:1712.02390.

7 Appendix

(A) Gradients of Variational family of BBVI

In this section, we derive the analytical solution for BBVI with score function estimator. With q as in (12), for $j = 1, \dots, K(n)$

$$\nabla_{m_{jn}} \mathcal{L}_{\mathcal{V}_q} = E_{q(\cdot|\mathcal{V}_q)} \left[\left(\frac{\theta_{jn} - m_{jn}}{s_{jn}^2} \right) (\log \pi(\boldsymbol{\Theta}_n, \mathbf{y}_n, \mathbf{X}_n) - \log q(\boldsymbol{\Theta}_n|\mathcal{V}_q)) \right]$$

$$g^{m_{jn}} = \frac{1}{S} \sum_{w=1}^S \left(\frac{\theta_{jn}[w] - m_{jn}}{s_{jn}^2} \right) (\log \pi(\boldsymbol{\theta}_n[w], \mathbf{y}_n, \mathbf{X}_n) - \log q(\boldsymbol{\theta}_n[w]|\mathcal{V}_q))$$

$$\nabla_{s_{jn}} \mathcal{L}_{\mathcal{V}_q} = E_{q(\cdot|\mathcal{V}_q)} \left[\left(\frac{(\theta_{jn} - m_{jn})^2}{s_{jn}^3} - \frac{1}{s_{jn}} \right) (\log \pi(\boldsymbol{\Theta}_n, \mathbf{y}_n, \mathbf{X}_n) - \log q(\boldsymbol{\Theta}_n|\mathcal{V}_q)) \right]$$

$$g^{s_{jn}} = \frac{1}{S} \sum_{w=1}^S \left(\frac{(\theta_{jn}[w] - m_{jn})^2}{s_{jn}^3} - \frac{1}{s_{jn}} \right) (\log \pi(\boldsymbol{\theta}_n[w], \mathbf{y}_n, \mathbf{X}_n) - \log q(\boldsymbol{\theta}_n[w]|\mathcal{V}_q))$$

With $s_{jn} = \log(1 + e^{r_{jn}})$

$$\nabla_{r_{jn}} \mathcal{L}_{\mathcal{V}_q} = \left(\frac{e^{r_{jn}}}{1 + e^{r_{jn}}} \right) (\nabla_{s_{jn}} \mathcal{L}_{\mathcal{V}_q} |_{s_{jn}=\log(1+e^{r_{jn}})})$$

$$g^{r_{jn}} = \left(\frac{e^{r_{jn}}}{1 + e^{r_{jn}}} \right) (g^{s_{jn}} |_{s_{jn}=\log(1+e^{r_{jn}})})$$

(B) Consistency of the variational posterior

7.1 Definitions

Definition 7.1 For a vector $\boldsymbol{\alpha}$ and a function g ,

1. $\|\boldsymbol{\alpha}\|_1 = \sum_i |\alpha_i|$, $\|\boldsymbol{\alpha}\|_2 = \sqrt{\sum_i \alpha_i^2}$, $\|\boldsymbol{\alpha}\|_\infty = \max_i |\alpha_i|$.

2. $\|g\|_1 = \int_{\mathbf{x} \in \mathcal{X}} |g(\mathbf{x})| d\mathbf{x}$, $\|g\|_2 = \sqrt{\int_{\mathbf{x} \in \mathcal{X}} g(\mathbf{x})^2 d\mathbf{x}}$, $\|g\|_\infty = \sup_{\mathbf{x} \in \mathcal{X}} |g(\mathbf{x})|$

Definition 7.2 For any two functions l and u , define the bracket $[l, u]$ as the set of all functions f such that $l \leq f \leq u$. Let $\|\cdot\|$ be a metric. Define an ε -bracket as a bracket with $\|u - l\| \leq \varepsilon$.

Define the bracketing number of a set of functions \mathcal{F}^* as the minimum number of ε -brackets needed to cover \mathcal{F}^* , and denote it by $N_{[]}(\varepsilon, \mathcal{F}^*, \|\cdot\|)$. Finally, the bracketing entropy, denoted $H_{[]}(\varepsilon, \mathcal{F}^*, \|\cdot\|)$, is the natural logarithm of the bracketing number Pollard (1990).

7.2 Lemmas

Lemma 7.3 Let $H_{[]}(\varepsilon, \tilde{\mathcal{F}}_n, \|\cdot\|_2) \leq K(n) \log(M_n/\varepsilon)$ then

$$\int_0^\varepsilon H_{[]}(\varepsilon, \tilde{\mathcal{F}}_n, \|\cdot\|_2) d\varepsilon \lesssim \varepsilon \sqrt{K(n)(\log M_n - \log \varepsilon)}$$

where $H_{[]}(\varepsilon, \tilde{\mathcal{F}}_n, \|\cdot\|_2)$ is defined in Definition 7.2.

Proof. See proof of lemma 7.12 in Bhattacharya and Maiti (2020).

Lemma 7.4 Suppose q satisfies

$$\int d_{KL}(\ell_0, \ell_{\boldsymbol{\theta}_n}) q(\boldsymbol{\theta}_n) d\boldsymbol{\theta}_n \leq \varepsilon,$$

then for any $\nu > 0$,

$$P_0^n \left(\left| \int q(\boldsymbol{\theta}_n) \log \frac{L(\boldsymbol{\theta}_n)}{L_0} d\boldsymbol{\theta}_n \right| \geq n\nu \right) \leq \frac{\varepsilon}{\nu}$$

Proof. See proof of lemma 7.11 in Bhattacharya and Maiti (2020).

Lemma 7.5 Suppose $\mathcal{N}_\varepsilon = \{\boldsymbol{\theta}_n : d_{KL}(\ell_0, \ell_{\boldsymbol{\theta}_n}) < \varepsilon\}$ and $p(\boldsymbol{\theta}_n)$ satisfies

$$\int_{\mathcal{N}_\varepsilon} p(\boldsymbol{\theta}_n) d\boldsymbol{\theta}_n \geq e^{-n\varepsilon}, n \rightarrow \infty$$

then for any $\nu > 0$,

$$P_0^n \left(\left| \log \int \frac{L(\boldsymbol{\theta}_n)}{L_0} p(\boldsymbol{\theta}_n) d\boldsymbol{\theta}_n \right| \geq n\nu \right) \leq \frac{2\varepsilon}{\nu}$$

Proof. See proof of lemma 7.10 in Bhattacharya and Maiti (2020).

Lemma 7.6 Suppose, $p(\boldsymbol{\theta}_n)$ satisfies

$$\int_{\mathcal{F}_n^c} p(\boldsymbol{\theta}_n) d\boldsymbol{\theta}_n \leq e^{-n\varepsilon}, n \rightarrow \infty$$

for any $\varepsilon > 0$. Then, for every $\tilde{\varepsilon} < \varepsilon$.

$$P_0^n \left(\int_{\boldsymbol{\theta}_n \in \mathcal{F}_n^c} \frac{L(\boldsymbol{\theta}_n)}{L_0} p(\boldsymbol{\theta}_n) d\boldsymbol{\theta}_n \geq e^{-n\tilde{\varepsilon}} \right) \leq e^{-n(\varepsilon - \tilde{\varepsilon})}$$

Proof. See proof of lemma 7.14 in Bhattacharya and Maiti (2020).

Lemma 7.7 Let $\eta_{\mathbf{t}_n}(\mathbf{x}) = \beta_0^{\mathbf{t}} + \sum_{j=1}^{k_n} \beta_j^{\mathbf{t}} \psi(\gamma_j^{\mathbf{t}\top} \mathbf{x})$ be a fixed neural network satisfying

$$|\theta_{jn} - t_{jn}| \leq \varepsilon, \quad j = 1, \dots, K(n).$$

Then,

$$\int_{\mathbf{x} \in [0,1]^p} |\eta_{\boldsymbol{\theta}_n}(\mathbf{x}) - \eta_{\mathbf{t}_n}(\mathbf{x})| dx \leq 8 \left(K(n) + (p+1) \sum_{j=1}^{K(n)} |t_{jn}| \right) \varepsilon$$

Proof. See proof of lemma 7.2 in Bhattacharya and Maiti (2020).

Lemma 7.8 If $|\eta_0(\mathbf{x}) - \eta_{\boldsymbol{\theta}_n}(\mathbf{x})| \leq \varepsilon$, then $|h_{\boldsymbol{\theta}_n}(\mathbf{x})| \leq 2\varepsilon$ where

$$h_{\boldsymbol{\theta}_n}(\mathbf{x}) = \sigma(\eta_0(\mathbf{x}))(\eta_0(\mathbf{x}) - \eta_{\boldsymbol{\theta}_n}(\mathbf{x})) + \log(1 - \sigma(\eta_0(\mathbf{x}))) - \log(1 - \sigma(\eta_{\boldsymbol{\theta}_n}(\mathbf{x})))$$

Proof: Note that,

$$\begin{aligned} |h_{\boldsymbol{\theta}_n}(\mathbf{x})| &\leq |\sigma(\eta_0(\mathbf{x}))| |\eta_0(\mathbf{x}) - \eta_{\boldsymbol{\theta}_n}(\mathbf{x})| + |\log(1 - \sigma(\eta_0(\mathbf{x}))) - \log(1 - \sigma(\eta_{\boldsymbol{\theta}_n}(\mathbf{x})))| \\ &\leq |\eta_0(\mathbf{x}) - \eta_{\boldsymbol{\theta}_n}(\mathbf{x})| + |\log(1 + \sigma(\eta_0(\mathbf{x}))(e^{\eta_{\boldsymbol{\theta}_n}(\mathbf{x}) - \eta_0(\mathbf{x})} - 1))| \\ &\leq 2|\eta_0(\mathbf{x}) - \eta_{\boldsymbol{\theta}_n}(\mathbf{x})| \end{aligned}$$

where the second step follows by using $\sigma(x) = e^x/(1 + e^x) \leq 1$ and the proof of the third step is shown below.

Let $p = \sigma(\eta_0(\mathbf{x}))$, then $0 \leq p \leq 1$ and $r = \eta_{\boldsymbol{\theta}_n}(\mathbf{x}) - \eta_0(\mathbf{x})$, then

$$|\log(1 + \sigma(\eta_0(\mathbf{x}))(e^{\eta_{\boldsymbol{\theta}_n}(\mathbf{x}) - \eta_0(\mathbf{x})} - 1))| = |\log(1 + p(e^r - 1))|$$

$$r > 0: \quad |\log(1 + p(e^r - 1))| = \log(1 + p(e^r - 1)) \leq \log(1 + (e^r - 1)) = r = |r|$$

$$r < 0: \quad |\log(1 + p(e^r - 1))| = -\log(1 + p(e^r - 1)) \leq -\log(1 + (e^r - 1)) = -r = |r|$$

Lemma 7.9 For

$$h(\boldsymbol{\theta}_n) = \int_{\mathbf{x} \in [0,1]^p} |\eta_{\boldsymbol{\theta}_n}(\sigma(\eta_0(\mathbf{x}))(\eta_0(\mathbf{x}) - \eta_{\boldsymbol{\theta}_n}(\mathbf{x})) + \log(1 - \sigma(\eta_0(\mathbf{x}))) - \log(1 - \sigma(\eta_{\boldsymbol{\theta}_n}(\mathbf{x}))))| d\mathbf{x}$$

$$\sum_{j=1}^{K(n)} |(\nabla^2 h(\boldsymbol{\theta}_n))_{jj}| \leq (2(p+1) + 1)(K(n) + 1) + 2(p+1) \|\boldsymbol{\theta}_n\|_2^2$$

where A_{jj} denotes the j^{th} diagonal entry of a matrix.

Proof. First note that

$$\begin{aligned} \nabla^2 h(\boldsymbol{\theta}_n) &= - \int_{\mathbf{x} \in [0,1]^p} \underbrace{(\sigma(\eta_0(\mathbf{x})) + \sigma(\eta_{\boldsymbol{\theta}_n}(\mathbf{x})))}_{g_1(\mathbf{x})} \nabla^2 \eta_{\boldsymbol{\theta}_n}(\mathbf{x}) d\mathbf{x} \\ &\quad - \int_{\mathbf{x} \in [0,1]^p} \underbrace{(\sigma(\eta_{\boldsymbol{\theta}_n}(\mathbf{x}))(1 - \sigma(\eta_{\boldsymbol{\theta}_n}(\mathbf{x}))))}_{g_2(\mathbf{x})} \nabla \eta_{\boldsymbol{\theta}_n}(\mathbf{x}) \nabla \eta_{\boldsymbol{\theta}_n}(\mathbf{x})^\top d\mathbf{x} \end{aligned}$$

For $r = \lfloor (j - k_n - 1)/p \rfloor$, $r' = (j - k_n - 1) \bmod p$

$$-b_{jj} = \begin{cases} \int g_2(\mathbf{x}) d\mathbf{x}, & r = 0, r' = 0 \\ \int g_2(\mathbf{x}) (\psi(\gamma_{r'}^\top \mathbf{x}))^2 d\mathbf{x}, & r = 0, r' = 1, \dots, k_n \\ \int g_1(\mathbf{x}) \beta_r \psi''(\gamma_r^\top \mathbf{x}) d\mathbf{x} + \int g_2(\mathbf{x}) \beta_r^2 (\psi'(\gamma_r^\top \mathbf{x}))^2 d\mathbf{x}, & r = 1, \dots, k_n, r' = 0 \\ \int g_1(\mathbf{x}) \beta_r \psi''(\gamma_r^\top \mathbf{x}) x_{r'}^2 d\mathbf{x} + \int g_2(\mathbf{x}) \beta_r^2 (\psi'(\gamma_r^\top \mathbf{x}))^2 x_{r'}^2 d\mathbf{x}, & r = 1, \dots, k_n, r' = 1, \dots, p \end{cases}$$

where the integral is over the set $\mathbf{x} \in [0, 1]^p$.

Note, $\psi(u) \leq 1$, $|g_1(\mathbf{x})| \leq 2$ and $|g_2(\mathbf{x})| \leq 1$. Also, $\psi(u), \psi'(u), \psi''(u), |x_{r'}^2| \leq 1$ which implies

$$\begin{aligned} \sum_{j=1}^{K(n)} |b_{jj}| &\leq (k_n + 1) + (p + 1) \sum_{j=1}^{k_n+1} (2|\beta_j| + |\beta_j|^2) \\ &\leq (k_n + 1) + (p + 1) \sum_{j=1}^{k_n+1} (2 + 2|\beta_j|^2) \\ &\leq (2(p+1) + 1)(K(n) + 1) + 2(p+1) \|\boldsymbol{\theta}_n\|_2^2 \end{aligned}$$

where the second inequality in the above step uses $|x| < x^2 + 1$.

Lemma 7.10 Let, $\tilde{\mathcal{F}}_n = \{\sqrt{\ell} : \ell_{\boldsymbol{\theta}_n}(y, \mathbf{x}), \boldsymbol{\theta}_n \in \mathcal{F}_n\}$ where $\ell_{\boldsymbol{\theta}_n}(y, \mathbf{x})$ is same as in (6) and \mathcal{F}_n

is same as in (39). Then,

$$\int_{\varepsilon^2/8}^{\sqrt{2\varepsilon}} \sqrt{H_{\square}(u, \tilde{\mathcal{F}}_n, \|\cdot\|_2)} du \lesssim \varepsilon \sqrt{2K_n(\log K_n + 2 \log C_n - \log \varepsilon)}$$

where $H_{\square}(u, \tilde{\mathcal{F}}_n, \|\cdot\|_2)$ is defined in Definition 7.2.

Proof. In this proof, let $\boldsymbol{\theta} = \boldsymbol{\theta}_n$. Note, by lemma 4.1 in Pollard (1990),

$$N(\varepsilon, \mathcal{F}_n, \|\cdot\|_{\infty}) \leq \left(\frac{3C_n}{\varepsilon} \right)^{K(n)}.$$

For $\boldsymbol{\theta}_1, \boldsymbol{\theta}_2 \in \mathcal{F}_n$, let $\tilde{\ell}(u) = \sqrt{\ell_{u\boldsymbol{\theta}_1 + (1-u)\boldsymbol{\theta}_2}(\mathbf{x}, y)}$.

Following equation (52) in Bhattacharya and Maiti (2020), we get

$$\sqrt{\ell_{\boldsymbol{\theta}_1}(\mathbf{x}, y)} - \sqrt{\ell_{\boldsymbol{\theta}_2}(\mathbf{x}, y)} \leq K(n) \sup_j \left| \frac{\partial \tilde{\ell}}{\partial \theta_j} \right| \|\boldsymbol{\theta}_1 - \boldsymbol{\theta}_2\|_{\infty} \leq F(\mathbf{x}, y) \|\boldsymbol{\theta}_1 - \boldsymbol{\theta}_2\|_{\infty} \quad (43)$$

where the upper bound $F(\mathbf{x}, y) = K(n)C_n/2$. This is because $|\partial \tilde{\ell} / \partial \theta_j|$, the derivative of $\sqrt{\ell}$ w.r.t. is bounded above by $|\partial \eta_{\boldsymbol{\theta}}(\mathbf{x}) / \partial \theta_j|$ as shown below.

$$\begin{aligned} \left| \frac{\partial \tilde{\ell}}{\partial \theta_j} \right| &= \left| \frac{1}{2} \frac{\partial \eta_{\boldsymbol{\theta}}(\mathbf{x})}{\partial \theta_j} \left(y - \frac{e^{\eta_{\boldsymbol{\theta}}(\mathbf{x})}}{1 + e^{\eta_{\boldsymbol{\theta}}(\mathbf{x})}} \right) \sqrt{e^{(y\eta_{\boldsymbol{\theta}}(\mathbf{x}) - \log(1 + e^{\eta_{\boldsymbol{\theta}}(\mathbf{x}))})} \right| \\ &\leq \frac{1}{2} \frac{\partial \eta_{\boldsymbol{\theta}}(\mathbf{x})}{\partial \theta_j} \left(\frac{e^{\eta_{\boldsymbol{\theta}}(\mathbf{x})}}{1 + e^{\eta_{\boldsymbol{\theta}}(\mathbf{x})}} \right)^{1/2} \left(\frac{1}{1 + e^{\eta_{\boldsymbol{\theta}}(\mathbf{x})}} \right)^{1/2} \end{aligned}$$

Thus, using $e^{\eta_{\boldsymbol{\theta}}(\mathbf{x})} / (1 + e^{\eta_{\boldsymbol{\theta}}(\mathbf{x})})$, $1 / (1 + e^{\eta_{\boldsymbol{\theta}}(\mathbf{x})}) \leq 1$, we get

$$2 \left| \frac{\partial \tilde{\ell}}{\partial \theta_j} \right| \leq \left| \frac{\partial \eta_{\boldsymbol{\theta}}(\mathbf{x})}{\partial \theta_j} \right| \leq \begin{cases} 1, & \theta_j = \beta_r \text{ for some } r = 0, \dots, k_n \\ |\beta_r \psi'(\gamma_r^{\top} \mathbf{x}) x_{r'}|, & \theta_j = \gamma_{rr'} \text{ for some } r = 0, \dots, k_n, r' = 0, \dots, p \end{cases}$$

Using $|\psi'(u)| \leq 1$, $|x_{r'}| \leq 1$, $|\beta_r| \leq C_n$, the bound $F(\mathbf{x}, y)$ follows.

In view of (43) and theorem 2.7.11 in van der Vaart and Wellner (1996), we have

$$N_{\square}(\varepsilon, \tilde{\mathcal{F}}_n, \|\cdot\|_2) \leq \left(\frac{3K(n)C_n^2}{2\varepsilon} \right)^{K(n)} \implies H_{\square}(\varepsilon, \tilde{\mathcal{F}}_n, \|\cdot\|_2) \lesssim K(n) \log \frac{K(n)C_n^2}{\varepsilon}$$

where N_{\square} and H_{\square} denote the bracketing number and bracketing entropy as in definition 7.2.

Using, lemma 7.3 with $M_n = K(n)C_n^2$, we get

$$\int_0^\varepsilon \sqrt{H_{\square}(u, \tilde{\mathcal{F}}_n, \|\cdot\|_2)} du \lesssim \varepsilon \sqrt{K(n)(\log K(n)C_n^2 - \log \varepsilon)}$$

Therefore,

$$\begin{aligned} \int_{\varepsilon^2/8}^{\sqrt{2}\varepsilon} H_{\square}(u, \tilde{\mathcal{F}}_n, \|\cdot\|_2) du &\leq \int_0^{\sqrt{2}\varepsilon} H_{\square}(u, \tilde{\mathcal{F}}_n, \|\cdot\|_2) du \\ &\lesssim \sqrt{2}\varepsilon \sqrt{K(n)(\log K(n)C_n^2 - \log \sqrt{2}\varepsilon)} \end{aligned}$$

The proof follows by noting $\log \sqrt{2}\varepsilon \geq \log \varepsilon$.

7.3 Propositions

Proposition 7.11 *Let $q(\boldsymbol{\theta}_n) = \text{MVN}(\mathbf{t}_n, I_{K(n)}/\sqrt{n})$ and $p(\boldsymbol{\theta}_n) = \text{MVN}(\boldsymbol{\mu}_n, \boldsymbol{\Sigma}_n)$, where $\boldsymbol{\Sigma}_n = \text{diag}(\boldsymbol{\zeta}_n)$ and $\boldsymbol{\zeta}_n^* = 1/\boldsymbol{\zeta}_n$. Let $n\epsilon_n^2 \rightarrow \infty$, $K(n) \log n = o(n\epsilon_n^2)$, $\|\mathbf{t}_n\|_2^2 = o(n\epsilon_n^2)$, $\|\boldsymbol{\mu}_n\|_2^2 = o(n\epsilon_n^2)$, then for any $\nu > 0$,*

$$d_{\text{KL}}(q, p) \leq n\epsilon_n^2 \nu$$

provided $\|\boldsymbol{\zeta}_n\|_\infty = O(n)$, $\|\boldsymbol{\zeta}_n^*\|_\infty = O(1)$.

Proof:

$$\begin{aligned} d_{\text{KL}}(q, p) &= \sum_{j=1}^{K(n)} \left(\log \sqrt{n}\zeta_{jn} + \frac{1}{n\zeta_{jn}^2} + \frac{(t_{jn} - \mu_{jn})^2}{\zeta_{jn}^2} - \frac{1}{2} \right) \\ &\leq \frac{K(n)}{2}(\log n - 1) + \sum_{j=1}^{K(n)} \log \zeta_{jn} + \frac{1}{n} \sum_{j=1}^{K(n)} \frac{1}{\zeta_{jn}^2} + 2 \sum_{j=1}^{K(n)} \frac{t_{jn}^2}{\zeta_{jn}^2} + 2 \sum_{j=1}^{K(n)} \frac{\mu_{jn}^2}{\zeta_{jn}^2} - \frac{K(n)}{2} \\ &\leq \frac{K(n)}{2}(\log n - 1) + K(n) \log \|\boldsymbol{\zeta}_n\|_\infty + \frac{K(n)}{n} \|\boldsymbol{\zeta}_n^*\|_\infty \\ &\quad + 2\|\mathbf{t}_n\|_2^2 \|\boldsymbol{\zeta}_n^*\|_\infty + 2\|\boldsymbol{\mu}_n\|_2^2 \|\boldsymbol{\zeta}_n^*\|_\infty = o(n\epsilon_n^2) \end{aligned} \tag{44}$$

where the second last inequality uses $\boldsymbol{\zeta}_n^* = 1/\boldsymbol{\zeta}_n$. The last equality follows since $\|\boldsymbol{\zeta}_n\| = O(n)$, $\|\boldsymbol{\zeta}_n^*\|_\infty = O(1)$, $K(n) \log n = o(n\epsilon_n^2)$, $\|\mathbf{t}_n\|_2^2 = o(n\epsilon_n^2)$ and $\|\boldsymbol{\mu}_n\|_2^2 = o(n\epsilon_n^2)$.

Proposition 7.12 Let $p(\boldsymbol{\theta}_n)$ as in (10). Define

$$\mathcal{N}_\varepsilon = \{\boldsymbol{\theta}_n : d_{\text{KL}}(\ell_0, \ell_{\boldsymbol{\theta}_n}) < \varepsilon\} \quad (45)$$

where

$$d_{\text{KL}}(\ell_0, \ell_{\boldsymbol{\theta}_n}) = \int_{\mathbf{x} \in [0,1]^p} \left(\sigma(\eta_0(\mathbf{x}))(\eta_0(\mathbf{x}) - \eta_{\boldsymbol{\theta}_n}(\mathbf{x})) + \log \frac{1 - \sigma(\eta_0(\mathbf{x}))}{1 - \sigma(\eta_{\boldsymbol{\theta}_n}(\mathbf{x}))} \right) d\mathbf{x}$$

Let $\|\eta_0 - \eta_{\mathbf{t}_n}\|_\infty \leq \varepsilon \varepsilon_n^2/4$, $n \varepsilon_n^2 \rightarrow \infty$. If $K(n) \log n = o(n \varepsilon_n^2)$, $\|\mathbf{t}_n\|_2^2 = o(n \varepsilon_n^2)$, $\|\boldsymbol{\mu}_n\|_2^2 = o(n \varepsilon_n^2)$, then

$$\int_{\boldsymbol{\theta}_n \in \mathcal{N}_{\varepsilon \varepsilon_n^2}} p(\boldsymbol{\theta}_n) d\boldsymbol{\theta}_n \geq e^{-n \varepsilon_n^2 \nu} \quad \forall \nu > 0$$

provided $\|\boldsymbol{\zeta}_n\|_\infty = O(n)$, $\|\boldsymbol{\zeta}_n^*\|_\infty = O(1)$ where $\boldsymbol{\zeta}_n^* = 1/\boldsymbol{\zeta}_n$.

Proof. Let $\eta_{\mathbf{t}_n}(\mathbf{x}) = \beta_0^{\mathbf{t}} + \sum_{j=1}^{k_n} \beta_j^{\mathbf{t}} \sigma(\gamma_j^{\mathbf{t}^\top} \mathbf{x})$ be the neural network such that

$$\|\eta_{\mathbf{t}_n} - \eta_0\|_1 \leq \frac{\varepsilon \varepsilon_n^2}{4} \quad (46)$$

Such a neural network exists since $\|\eta_0 - \eta_{\mathbf{t}_n}\|_1 \leq \|\eta_0 - \eta_{\mathbf{t}_n}\|_\infty \leq \varepsilon \varepsilon_n^2/4$.

Next define neighborhood \mathcal{M}_ε as follows

$$\mathcal{M}_{\varepsilon \varepsilon_n^2} = \left\{ \boldsymbol{\theta}_n : |\theta_{jn} - t_{jn}| < \frac{\varepsilon \varepsilon_n^2}{8(K(n) + (p+1)\|\mathbf{t}_n\|_1)}, j = 1, \dots, K(n) \right\}$$

For every $\boldsymbol{\theta}_n \in \mathcal{M}_{\varepsilon \varepsilon_n^2}$, by lemma 7.7, we have

$$\|\eta_{\boldsymbol{\theta}_n} - \eta_{\mathbf{t}_n}\|_1 \leq \frac{\varepsilon \varepsilon_n^2}{2} \quad (47)$$

Combining (46) and (47), we get for $\boldsymbol{\theta}_n \in \mathcal{M}_{\varepsilon \varepsilon_n^2}$, $\|\eta_{\boldsymbol{\theta}_n} - \eta_0\|_1 \leq \varepsilon \varepsilon_n^2/2$.

This, in view of lemma 7.8, $d_{\text{KL}}(\ell_0, \ell_{\boldsymbol{\theta}_n}) \leq \varepsilon \varepsilon_n^2$.

Let $\boldsymbol{\theta}_n \in \mathcal{N}_{\varepsilon \varepsilon_n^2}$ for every $\boldsymbol{\theta}_n \in \mathcal{M}_{\varepsilon \varepsilon_n^2}$. Therefore,

$$\int_{\boldsymbol{\theta}_n \in \mathcal{N}_{\varepsilon \varepsilon_n^2}} p(\boldsymbol{\theta}_n) d\boldsymbol{\theta}_n \geq \int_{\boldsymbol{\theta}_n \in \mathcal{M}_{\varepsilon \varepsilon_n^2}} p(\boldsymbol{\theta}_n) d\boldsymbol{\theta}_n$$

Let $\delta_n = \varepsilon \epsilon_n^2 / (8(K(n) + (p+1)\|\mathbf{t}_n\|_1))$, then

$$\begin{aligned}
\int_{\boldsymbol{\theta}_n \in \mathcal{M}_{\varepsilon \epsilon_n^2}} p(\boldsymbol{\theta}_n) d\boldsymbol{\theta}_n &= \prod_{j=1}^{K(n)} \int_{t_{jn}-\delta_n}^{t_{jn}+\delta_n} \frac{1}{\sqrt{2\pi\zeta_{jn}^2}} e^{-\frac{(\theta_{jn}-\mu_{jn})^2}{2\zeta_{jn}^2}} d\theta_{jn} \\
&= \prod_{j=1}^{K(n)} \frac{2\delta_n}{\sqrt{2\pi\zeta_{jn}^2}} e^{-\frac{(\tilde{t}_{jn}-\mu_{jn})^2}{2\zeta_{jn}^2}}, \quad \tilde{t}_{jn} \in [t_{jn}-\delta_n, t_{jn}+\delta_n] \\
&= \prod_{j=1}^{K(n)} e^{-\left(-\frac{1}{2} \log \frac{2}{\pi} - \log \delta_n + \log \zeta_{jn} + \frac{(\tilde{t}_{jn}-\mu_{jn})^2}{2\zeta_{jn}^2}\right)}
\end{aligned} \tag{48}$$

where the second last equality holds by mean value theorem.

Note that $\tilde{t}_{jn} \in [t_{jn}-1, t_{jn}+1]$ since $\delta_n \rightarrow 0$, therefore

$$\frac{(\tilde{t}_{jn}-\mu_{jn})^2}{2\zeta_{jn}^2} \leq \frac{\max((t_{jn}-\mu_{jn}-1)^2, (t_{jn}-\mu_{jn}+1)^2)}{2\zeta_{jn}^2} \leq \frac{(t_{jn}-\mu_{jn})^2}{\zeta_{jn}^2} + \frac{1}{\zeta_{jn}^2}$$

where the last inequality follows since $(a+b)^2 \leq 2(a^2+b^2)$. Therefore

$$\begin{aligned}
\sum_{j=1}^{K(n)} \frac{(\tilde{t}_{jn}-\mu_{jn})^2}{2\zeta_{jn}^2} &\leq 2 \sum_{j=1}^{K(n)} \frac{t_{jn}^2}{\zeta_{jn}^2} + 2 \sum_{j=1}^{K(n)} \frac{\mu_{jn}^2}{\zeta_{jn}^2} + \sum_{j=1}^{K(n)} \frac{1}{\zeta_{jn}^2} \\
&\leq 2(\|\mathbf{t}_n\|_2^2 + \|\boldsymbol{\mu}_n\|_2^2 + 1) \|\boldsymbol{\zeta}_n^*\|_\infty \leq n\nu\epsilon_n^2
\end{aligned} \tag{49}$$

since $\|\mathbf{t}_n\|_2^2 = o(n\epsilon_n^2)$, $\|\boldsymbol{\mu}_n\|_2^2 = o(n\epsilon_n^2)$ and $\|\boldsymbol{\zeta}_n^*\|_\infty = O(1)$ and $n\epsilon_n^2 \rightarrow \infty$. Also,

$$\begin{aligned}
-\log \delta_n + \log \zeta_{jn} &= \log 8 + \log(K(n) + (p+1)\|\mathbf{t}_n\|_1) + \log \zeta_{jn} - \log \varepsilon \epsilon_n^2 \\
&\leq \log 8 + \log(K(n) + (p+1)\sqrt{K(n)}\|\mathbf{t}_n\|_2) + \log \zeta_{jn} - \log \varepsilon - 2 \log \epsilon_n \\
&\leq \log 8 + \log K(n) + \log(1 + \|\mathbf{t}_n\|_2) + \log \zeta_{jn} - \log \varepsilon - 2 \log \epsilon_n
\end{aligned}$$

where the second inequality is an outcome of Cauchy Schwartz and the third inequality follows

since $(p+1) \leq \sqrt{K(n)}$, $n \rightarrow \infty$. Therefore,

$$\begin{aligned}
\sum_{j=1}^{K(n)} -\frac{1}{2} \log \frac{2}{\pi} - \log \delta_n + \log \zeta_{jn} &\leq K(n) \log 8 + K(n) \log K(n) + K(n) \log(1 + \|\mathbf{t}_n\|_2) \\
&\quad + K(n) \log \|\boldsymbol{\zeta}_n\|_\infty - K(n) \log \varepsilon - 2K(n) \log \epsilon_n \leq n\nu\epsilon_n^2
\end{aligned} \tag{50}$$

where the last inequality follows since $K(n) \log n = o(n\epsilon_n^2)$, $\|\zeta_n\|_\infty = O(n)$, $\|\mathbf{t}_n\|_2 = o(\sqrt{n}\epsilon_n) = o(n)$ and $1/n\epsilon_n^2 = o(1)$ which implies $-2 \log \epsilon_n = o(\log n)$.

Combining (49) and (50) and replacing (48), the proof follows.

Proposition 7.13 *Let $q(\boldsymbol{\theta}_n) \sim \text{MVN}(\mathbf{t}_n, I_{K(n)}/\sqrt{n})$. Define*

$$h(\boldsymbol{\theta}_n) = \int_{\mathbf{x} \in [0,1]^p} \left(\sigma(\eta_0(\mathbf{x}))(\eta_0(\mathbf{x}) - \eta_{\boldsymbol{\theta}_n}(\mathbf{x})) + \log \frac{1 - \sigma(\eta_0(\mathbf{x}))}{1 - \sigma(\eta_{\boldsymbol{\theta}_n}(\mathbf{x}))} \right) d\mathbf{x}$$

Let $\|\eta_0 - \eta_{\mathbf{t}_n}\|_\infty \leq \epsilon \epsilon_n^2/4$ where $n\epsilon_n^2 \rightarrow \infty$. If $K(n) \log n = o(n\epsilon_n^2)$, $\|\mathbf{t}_n\|_2^2 = o(n\epsilon_n^2)$, then

$$\int h(\boldsymbol{\theta}_n) q(\boldsymbol{\theta}_n) d\boldsymbol{\theta}_n \leq \epsilon \epsilon_n^2$$

provided $\|\zeta_n\|_\infty = O(n)$, $\|\zeta_n^*\|_\infty = O(1)$ where $\zeta_n^* = 1/\zeta_n$.

Proof. Since $h(\boldsymbol{\theta}_n)$ is a KL-distance, $h(\boldsymbol{\theta}_n) > 0$. We shall thus establish an upper bound.

Let $A = \{\boldsymbol{\theta}_n : \bigcap_{j=1}^{K(n)} |\theta_{jn} - t_{jn}| \leq \sqrt{\epsilon \epsilon_n^2 / K(n)}\}$, then

$$\int h(\boldsymbol{\theta}_n) q(\boldsymbol{\theta}_n) d\boldsymbol{\theta}_n = \int_A h(\boldsymbol{\theta}_n) q(\boldsymbol{\theta}_n) d\boldsymbol{\theta}_n + \int_{A^c} h(\boldsymbol{\theta}_n) q(\boldsymbol{\theta}_n) d\boldsymbol{\theta}_n \quad (51)$$

By Taylor expansion, the first term is equal to

$$\begin{aligned} &= \int_A \left(h(\mathbf{t}_n) + (\boldsymbol{\theta}_n - \mathbf{t}_n)^\top \nabla h(\mathbf{t}_n) + \frac{1}{2} (\boldsymbol{\theta}_n - \mathbf{t}_n)^\top \nabla^2 h(\mathbf{t}_n) (\boldsymbol{\theta}_n - \mathbf{t}_n) \right) q(\boldsymbol{\theta}_n) d\boldsymbol{\theta}_n + o(\epsilon \epsilon_n^2) \\ &\leq |h(\mathbf{t}_n)| + \frac{1}{2} \int (\boldsymbol{\theta}_n - \mathbf{t}_n)^\top \nabla^2 h(\mathbf{t}_n) (\boldsymbol{\theta}_n - \mathbf{t}_n) q(\boldsymbol{\theta}_n) d\boldsymbol{\theta}_n + o(\epsilon \epsilon_n^2) \\ &= \frac{\epsilon \epsilon_n^2}{2} + \frac{1}{2} \int (\boldsymbol{\theta}_n - \mathbf{t}_n)^\top \nabla^2 h(\mathbf{t}_n) (\boldsymbol{\theta}_n - \mathbf{t}_n) q(\boldsymbol{\theta}_n) d\boldsymbol{\theta}_n + o(\epsilon \epsilon_n^2) \\ &= \frac{\epsilon \epsilon_n^2}{2} + o(\epsilon \epsilon_n^2) \leq \frac{3\epsilon \epsilon_n^2}{4} \end{aligned} \quad (52)$$

where the second step holds because $q(\boldsymbol{\theta}_n)$ is symmetric around \mathbf{t}_n . The third step holds in view of lemma 7.8 and the fact that \mathbf{t}_n satisfies $\|\eta_{\mathbf{t}_n} - \eta_0\|_\infty \leq \epsilon \epsilon_n^2/4$.

The final step is justified next. With $J = \{1, \dots, K(n)\}$, let $\nabla^2 h(\mathbf{t}_n) = ((b_{jj'}))_{j \in J, j' \in J}$

$$\int_A (\boldsymbol{\theta}_n - \mathbf{t}_n)^\top \nabla^2 h(\mathbf{t}_n) (\boldsymbol{\theta}_n - \mathbf{t}_n) q(\boldsymbol{\theta}_n) d\boldsymbol{\theta}_n = \sum_{j=1}^{K(n)} b_{jj} \int_{|\theta_{jn} - t_{jn}| \leq \sqrt{\epsilon \epsilon_n^2 / K(n)}} (\theta_{jn} - t_{jn})^2 q(\theta_{jn}) d\theta_{jn}$$

where the cross covariance terms disappear since θ_{jn} 's are independent and $q(\boldsymbol{\theta}_n)$ is symmetric around \mathbf{t}_n . Thus,

$$\int_A (\boldsymbol{\theta}_n - \mathbf{t}_n)^\top \nabla^2 h(\mathbf{t}_n) (\boldsymbol{\theta}_n - \mathbf{t}_n) q(\boldsymbol{\theta}_n) d\boldsymbol{\theta}_n \leq \sum_{j=1}^{K(n)} |b_{jj}| \int (\theta_{jn} - t_{jn})^2 q(\theta_{jn}) d\theta_{jn} = \frac{1}{n} \sum_{j=1}^{K(n)} |b_{jj}|$$

Using lemma 7.9, we get

$$\begin{aligned} \int_A (\boldsymbol{\theta}_n - \mathbf{t}_n)^\top \nabla^2 h(\mathbf{t}_n) (\boldsymbol{\theta}_n - \mathbf{t}_n) q(\boldsymbol{\theta}_n) d\boldsymbol{\theta}_n &\leq \frac{1}{n} ((2(p+1) + 1)(K(n) + 1) + 2(p+1) \|\mathbf{t}_n\|_2^2) \\ &= o(\varepsilon \epsilon_n^2) \end{aligned} \quad (53)$$

where the last equality holds since $K(n) \log n = o(n\epsilon_n^2)$ and $\|\mathbf{t}_n\|_2^2 = o(\varepsilon \epsilon_n^2)$. We next handle the second term in (51). Using lemma 7.8, note that

$$\begin{aligned} \int_{A^c} h(\boldsymbol{\theta}_n) q(\boldsymbol{\theta}_n) d\boldsymbol{\theta}_n &\leq 2 \int_{A^c} \left(\int_{\mathbf{x} \in [0,1]^p} |\eta_0(\mathbf{x}) - \eta_{\boldsymbol{\theta}_n}(\mathbf{x})| d\mathbf{x} \right) q(\boldsymbol{\theta}_n) d\boldsymbol{\theta}_n \\ &\leq 2 \int_{\mathbf{x} \in [0,1]^p} |\eta_0(\mathbf{x})| d\mathbf{x} \int_{A^c} q(\boldsymbol{\theta}_n) d\boldsymbol{\theta}_n + 2 \int_{A^c} \int_{\mathbf{x} \in [0,1]^p} |\eta_{\boldsymbol{\theta}_n}(\mathbf{x})| d\mathbf{x} q(\boldsymbol{\theta}_n) d\boldsymbol{\theta}_n \end{aligned}$$

First, note using $|\psi(u)| \leq 1$, we get $|\eta_{\boldsymbol{\theta}_n}(\mathbf{x})| \leq \sum_{j=0}^{k_n} |\beta_j^{\mathbf{t}}|$. Thus, $|\eta_{\boldsymbol{\theta}_n}(\mathbf{x})| \leq \sum_{j=0}^{k_n} |\beta_j^{\mathbf{t}}| + \sum_{j=0}^{k_n} |\beta_j - \beta_j^{\mathbf{t}}|$ which implies

$$\frac{1}{2} \int_{A^c} h(\boldsymbol{\theta}_n) q(\boldsymbol{\theta}_n) d\boldsymbol{\theta}_n \leq Q(A^c) \left(\int_{\mathbf{x} \in [0,1]^p} |\eta_0(\mathbf{x})| d\mathbf{x} + \sum_{j=0}^{k_n} |\beta_j^{\mathbf{t}}| \right) + \int_{A^c} \left(\sum_{j=0}^{k_n} |\beta_j - \beta_j^{\mathbf{t}}| \right) q(\boldsymbol{\theta}_n) d\boldsymbol{\theta}_n \quad (54)$$

First note that $A^c = \cup_{j=1}^{K(n)} A_j^c$ where $A_j = \{|\theta_{jn} - t_{jn}| \leq \sqrt{\varepsilon \epsilon_n^2 / K_n}\}$. Therefore,

$$\begin{aligned} Q(A^c) &= Q(\cup_{j=1}^{K(n)} A_j^c) \leq \sum_{j=1}^{K(n)} Q(A_j^c) = \sum_{j=1}^{K(n)} \int_{|\theta_{jn} - t_{jn}| > \sqrt{\varepsilon \epsilon_n^2 / K(n)}} q(\theta_{jn}) d\theta_{jn} \\ &= 2K(n) \left(1 - \Phi \left(\sqrt{\frac{n\varepsilon \epsilon_n^2}{K(n)}} \right) \right) \end{aligned} \quad (55)$$

Using (55) in the first term of (54), we get

$$\begin{aligned}
Q(A^c) \left(\int_{\mathbf{x} \in [0,1]^p} |\eta_0(\mathbf{x})| d\mathbf{x} + \sum_{j=0}^{k_n} |\beta_j^t| \right) &\lesssim 2(\|\eta_0\|_1 + \|\mathbf{t}_n\|_1) K(n) \left(1 - \Phi \left(\sqrt{\frac{n\varepsilon\epsilon_n^2}{K(n)}} \right) \right) \\
&\stackrel{\text{Cauchy Schwartz}}{\leq} 2(\|\eta_0\|_1 + \sqrt{K(n)}\|\mathbf{t}_n\|_2) K(n) \left(1 - \Phi \left(\sqrt{\frac{n\varepsilon\epsilon_n^2}{K(n)}} \right) \right) \\
&\leq 4n\epsilon_n^2 K(n) \left(1 - \Phi \left(\sqrt{\frac{n\varepsilon\epsilon_n^2}{K(n)}} \right) \right) \\
&\leq 4nK(n) \left(1 - \Phi \left(\sqrt{\frac{n\varepsilon\epsilon_n^2}{K(n)}} \right) \right) \\
&\stackrel{\text{Mill's ratio}}{\sim} 4nK(n) \sqrt{\frac{K(n)}{n\varepsilon\epsilon_n^2}} e^{-\frac{n\varepsilon\epsilon_n^2}{2K(n)}} \\
&\leq 4nK(n) e^{-\frac{n\varepsilon\epsilon_n^2}{2K(n)}} = o(\varepsilon\epsilon_n^2) \tag{56}
\end{aligned}$$

where the third step holds because $\|\mathbf{t}_n\|_2 = o(\sqrt{n\epsilon_n^2})$ and $\sqrt{K(n)} = o(\sqrt{n\epsilon_n^2})$ and $\|\eta_0\|_1$ is fixed and fourth step holds because $\epsilon_n^2 \leq 1$. The last equality in the above step holds because

$$-\frac{n\epsilon_n^2}{K(n)} + \log K(n) + \log n - \log \varepsilon \leq -\frac{n\epsilon_n^2}{K(n)} + 3 \log n = -\log n \left(\frac{n\epsilon_n^2}{K(n) \log n} - 3 \right) \rightarrow -\infty$$

where the first inequality holds since $K(n) \leq n$.

For the second term in (54), let $A_{\beta_j} = \{|\beta_j - \beta_j^t| > \sqrt{\varepsilon\epsilon_n^2/K_n}\}$

$$\begin{aligned}
\int_{A^c} \left(\sum_{j=0}^{k_n} |\beta_j - \beta_j^t| \right) q(\boldsymbol{\theta}_n) d\boldsymbol{\theta}_n &= \sum_{j=0}^{k_n} \int_{A^c} |\beta_j - \beta_j^t| q(\boldsymbol{\theta}_n) d\boldsymbol{\theta}_n \\
&= \sum_{j=0}^{k_n} \left(\int_{A^c \cap A_{\theta_j}} |\beta_j - \beta_j^t| q(\boldsymbol{\theta}_n) d\boldsymbol{\theta}_n + \int_{A^c \cap A_{\beta_j}^c} |\beta_j - \beta_j^t| q(\boldsymbol{\theta}_n) d\boldsymbol{\theta}_n \right) \\
&\leq \sum_{j=0}^{k_n} \left(\int_{A_{\beta_j}} |\beta_j - \beta_j^t| q(\beta_j) d\beta_j + E_{q(\beta_j)} |\beta_j - \beta_j^t| \int_{\tilde{A}^c} q(\tilde{\boldsymbol{\theta}}_n) d\tilde{\boldsymbol{\theta}}_n \right) \tag{57}
\end{aligned}$$

where $\tilde{\boldsymbol{\theta}}_n$ has all coordinates of $\boldsymbol{\theta}_n$ except β_j and \tilde{A}^c is the union of all A_j^c except $A_{\beta_j}^c$.

$$\begin{aligned}
\sum_{j=0}^{k_n} \int_{A_{\beta_j}} |\theta_j - \beta_j^t| q(\beta_j) d\beta_j &= \sum_{j=0}^{k_n} \int_{|\beta_j - \beta_j^t| > \sqrt{\varepsilon \epsilon_n^2 / K(n)}} \sqrt{\frac{n}{2\pi}} |\beta_j - \beta_j^t| e^{-\frac{n}{2} |\beta_j - \beta_j^t|^2} d\beta_j \\
&= \frac{2}{\sqrt{n}} \sum_{j=0}^{k_n} \int_{\sqrt{n\varepsilon \epsilon_n^2 / K(n)}}^{\infty} \frac{u}{\sqrt{2\pi}} e^{-\frac{1}{2} u^2} du \\
&\leq 2K(n) e^{-\frac{n\varepsilon \epsilon_n^2}{2K(n)}} = o(\varepsilon \epsilon_n^2)
\end{aligned} \tag{58}$$

where the last equality is a consequence of (56).

Note $E_{q(\beta_j)} |\beta_j - \beta_j^t| = \sqrt{2/\pi} (1/n)$. Thus

$$\begin{aligned}
\sum_{j=0}^{k(n)} E_{q(\beta_j)} |\beta_j - \beta_j^t| \int_{\tilde{A}^c} q(\tilde{\boldsymbol{\theta}}_n) d\tilde{\boldsymbol{\theta}}_n &= \frac{2K(n)}{n\sqrt{2\pi}} Q(\tilde{A}^c) \\
&\sim \frac{2K(n)^2}{n\sqrt{2\pi}} \left(1 - \Phi \left(\sqrt{\frac{n\varepsilon}{K(n)}} \right) \right) \\
&\leq 2K(n) \left(1 - \Phi \left(\sqrt{\frac{n\varepsilon}{K(n)}} \right) \right) = o(\varepsilon \epsilon_n^2)
\end{aligned} \tag{59}$$

where the asymptotic equality in the second line follows from (55) because $Q(\tilde{A}^c)$ shares the same form as $Q(A^c)$. The third line follow from $K(n) \leq n$ and Relation (56).

Combining (56), (58), (59), we get

$$\int_{A^c} h(\boldsymbol{\theta}_n) q(\boldsymbol{\theta}_n) d\boldsymbol{\theta}_n = o(\varepsilon \epsilon_n^2) \leq \frac{\varepsilon \epsilon_n^2}{4} \tag{60}$$

This together with (52) completes the proof.

Proposition 7.14 *Let $n\epsilon_n^2 \rightarrow \infty$. Suppose $p(\boldsymbol{\theta}_n)$ satisfies (10) with $\|\boldsymbol{\mu}_n\|_2^2 = o(n\epsilon_n^2)$ and $\|\boldsymbol{\zeta}_n\|_\infty = O(n)$. Suppose for some $0 < b < 1$, $K(n) \log n = o(n^b \epsilon_n^2)$, then for $C_n = e^{n^b \epsilon_n^2 / K(n)}$ and \mathcal{F}_n as in (39), we have for any $\varepsilon > 0$,*

$$\int_{\boldsymbol{\theta}_n \in \mathcal{F}_n^c} p(\boldsymbol{\theta}_n) d\boldsymbol{\theta}_n \leq e^{-n\varepsilon \epsilon_n^2}$$

Proof: Let $\mathcal{F}_{jn} = \{\theta_{jn} : |\theta_{jn}| \leq C_n\}$

$$\mathcal{F}_n = \bigcap_{j=1}^{K(n)} \mathcal{F}_{jn} \implies \mathcal{F}_n^c = \bigcap_{j=1}^{K(n)} \mathcal{F}_{jn}^c$$

Note that

$$\begin{aligned}
\int_{\boldsymbol{\theta}_n \in \mathcal{F}_n^c} p(\boldsymbol{\theta}_n) d\boldsymbol{\theta}_n &\leq \sum_{j=1}^{K(n)} \int_{\mathcal{F}_{j_n}^c} \frac{1}{\sqrt{2\pi\zeta_{j_n}^2}} e^{-\frac{(\theta_{j_n} - \mu_{j_n})^2}{2\zeta_{j_n}^2}} d\theta_{j_n} \\
&= \sum_{j=1}^{K(n)} \int_{-\infty}^{-C_n} \frac{1}{\sqrt{2\pi\zeta_{j_n}^2}} e^{-\frac{(\theta_{j_n} - \mu_{j_n})^2}{2\zeta_{j_n}^2}} d\theta_{j_n} + \sum_{j=1}^{K(n)} \int_{C_n}^{\infty} \frac{1}{\sqrt{2\pi\zeta_{j_n}^2}} e^{-\frac{(\theta_{j_n} - \mu_{j_n})^2}{2\zeta_{j_n}^2}} d\theta_{j_n} \\
&= \sum_{j=1}^{K(n)} \left(1 - \Phi\left(\frac{C_n - \mu_{j_n}}{\zeta_{j_n}}\right) \right) + \sum_{j=1}^{K(n)} \left(1 - \Phi\left(\frac{C_n + \mu_{j_n}}{\zeta_{j_n}}\right) \right)
\end{aligned}$$

Since $\|\boldsymbol{\mu}_n\|_2^2 = o(n\epsilon_n^2) \implies \|\boldsymbol{\mu}_n\|_\infty = o(\sqrt{n}\epsilon_n)$. Also, $\|\boldsymbol{\zeta}_n\|_\infty = O(n)$, which implies for some $M > 0$,

$$\min\left(\frac{|C_n - \mu_{j_n}|}{\zeta_{j_n}}, \frac{|C_n + \mu_{j_n}|}{\zeta_{j_n}}\right) \geq \frac{C_n - \sqrt{n}}{nM} \geq e^{\log C_n - 2\log n} - \frac{1}{\sqrt{n}M} \sim e^{R_n \log n} \rightarrow \infty \quad (61)$$

where the last asymptotic relation holds because $1/\sqrt{n} \rightarrow 0$ and $R_n = (n^b \epsilon_n^2)/(K(n) \log n) - 2 \rightarrow \infty$ since $K(n) \log n = o(n^b \epsilon_n^2)$.

Thus, using Mill's ratio, we get:

$$\begin{aligned}
\int_{\boldsymbol{\theta}_n \in \mathcal{F}_n^c} p(\boldsymbol{\theta}_n) d\boldsymbol{\theta}_n &\lesssim \sum_{j=1}^{K(n)} \frac{\zeta_{j_n}}{C_n - \mu_{j_n}} e^{-\frac{(C_n - \mu_{j_n})^2}{2\zeta_{j_n}^2}} + \sum_{j=1}^{K(n)} \frac{\zeta_{j_n}}{C_n + \mu_{j_n}} e^{-\frac{(C_n + \mu_{j_n})^2}{2\zeta_{j_n}^2}} \\
&\leq 2K(n) e^{-\frac{(C_n - \sqrt{n})^2}{2n^2 M^2}} \lesssim e^{-\epsilon_n \epsilon_n^2}
\end{aligned}$$

where the last asymptotic inequality holds because

$$\frac{(C_n - \sqrt{n})^2}{2n^2 M^2} - \log 2K(n) \gtrsim \frac{1}{2} e^{2R_n \log n} - 2 \log n = n \left(\frac{e^{R_n}}{2} - \frac{2 \log n}{n} \right) \geq \epsilon_n \epsilon_n^2$$

In the above step, the first asymptotic inequality holds due to (61) and $K(n) \leq n$. The last inequality holds since $R_n \rightarrow \infty$ and $\log / n \rightarrow 0$.

Lemma 7.15 *Let $n\epsilon_n^2 \rightarrow \infty$. Suppose $K(n) \log n = o(n^b \epsilon_n^2)$ for some $0 < b < 1$ and $p(\boldsymbol{\theta}_n)$ satisfies (10) with $\|\boldsymbol{\mu}_n\|_2^2 = o(n\epsilon_n^2)$. Then for every $\varepsilon > 0$,*

$$\log \int_{\mathcal{U}_{\varepsilon \epsilon_n}^c} \frac{L(\boldsymbol{\theta}_n)}{L_0} p(\boldsymbol{\theta}_n) d\boldsymbol{\theta}_n \leq \log 2 - \varepsilon^2 n \epsilon_n^2 + o_{P_0^n}(1)$$

Proof. In this direction, we first show

$$P_0^n \left(\int_{\mathcal{U}_{\varepsilon\epsilon_n}^c} \frac{L(\boldsymbol{\theta}_n)}{L_0} p(\boldsymbol{\theta}_n) d\boldsymbol{\theta}_n > 2e^{-\varepsilon n \epsilon_n^2} \right) \rightarrow 0, \quad n \rightarrow \infty \quad (62)$$

$$\begin{aligned} & P_0^n \left(\int_{\mathcal{U}_{\varepsilon\epsilon_n}^c} \frac{L(\boldsymbol{\theta}_n)}{L_0} p(\boldsymbol{\theta}_n) d\boldsymbol{\theta}_n > 2e^{-\varepsilon^2 n \epsilon_n^2} \right) \\ & \leq P_0^n \left(\int_{\mathcal{U}_{\varepsilon\epsilon_n}^c \cap \mathcal{F}_n} \frac{L(\boldsymbol{\theta}_n)}{L_0} p(\boldsymbol{\theta}_n) d\boldsymbol{\theta}_n > e^{-\varepsilon^2 n \epsilon_n^2} \right) + P_0^n \left(\int_{\mathcal{F}_n^c} \frac{L(\boldsymbol{\theta}_n)}{L_0} p(\boldsymbol{\theta}_n) d\boldsymbol{\theta}_n > e^{-\varepsilon^2 n \epsilon_n^2} \right) \end{aligned}$$

Using lemma 7.10 with $\varepsilon = \varepsilon\epsilon_n$ and $C_n = e^{n^b \epsilon_n^2 / K(n)}$,

$$\begin{aligned} \int_{\varepsilon^2 \epsilon_n^2 / 8}^{\sqrt{2}\varepsilon\epsilon_n} H_{\square}(u, \tilde{\mathcal{F}}_n, \|\cdot\|_2) du & \lesssim \varepsilon\epsilon_n \sqrt{2K_n(\log K_n + 2\log C_n - \log \epsilon_n)} \\ & \leq \varepsilon\epsilon_n O(\max(\sqrt{K(n)\log K(n)}, \sqrt{K(n)\log C_n}, \sqrt{-\log \epsilon_n})) \\ & \leq \varepsilon\epsilon_n \max(o(\sqrt{n}\epsilon_n), O(\sqrt{n^b}\epsilon_n), O(\sqrt{\log n})) \leq \varepsilon^2 \epsilon_n^2 \sqrt{n} \end{aligned}$$

where $H_{\square}(u, \tilde{\mathcal{F}}_n, \|\cdot\|_2)$ is as in definition 7.2. The first inequality in the third step follows because $K(n) \leq n$ and $K(n) \log n = o(n\epsilon_n^2)$, $K(n) \log C_n = K(n)(n^b \epsilon_n^2 / K(n))$, $1/\epsilon_n^2 = o(n) \implies -\log \epsilon_n^2 \leq \log n$. The second inequality in the third step follows since $n^b/n = o(1)$ and $\log n = o(n\epsilon_n^2)$.

By theorem 1 in Wong and Shen (1995), for some constant $C > 0$, we have

$$\begin{aligned} P_0^n \left(\int_{\boldsymbol{\theta}_n \in \mathcal{U}_{\varepsilon\epsilon_n}^c \cap \mathcal{F}_n} \frac{L(\boldsymbol{\theta}_n)}{L_0} p(\boldsymbol{\theta}_n) d\boldsymbol{\theta}_n > e^{-\varepsilon^2 n \epsilon_n^2} \right) & \leq P_0^n \left(\sup_{\boldsymbol{\theta}_n \in \mathcal{U}_{\varepsilon\epsilon_n}^c \cap \mathcal{F}_n} \frac{L(\boldsymbol{\theta}_n)}{L_0} > e^{-\varepsilon^2 n \epsilon_n^2} \right) \\ & \leq 4 \exp(-C\varepsilon^2 n \epsilon_n^2) \rightarrow 0 \end{aligned} \quad (63)$$

Using proposition 7.14 with $\varepsilon = 2\varepsilon$, we have

$$\int_{\boldsymbol{\theta}_n \in \mathcal{F}_n^c} p(\boldsymbol{\theta}_n) d\boldsymbol{\theta}_n \leq e^{-2n\varepsilon^2 \epsilon_n^2}$$

Therefore, using lemma 7.6 with $\varepsilon = 2\varepsilon^2 \epsilon_n^2$ and $\tilde{\varepsilon} = \varepsilon^2 \epsilon_n^2$, we have

$$P_0^n \left(\int_{\mathcal{F}_n^c} \frac{L(\boldsymbol{\theta}_n)}{L_0} p(\boldsymbol{\theta}_n) d\boldsymbol{\theta}_n > e^{-\varepsilon^2 n \epsilon_n^2} \right) \leq e^{-\varepsilon^2 n \epsilon_n^2} \rightarrow 0. \quad (64)$$

Combining (63) and (64), (62) follows.

Finally, to complete the proof, let $\textcircled{1} = \log \int_{\mathcal{U}_{\varepsilon \epsilon_n}^c} (L(\boldsymbol{\theta}_n)/L_0) p(\boldsymbol{\theta}_n) d\boldsymbol{\theta}_n$.

$$\begin{aligned} \textcircled{1} &= \textcircled{1} I_{\{\textcircled{1} \leq \log 2 - \varepsilon^2 \epsilon_n^2\}} + \textcircled{1} I_{\{\textcircled{1} > \log 2 - \varepsilon^2 \epsilon_n^2\}} \leq \log 2 - \varepsilon^2 \epsilon_n^2 + \underbrace{\textcircled{1} I_{\{\textcircled{1} > \log 2 - \varepsilon^2 \epsilon_n^2\}}}_{\textcircled{2}} \\ &= \log 2 - \varepsilon^2 \epsilon_n^2 + o_{P_0^n}(1) \end{aligned}$$

where the last equality follows from (62) as below

$$P_0^n(|\textcircled{2}| > \nu) \leq P_0^n(I_{\{\textcircled{1} > \log 2 - \varepsilon^2 \epsilon_n^2\}} = 1) = P_0^n(\textcircled{1} > \log 2 - \varepsilon^2 \epsilon_n^2) \rightarrow 0.$$

Proposition 7.16 *Let $p(\boldsymbol{\theta}_n)$ satisfy (10) with $\|\boldsymbol{\zeta}_n\| = O(n)$ and $\|\boldsymbol{\zeta}_n^*\|_n = O(1)$, $\zeta_n^* = 1/\boldsymbol{\zeta}_n$.*

1. *If $K(n) \log n = o(n)$ and $\|\boldsymbol{\mu}_n\|_2^2 = o(n)$, then*

$$d_{\text{KL}}(\pi^*, \pi(\cdot | \mathbf{y}_n, \mathbf{X}_n)) = o_{P_0^n}(n) \quad (65)$$

2. *If $K(n) \log n = o(n \epsilon_n^2)$ and $\|\boldsymbol{\mu}_n\|_2^2 = o(n \epsilon_n^2)$ and there exists a neural network such $\|\eta_0 - \eta_{\mathbf{t}_n}\|_\infty = o(n \epsilon_n^2)$ and $\|\mathbf{t}_n\|_2^2 = o(n \epsilon_n^2)$, then*

$$d_{\text{KL}}(\pi^*, \pi(\cdot | \mathbf{y}_n, \mathbf{X}_n)) = o_{P_0^n}(n \epsilon_n^2) \quad (66)$$

Proof. For any $q \in \mathcal{Q}_n$.

$$\begin{aligned}
d_{\text{KL}}(q, \pi(\cdot | \mathbf{y}_n, \mathbf{X}_n)) &= \int q(\boldsymbol{\theta}_n) \log q(\boldsymbol{\theta}_n) d\boldsymbol{\theta}_n - \int q(\boldsymbol{\theta}_n) \log \pi(\boldsymbol{\theta}_n | \mathbf{y}_n, \mathbf{X}_n) d\boldsymbol{\theta}_n \\
&= \int q(\boldsymbol{\theta}_n) \log q(\boldsymbol{\theta}_n) d\boldsymbol{\theta}_n - \int q(\boldsymbol{\theta}_n) \log \frac{L(\boldsymbol{\theta}_n)p(\boldsymbol{\theta}_n)}{\int L(\boldsymbol{\theta}_n)p(\boldsymbol{\theta}_n) d\boldsymbol{\theta}_n} d\boldsymbol{\theta}_n \\
&= d_{\text{KL}}(q, p) - \int \log \frac{L(\boldsymbol{\theta}_n)}{L_0} q(\boldsymbol{\theta}_n) d\boldsymbol{\theta}_n + \log \int \frac{L(\boldsymbol{\theta}_n)}{L_0} p(\boldsymbol{\theta}_n) d\boldsymbol{\theta}_n \\
&\leq d_{\text{KL}}(q, p) + \left| \int \log \frac{L(\boldsymbol{\theta}_n)}{L_0} q(\boldsymbol{\theta}_n) d\boldsymbol{\theta}_n \right| + \left| \log \int \frac{L(\boldsymbol{\theta}_n)}{L_0} p(\boldsymbol{\theta}_n) d\boldsymbol{\theta}_n \right| \quad (67)
\end{aligned}$$

Since π^* satisfies minimizes the KL-distance to $\pi(\cdot | \mathbf{y}_n, \mathbf{X}_n)$ in the family \mathcal{Q}_n , therefore

$$P_0^n (d_{\text{KL}}(\pi^*, \pi(\cdot | \mathbf{y}_n, \mathbf{X}_n)) > \kappa) \leq P_0^n (d_{\text{KL}}(q, \pi(\cdot | \mathbf{y}_n, \mathbf{X}_n)) > \kappa) \quad (68)$$

for any $\kappa > 0$.

Proof of part 1. Note, $K(n) \log n = o(n)$, $\|\mu_n\|_2^2 = o(n)$, $\|\boldsymbol{\zeta}_n\|_\infty = O(n)$ and $\|\boldsymbol{\zeta}_n^*\|_\infty = O(1)$.

We take $q(\boldsymbol{\theta}_n) = \text{MVN}(\mathbf{t}_n, \mathbf{I}_{K(n)}/\sqrt{n})$ where \mathbf{t}_n is defined next.

For $N \geq 1$, let $\eta_{\mathbf{t}_N}$ be a neural satisfying $\|\eta_{\mathbf{t}_N} - \eta_0\|_\infty \leq \varepsilon/4$. The existence of such a neural network is always guaranteed by Hornik et al. (1989). Define \mathbf{t}_n as

$$\beta_j^{\mathbf{t}_n} = \begin{cases} \beta_j^{\mathbf{t}_N}, & j = 1, \dots, k_N \\ 0, & j = k_N + 1, \dots, k_n \end{cases} \quad \gamma_j^{\mathbf{t}_n} = \begin{cases} \gamma_j^{\mathbf{t}_N}, & j = 1, \dots, k_N \\ 0, & j = k_N + 1, \dots, k_n \end{cases}$$

The above choice guarantees $\|\eta_{\mathbf{t}_n} - \eta_0\|_\infty \leq \varepsilon/4$.

Step 1 (a): Using proposition 7.11, with $\epsilon_n = 1$, we get for any $\nu > 0$,

$$d_{\text{KL}}(q, p) \leq n\nu$$

where the above step follows $\|\mathbf{t}_n\|_2^2 = \|\mathbf{t}_N\|_2^2$ is bounded which implies $\|\mathbf{t}_n\|_2^2 = o(n)$. Therefore,

$$P_0^n (d_{\text{KL}}(q, p) > n\nu) = 0 \quad (69)$$

Step 1 (b): Next, note that

$$\begin{aligned} d_{\text{KL}}(\ell_0, \ell_{\boldsymbol{\theta}_n}) &= \int_{\mathbf{x} \in [0,1]^p} \left(\sigma(\eta_0(\mathbf{x})) \log \frac{\sigma(\eta_0(\mathbf{x}))}{\sigma(\eta_{\boldsymbol{\theta}_n}(\mathbf{x}))} + (1 - \sigma(\eta_0(\mathbf{x}))) \log \frac{1 - \sigma(\eta_0(\mathbf{x}))}{1 - \sigma(\eta_{\boldsymbol{\theta}_n}(\mathbf{x}))} \right) d\mathbf{x} \\ &= \int_{\mathbf{x} \in [0,1]^p} \left(\sigma(\eta_0(\mathbf{x}))(\sigma(\eta_{\boldsymbol{\theta}_n}(\mathbf{x})) - \sigma(\eta_0(\mathbf{x}))) + \log \frac{1 - \sigma(\eta_0(\mathbf{x}))}{1 - \sigma(\eta_{\boldsymbol{\theta}_n}(\mathbf{x}))} \right) d\mathbf{x} \end{aligned} \quad (70)$$

Since $\|\eta_0 - \eta_{\boldsymbol{\theta}_n}\|_\infty \leq \varepsilon/4$, using proposition 7.13 with $\epsilon_n = 1$ and $\varepsilon = \varepsilon$

$$\int d_{\text{KL}}(\ell_0, \ell_{\boldsymbol{\theta}_n}) q(\boldsymbol{\theta}_n) d\boldsymbol{\theta}_n \leq \varepsilon$$

where the above step follows since $\|\mathbf{t}_n\|_2^2 = \|\mathbf{t}_N\|_2^2$ is bounded which implies $\|\mathbf{t}_n\|_2^2 = o(n)$.

Therefore, by lemma 7.4,

$$P_0^n \left(\left| \int \log \frac{L(\boldsymbol{\theta}_n)}{L_0} q(\boldsymbol{\theta}_n) d\boldsymbol{\theta}_n \right| > n\nu \right) \leq \frac{\varepsilon}{\nu}. \quad (71)$$

Step 1 (c): Since $\|\eta_0 - \eta_{\boldsymbol{\theta}_n}\|_\infty \leq \varepsilon/4$, therefore using proposition 7.12 with $\epsilon_n = 1$ and $\nu = \varepsilon$ we get

$$\int_{\boldsymbol{\theta}_n \in \mathcal{N}_\varepsilon} p(\boldsymbol{\theta}_n) d\boldsymbol{\theta}_n \geq \exp(-n\varepsilon)$$

where the above step follows $\|\mathbf{t}_n\|_2^2 = \|\mathbf{t}_N\|_2^2$ is bounded which implies $\|\mathbf{t}_n\|_2^2 = o(n)$.

Therefore, using lemma 7.5, we get

$$P_0^n \left(\left| \log \int \frac{L(\boldsymbol{\theta}_n)}{L_0} p(\boldsymbol{\theta}_n) d\boldsymbol{\theta}_n \right| > n\nu \right) \leq \frac{2\varepsilon}{\nu} \quad (72)$$

Step 1 (d): From (68) and (67) we get

$$\begin{aligned} &P_0^n(d_{\text{KL}}(\pi^*, \pi(\cdot | \mathbf{y}_n, \mathbf{X}_n)) > 3n\nu) \leq P_0^n(d_{\text{KL}}(q, p) > n\nu) \\ &+ P_0^n \left(\left| \int \log \frac{L(\boldsymbol{\theta}_n)}{L_0} q(\boldsymbol{\theta}_n) d\boldsymbol{\theta}_n \right| > n\nu \right) + P_0^n \left(\left| \log \int \frac{L(\boldsymbol{\theta}_n)}{L_0} p(\boldsymbol{\theta}_n) d\boldsymbol{\theta}_n \right| > n\nu \right) \leq \frac{3\varepsilon}{\nu} \end{aligned} \quad (73)$$

where the last inequality is a consequence of (69), (71) and (72).

Since ε is arbitrary, taking $\varepsilon \rightarrow 0$ completes the proof.

Proof of part 2. Note, $K(n) \log n = o(n\varepsilon_n^2)$, $\|\mu_n\|_2^2 = o(n\varepsilon_n^2)$, $\|\boldsymbol{\zeta}_n\|_\infty = O(n)$ and $\|\boldsymbol{\zeta}_n^*\|_\infty =$

$O(1)$. We take $q(\boldsymbol{\theta}_n) = MVN(\mathbf{t}_n, \mathbf{I}_{K(n)}/\sqrt{n})$ where \mathbf{t}_n is defined next.

Let $\eta_{\mathbf{t}_n}$ be the neural satisfying

$$\|\eta_{\mathbf{t}_n} - \eta_0\|_\infty \leq \varepsilon \epsilon_n^2/4 \quad \|\mathbf{t}_n\|_2^2 = o(n\epsilon_n^2)$$

The existence of such a neural network is guaranteed since $\|\eta_{\mathbf{t}_n} - \eta_0\|_\infty = o(\epsilon_n^2)$.

Step 2 (a): Since $\|\mathbf{t}_n\|_2^2 = o(n\epsilon_n^2)$, by proposition 7.11,

$$d_{\text{KL}}(q, p) \leq n\epsilon_n^2\nu$$

which implies

$$P_0^n(d_{\text{KL}}(q, p) > \nu n\epsilon_n^2) = 0 \tag{74}$$

Step 2 (b): Since $\|\eta_{\mathbf{t}_n} - \eta_0\|_\infty \leq \varepsilon \epsilon_n^2/4$ and $\|\mathbf{t}_n\|_2^2 = o(n\epsilon_n^2)$, by proposition 7.13,

$$\int d_{\text{KL}}(\ell_0, \ell_{\boldsymbol{\theta}_n}) q(\boldsymbol{\theta}_n) d\boldsymbol{\theta}_n \leq \varepsilon \epsilon_n^2$$

Therefore, by lemma 7.4,

$$P_0^n \left(\left| \int \log \frac{L(\boldsymbol{\theta}_n)}{L_0} q(\boldsymbol{\theta}_n) d\boldsymbol{\theta}_n \right| > \nu n\epsilon_n^2 \right) \leq \frac{\varepsilon}{\nu}. \tag{75}$$

Step 2 (c): Since $\|\eta_0 - \eta_{\mathbf{t}_n}\|_\infty \leq \varepsilon \epsilon_n^2/4$ and $\|\mathbf{t}_n\|_2^2 = o(n\epsilon_n^2)$, by proposition 7.12,

$$\int_{\boldsymbol{\theta}_n \in \mathcal{N}_{\varepsilon \epsilon_n^2}} p(\boldsymbol{\theta}_n) d\boldsymbol{\theta}_n \geq \exp(-\varepsilon n\epsilon_n^2)$$

Therefore, using lemma 7.5, we get

$$P_0^n \left(\left| \log \int \frac{L(\boldsymbol{\theta}_n)}{L_0} q(\boldsymbol{\theta}_n) d\boldsymbol{\theta}_n \right| > \nu n\epsilon_n^2 \right) \leq \frac{2\varepsilon}{\nu} \tag{76}$$

Step 2 (d): From (68) and (67) we get

$$\begin{aligned} & P_0^n(d_{\text{KL}}(\pi^*, \pi(\cdot | \mathbf{y}_n, \mathbf{X}_n)) > 3\nu n\epsilon_n^2) \leq P_0^n(d_{\text{KL}}(q, p) > \nu n\epsilon_n^2) \\ & + P_0^n \left(\left| \int \log \frac{L(\boldsymbol{\theta}_n)}{L_0} q(\boldsymbol{\theta}_n) d\boldsymbol{\theta}_n \right| > \nu n\epsilon_n^2 \right) + P_0^n \left(\left| \log \int \frac{L(\boldsymbol{\theta}_n)}{L_0} p(\boldsymbol{\theta}_n) d\boldsymbol{\theta}_n \right| > \nu n\epsilon_n^2 \right) \leq \frac{3\varepsilon}{\nu} \end{aligned} \tag{77}$$

where the last inequality is a consequence of (74), (75) and (76).

Since ε is arbitrary, taking $\varepsilon \rightarrow 0$ completes the proof.

7.4 Theorems and Corollaries

Let \mathcal{U}_ε be as in (35). Let $\pi(\cdot|\mathbf{y}_n, \mathbf{X}_n)$ and π^* be the posterior and the variational posterior as in (11) and (13) respectively.

Proof of Theorem 4.1:

We assume Relation (38) holds with A_n and B_n are same as in (37).

By assumptions (A1) and (A2), the prior parameters satisfy

$$\|\boldsymbol{\mu}_n\|_2^2 = o(n), \quad \|\boldsymbol{\zeta}_n\|_\infty = O(n), \quad \|\boldsymbol{\zeta}_n^*\|_\infty = O(1), \quad \boldsymbol{\zeta}_n^* = 1/\boldsymbol{\zeta}_n.$$

Note $K(n) \sim k_n \sim n^a$, $0 < a < 1$ which implies $K(n) \log n = o(n)$.

By proposition 7.16 part 1.,

$$d_{\text{KL}}(\pi^*, \pi(\cdot|\mathbf{y}_n, \mathbf{X}_n)) = o_{P_0^n}(n). \quad (78)$$

By step 1 (c) in the proof of proposition 7.16

$$B_n = o_{P_0^n}(n) \quad (79)$$

Since, $K(n) \sim n^a$, $K(n) \log n = o(n^b)$, $a < b < 1$. Using proposition 7.15 with $\epsilon_n = 1$,

$$-\pi^*(\mathcal{U}_\varepsilon^c)A_n \geq n\varepsilon^2\pi^*(\mathcal{U}_\varepsilon^c) - \log 2 + o_{P_0^n}(1) = n\varepsilon^2\pi^*(\mathcal{U}_\varepsilon^c) + O_{P_0^n}(1) \quad (80)$$

Thus, using (78), (79) and (80) in (38), we get

$$n\varepsilon^2\pi^*(\mathcal{U}_\varepsilon^c) + O_{P_0^n}(1) \leq o_{P_0^n}(n) + o_{P_0^n}(n) \implies \pi^*(\mathcal{U}_\varepsilon^c) = o_{P_0^n}(1)$$

Proof of Theorem 4.2:

We assume Relation (38) holds with A_n and B_n are same as in (37).

Let $k_n \sim n^a$ and $\epsilon_n^2 \sim n^{-\delta}$, $0 < \delta < 1 - a$. This implies $K(n) \log n = o(n\epsilon_n^2)$.

By assumptions (A1) and (A4), the prior parameters satisfy

$$\|\boldsymbol{\mu}_n\|_2^2 = o(n\epsilon_n^2), \quad \|\boldsymbol{\zeta}_n\|_\infty = O(n), \quad \|\boldsymbol{\zeta}_n^*\|_\infty = O(1), \quad \boldsymbol{\zeta}_n^* = 1/\boldsymbol{\zeta}_n.$$

Also by assumption (A3),

$$\|\eta_0 - \eta_{\mathbf{t}_n}\|_\infty = o(\epsilon_n^2), \quad \|\mathbf{t}_n\|_2^2 = o(n\epsilon_n^2)$$

By proposition 7.16 part 2.,

$$d_{\text{KL}}(\pi^*, \pi(\cdot | \mathbf{y}_n, \mathbf{X}_n)) = o_{P_0^n}(n\epsilon_n^2). \quad (81)$$

By step 2 (c) in the proof of proposition 7.16

$$B_n = o_{P_0^n}(n\epsilon_n^2) \quad (82)$$

Since $K(n) \sim n^a$, $K(n) \log n = o(n^b \epsilon_n^2)$, $a + \delta < b < 1$. Using proposition 7.15, it follows that

$$-\pi^*(\mathcal{U}_{\epsilon\epsilon_n}^c)A_n \geq \varepsilon^2 n \epsilon_n^2 \pi^*(\mathcal{U}_{\epsilon\epsilon_n}^c) - \log 2 + o_{P_0^n}(1) = \varepsilon^2 n \epsilon_n^2 \pi^*(\mathcal{U}_{\epsilon\epsilon_n}^c) + O_{P_0^n}(1) \quad (83)$$

Thus, using (81), (82) and (83) in (38), we get

$$n\varepsilon^2 \epsilon_n^2 \pi^*(\mathcal{U}_{\epsilon\epsilon_n}^c) + O_{P_0^n}(1) \leq o_{P_0^n}(n\epsilon_n^2) + o_{P_0^n}(n\epsilon_n^2) \implies \pi^*(\mathcal{U}_{\epsilon\epsilon_n}^c) = o_{P_0^n}(1)$$

Proof of Corollary 1.

Let $\hat{\ell}_n(y, \mathbf{x}) = \int \ell_{\boldsymbol{\theta}_n}(y, \mathbf{x}) \pi^*(\boldsymbol{\theta}_n) d\boldsymbol{\theta}_n$.

$$\begin{aligned} d_{\text{H}}(\hat{\ell}_n, \ell_0) &= d_{\text{H}}\left(\int \ell_{\boldsymbol{\theta}_n} \pi^*(\boldsymbol{\theta}_n) d\boldsymbol{\theta}_n, \ell_0\right) \\ &\leq \int d_{\text{H}}(\ell_{\boldsymbol{\theta}_n}, \ell_0) \pi^*(\boldsymbol{\theta}_n) d\boldsymbol{\theta}_n \quad \text{Jensen's inequality} \\ &= \int_{\mathcal{U}_\varepsilon} d_{\text{H}}(\ell_{\boldsymbol{\theta}_n}, \ell_0) \pi^*(\boldsymbol{\theta}_n) d\boldsymbol{\theta}_n + \int_{\mathcal{U}_\varepsilon^c} d_{\text{H}}(\ell_{\boldsymbol{\theta}_n}, \ell_0) \pi^*(\boldsymbol{\theta}_n) d\boldsymbol{\theta}_n \\ &\leq \varepsilon + o_{P_0^n}(1) \end{aligned}$$

Taking $\varepsilon \rightarrow 0$, we get $d_{\text{H}}(\hat{\ell}_n, \ell_0) = o_{P_0^n}(1)$.

By (31), note that $\hat{\eta}(y, \mathbf{x}) = \sigma^{-1} \hat{\ell}_n(y, \mathbf{x}) = \log \frac{\hat{\ell}_n(1, \mathbf{x})}{\hat{\ell}_n(0, \mathbf{x})}$, then

$$\begin{aligned}
2d_{\text{H}}^2(\hat{\ell}_n, \ell_0) &= \int_{\mathbf{x} \in [0,1]^p} \sum_{y \in \{0,1\}} \left(\sqrt{\hat{\ell}_n(y, \mathbf{x})} - \sqrt{\ell_0(y, \mathbf{x})} \right)^2 d\mathbf{x} \\
&= 2 - 2 \int_{\mathbf{x} \in [0,1]^p} \sum_{y \in \{0,1\}} \sqrt{\hat{\ell}_n(y, \mathbf{x}) \ell_0(y, \mathbf{x})} d\mathbf{x} \\
&= 2 - 2 \int_{\mathbf{x} \in [0,1]^p} \sum_{y \in \{0,1\}} e^{\left\{ \frac{1}{2} (y \hat{\eta}(\mathbf{x}) - \log(1 + e^{\hat{\eta}(\mathbf{x})}) + y \eta_0(\mathbf{x}) - \log(1 + e^{\eta_0(\mathbf{x})})) \right\}} d\mathbf{x} \\
&= 2 - 2 \int_{\mathbf{x} \in [0,1]^p} \left(\sqrt{\sigma(\eta_0(\mathbf{x})) \sigma(\hat{\eta}(\mathbf{x}))} + \sqrt{(1 - \sigma(\eta_0(\mathbf{x}))) (1 - \sigma(\hat{\eta}(\mathbf{x})))} \right) d\mathbf{x} \\
&\geq 2 - 2 \int_{\mathbf{x} \in [0,1]^p} \sqrt{1 - (\sqrt{\sigma(\eta_0(\mathbf{x}))} - \sqrt{\sigma(\hat{\eta}(\mathbf{x}))})^2} d\mathbf{x} \\
&\geq \int_{\mathbf{x} \in [0,1]^p} (\sqrt{\sigma(\eta_0(\mathbf{x}))} - \sqrt{\sigma(\hat{\eta}(\mathbf{x}))})^2 d\mathbf{x} \\
&\geq \frac{1}{4} \int_{\mathbf{x} \in [0,1]^p} (\sigma(\eta_0(\mathbf{x})) - \sigma(\hat{\eta}(\mathbf{x})))^2 d\mathbf{x} \tag{84}
\end{aligned}$$

In the above equation, the sixth and the seventh step hold because $\sqrt{1-x} \leq 1-x/2$ and $|p_1 - p_2| \leq |\sqrt{p_1} + \sqrt{p_2}| |\sqrt{p_1} - \sqrt{p_2}| \leq 2|\sqrt{p_1} - \sqrt{p_2}|$ respectively. The fifth step holds because

$$\begin{aligned}
\left(\sqrt{p_1 p_2} + \sqrt{(1-p_1)(1-p_2)} \right)^2 &= p_1 p_2 + 1 - p_1 - p_2 + \sqrt{p_1 p_2 (1-p_1)(1-p_2)} \\
&\leq \sqrt{p_1 p_2} + 1 - p_1 - p_2 + \sqrt{p_1 p_2} = 1 - (\sqrt{p_1} - \sqrt{p_2})^2
\end{aligned}$$

By (84) and Cauchy Schwartz inequality,

$$\begin{aligned}
\int_{\mathbf{x} \in [0,1]^p} |\sigma(\eta_0(\mathbf{x})) - \sigma(\hat{\eta}(\mathbf{x}))| d\mathbf{x} &\leq \left(\int_{\mathbf{x} \in [0,1]^p} (\sigma(\eta_0(\mathbf{x})) - \sigma(\hat{\eta}(\mathbf{x})))^2 d\mathbf{x} \right)^{1/2} \\
&\leq 2\sqrt{2} d_{\text{H}}(\hat{\ell}_n, \ell_0) = o_{P_0^n}(1) \tag{85}
\end{aligned}$$

The proof follows in lieu of (41).

Proof of Corollary 2.

We assume Relation (38) holds with A_n and B_n are same as in (37).

Let $k_n \sim n^a$ and $\epsilon_n^2 \sim n^{-\delta}$, $0 < \delta < 1 - a$. This implies $K(n) \log n = o(n \epsilon_n^2)$.

Also $K(n) \log n = o(n^b \epsilon_n^2)$, $a + \delta < b < 1$. This implies $K(n) \log n = o(n^b (\epsilon_n^2)^\kappa)$, $0 \leq \kappa \leq 1$.

Thus, using proposition 7.15 with $\epsilon_n = \epsilon_n^k$, we get

$$-\pi^*(\mathcal{U}_{\epsilon_n^k}^c)A_n \geq \varepsilon^2 n \epsilon_n^{2\kappa} \pi^*(\mathcal{U}_{\epsilon_n^k}^c) - \log 2 + o_{P_0^n}(1) = \varepsilon^2 n \epsilon_n^{2\kappa} \pi^*(\mathcal{U}_{\epsilon_n^k}^c) + O_{P_0^n}(1) \quad (86)$$

This together with (81), (82) and (38) implies

$$\pi^*(\mathcal{U}_{\epsilon_n^k}^c) = o_{P_0^n}(\epsilon_n^{2-2\kappa})$$

Let $\hat{\ell}_n(y, \mathbf{x}) = \int \ell_{\boldsymbol{\theta}_n}(y, \mathbf{x}) \pi^*(\boldsymbol{\theta}_n) d\boldsymbol{\theta}_n$.

$$\begin{aligned} d_H(\hat{\ell}_n, \ell_0) &\leq \int_{\mathcal{U}_{\epsilon_n^k}^c} d_H(\ell_{\boldsymbol{\theta}_n}, \ell_0) \pi^*(\boldsymbol{\theta}_n) d\boldsymbol{\theta}_n + \int_{\mathcal{U}_{\epsilon_n^k}^c} d_H(\ell_{\boldsymbol{\theta}_n}, \ell_0) \pi^*(\boldsymbol{\theta}_n) d\boldsymbol{\theta}_n \\ &\leq \varepsilon \epsilon_n^k + o_{P_0^n}(\epsilon_n^{2-2\kappa}) \end{aligned}$$

Dividing by ϵ_n^k on both sides we get

$$\frac{1}{\epsilon_n^k} d_H(\hat{\ell}_n, \ell_0) = o_{P_0^n}(\epsilon_n^{2-3\kappa}) + o_{P_0^n}(1) = o_{P_0^n}(1), \quad 0 \leq \kappa \leq 2/3.$$

By (85), for every $0 \leq \kappa \leq 2/3$,

$$\frac{1}{\epsilon_n^k} \int_{\mathbf{x} \in U_{[0,1]^p}} |\sigma(\eta_0(\mathbf{x})) - \sigma(\hat{\eta}(\mathbf{x}))| d\mathbf{x} \leq \frac{1}{\epsilon_n^k} 2\sqrt{2} d_H(\hat{\ell}_n, \ell_0) = o_{P_0^n}(1).$$

The proof follows in lieu of (41).

(C) Consistency of the true posterior.

Theorem 7.17 *Suppose $k_n \sim n^a$, $0 < a < 1$. Additionally, the prior parameters in (10) satisfies assumption (A1) and (A2). Then,*

1.

$$P_0^n \left(\pi(\mathcal{U}_\varepsilon^c | \mathbf{y}_n, \mathbf{X}_n) \leq 2e^{-n\varepsilon^2/2} \right) \rightarrow 1, n \rightarrow \infty$$

2.

$$P_0^n (|R(\hat{C}) - R(C^{\text{Bayes}})| \leq 4\sqrt{2}\varepsilon) \rightarrow 1, n \rightarrow \infty$$

where R is the risk defined in (2).

Proof. From (11), note that

$$\begin{aligned}\pi(\mathcal{U}_\varepsilon^c | \mathbf{y}_n, \mathbf{X}_n) &= \frac{\int_{\mathcal{U}_\varepsilon^c} L(\boldsymbol{\theta}_n) p(\boldsymbol{\theta}_n) d\boldsymbol{\theta}_n}{\int L(\boldsymbol{\theta}_n) p(\boldsymbol{\theta}_n) d\boldsymbol{\theta}_n} \\ &= \frac{\int_{\mathcal{U}_\varepsilon^c} (L(\boldsymbol{\theta}_n)/L_0) p(\boldsymbol{\theta}_n) d\boldsymbol{\theta}_n}{\int (L(\boldsymbol{\theta}_n)/L_0) p(\boldsymbol{\theta}_n) d\boldsymbol{\theta}_n}\end{aligned}\quad (87)$$

By assumptions (A1) and (A2), the prior parameters satisfy

$$\|\boldsymbol{\mu}_n\|_2^2 = o(n), \quad \|\boldsymbol{\zeta}_n\|_\infty = O(n), \quad \|\boldsymbol{\zeta}_n^*\|_\infty = O(1), \quad \boldsymbol{\zeta}_n^* = 1/\boldsymbol{\zeta}_n.$$

Note $K(n) \sim k_n \sim n^a$, $0 < a < 1$ which implies $K(n) \log n = o(n)$. Thus, the conditions of proposition 7.12 hold with $\epsilon_n = 1$.

$$P_0^n \left(\int \frac{L(\boldsymbol{\theta}_n)}{L_0} p(\boldsymbol{\theta}_n) d\boldsymbol{\theta}_n \leq e^{-n\nu} \right) \leq P_0^n \left(\left| \log \int \frac{L(\boldsymbol{\theta}_n)}{L_0} p(\boldsymbol{\theta}_n) d\boldsymbol{\theta}_n \right| > n\nu \right) \rightarrow 0, n \rightarrow \infty \quad (88)$$

where the above convergence follows from (72) in step 1 (c) in the proof of proposition 7.16.

Also, since $K(n) \log n = o(n^b)$, $a < b < 1$. Thus, conditions of proposition 7.15 hold with $\epsilon_n = 1$.

$$P_0^n \left(\int_{\mathcal{U}_\varepsilon} \frac{L(\boldsymbol{\theta}_n)}{L_0} p(\boldsymbol{\theta}_n) d\boldsymbol{\theta}_n \geq 2e^{-n\varepsilon^2} \right) \rightarrow 0, n \rightarrow \infty \quad (89)$$

where the last equality follows from (62) with $\epsilon_n = 1$ in the proof of Proposition 7.15.

Using (88) and (89) with (87), we get

$$P_0^n \left(\pi(\mathcal{U}_\varepsilon^c | \mathbf{y}_n, \mathbf{X}_n) \geq 2e^{-n(\varepsilon^2 - \nu)} \right) \rightarrow 0, n \rightarrow \infty$$

Take $\nu = \varepsilon^2/2$ to complete the proof.

Let $\hat{\ell}_n(y, \mathbf{x}) = \int \ell_{\boldsymbol{\theta}_n}(y, \mathbf{x}) \pi(\boldsymbol{\theta}_n | \mathbf{y}_n, \mathbf{X}_n) d\boldsymbol{\theta}_n$. Mimicking the steps in the proof of corollary

4.3, we get

$$\begin{aligned}
d_{\text{H}}(\hat{\ell}_n, \ell_0) &= d_{\text{H}}\left(\int \ell_{\boldsymbol{\theta}_n} \pi(\boldsymbol{\theta}_n | \mathbf{y}_n, \mathbf{X}_n) d\boldsymbol{\theta}_n, \ell_0\right) \\
&\leq \int d_{\text{H}}(\ell_{\boldsymbol{\theta}_n}, \ell_0) \pi(\boldsymbol{\theta}_n | \mathbf{y}_n, \mathbf{X}_n) d\boldsymbol{\theta}_n \quad \text{Jensen's inequality} \\
&= \int_{\mathcal{U}_\varepsilon} d_{\text{H}}(\ell_{\boldsymbol{\theta}_n}, \ell_0) \pi(\boldsymbol{\theta}_n | \mathbf{y}_n, \mathbf{X}_n) d\boldsymbol{\theta}_n + \int_{\mathcal{U}_\varepsilon^c} d_{\text{H}}(\ell_{\boldsymbol{\theta}_n}, \ell_0) \pi(\boldsymbol{\theta}_n | \mathbf{y}_n, \mathbf{X}_n) d\boldsymbol{\theta}_n \\
&\leq \varepsilon + 2e^{-n\varepsilon^2/2} \leq 2\varepsilon, \quad \text{with probability tending to 1 as } n \rightarrow \infty
\end{aligned}$$

where the second last inequality is a consequence of part 1. in theorem 7.17. The remaining part of the proof follows by (85) and (41).

Theorem 7.18 *Suppose $k_n \sim n^a$, $0 < a < 1$, $\epsilon_n^2 \sim n^{-\delta}$, $0 < \delta < 1 - a$. Additionally, the prior parameters in (10) satisfies assumption (A1) and (A4). Then,*

1.

$$P_0^n \left(\pi(\mathcal{U}_{\varepsilon\epsilon_n}^c | \mathbf{y}_n, \mathbf{X}_n) \leq 2e^{-n\epsilon_n^2\varepsilon^2/2} \right) \rightarrow 1, n \rightarrow \infty$$

2.

$$P_0^n (|R(\hat{C}) - R(C^{\text{Bayes}})| \leq 4\sqrt{2\varepsilon\epsilon_n}) \rightarrow 1, n \rightarrow \infty$$

Proof. By assumptions (A1) and (A4), the prior parameters satisfy

$$\|\boldsymbol{\mu}_n\|_2^2 = o(n\epsilon_n^2), \quad \|\boldsymbol{\zeta}_n\|_\infty = O(n), \quad \|\boldsymbol{\zeta}_n^*\|_\infty = O(1), \quad \boldsymbol{\zeta}_n^* = 1/\boldsymbol{\zeta}_n.$$

Also by assumption (A3),

$$\|\eta_0 - \eta_{\mathbf{t}_n}\|_\infty = o(\epsilon_n^2), \quad \|\mathbf{t}_n\|_2^2 = o(n\epsilon_n^2)$$

Note $K(n) \sim k_n \sim n^a$, $0 < a < 1$ and $\epsilon_n \sim n^{-\delta}$, $0 < \delta < 1 - a$, thus $K(n) \log n = o(n\epsilon_n^2)$.

Thus, the conditions of proposition 7.12 hold.

$$P_0^n \left(\int \frac{L(\boldsymbol{\theta}_n)}{L_0} p(\boldsymbol{\theta}_n) d\boldsymbol{\theta}_n \leq e^{-n\epsilon_n^2\nu} \right) \leq P_0^n \left(\left| \log \int \frac{L(\boldsymbol{\theta}_n)}{L_0} p(\boldsymbol{\theta}_n) d\boldsymbol{\theta}_n \right| > n\epsilon_n^2\nu \right) \rightarrow 0, n \rightarrow \infty \quad (90)$$

where the above convergence follows from (76) in step 2 (c) in the proof of proposition 7.16. Also, since $K(n) \log n = o(n^b \epsilon_n^2)$, $a + \delta < b < 1$. Thus conditions of proposition 7.15 hold.

$$P_0^n \left(\int_{\mathcal{U}_{\epsilon_n}^c} \frac{L(\boldsymbol{\theta}_n)}{L_0} p(\boldsymbol{\theta}_n) d\boldsymbol{\theta}_n \geq 2e^{-n\epsilon_n^2 \epsilon^2} \right) \rightarrow 0, n \rightarrow \infty \quad (91)$$

where the last equality follows from (62) in the proof of proposition 7.15.

Using (90) and (91) with (87), we get

$$P_0^n \left(\pi(\mathcal{U}_{\epsilon_n}^c | \mathbf{y}_n, \mathbf{X}_n) \geq 2e^{-n\epsilon_n^2(\epsilon^2 - \nu)} \right) \rightarrow 0, n \rightarrow \infty$$

Take $\nu = \epsilon^2/2$ to complete the proof.

Let $\hat{\ell}_n(y, \mathbf{x}) = \int \ell_{\boldsymbol{\theta}_n}(y, \mathbf{x}) \pi(\boldsymbol{\theta}_n | \mathbf{y}_n, \mathbf{X}_n) d\boldsymbol{\theta}_n$. Mimicking the steps in the proof of corollary 4.3, we get

$$\begin{aligned} d_H(\hat{\ell}_n, \ell_0) &= d_H \left(\int \ell_{\boldsymbol{\theta}_n} \pi(\boldsymbol{\theta}_n | \mathbf{y}_n, \mathbf{X}_n) d\boldsymbol{\theta}_n, \ell_0 \right) \\ &\leq \int d_H(\ell_{\boldsymbol{\theta}_n}, \ell_0) \pi(\boldsymbol{\theta}_n | \mathbf{y}_n, \mathbf{X}_n) d\boldsymbol{\theta}_n \quad \text{Jensen's inequality} \\ &= \int_{\mathcal{U}_{\epsilon_n}} d_H(\ell_{\boldsymbol{\theta}_n}, \ell_0) \pi(\boldsymbol{\theta}_n | \mathbf{y}_n, \mathbf{X}_n) d\boldsymbol{\theta}_n + \int_{\mathcal{U}_{\epsilon_n}^c} d_H(\ell_{\boldsymbol{\theta}_n}, \ell_0) \pi(\boldsymbol{\theta}_n | \mathbf{y}_n, \mathbf{X}_n) d\boldsymbol{\theta}_n \\ &\leq \epsilon \epsilon_n + 2e^{-2n\epsilon_n^2 \epsilon^2} \leq 2\epsilon \epsilon_n, \quad \text{with probability tending to 1 as } n \rightarrow \infty \end{aligned}$$

where the second last inequality is a consequence of part 1. in theorem 7.18 and the last inequality last equality follows since $\epsilon_n \sim n^{-\delta}$. Dividing by ϵ_n on both sides we get

$$\epsilon_n^{-1} d_H(\hat{\ell}_n, \ell_0) \leq 2\epsilon, \quad \text{with probability tending to 1 as } n \rightarrow \infty$$

The remaining part of the proof follows by (85) and (41).

(D) Tables

Characteristics	MCI-S	MCI-C	Test statistic	P-value
Age(years)	74.34 ± 7.78	74.84 ± 6.83	-0.528	> 0.5 ^a
Education(years)	15.57 ± 2.94	15.73 ± 2.91	-0.527	> 0.5 ^b
APOE4 %	34.65%	62.19%	17.900	< 0.001 ^a
CDRSB	1.23 ± 0.61	1.72 ± 0.92	-5.237	< 0.001 ^a
MMSE	27.61 ± 1.74	26.82 ± 1.71	3.645	< 0.001 ^a
ADAS11	8.89 ± 3.79	12.29 ± 4.16	-6.823	< 0.001 ^a
ADAS13	14.48 ± 5.50	20.01 ± 5.79	-7.795	< 0.001 ^a
ASASQ4	4.76 ± 2.19	6.77 ± 2.21	-7.339	< 0.001 ^a
RAVLT1	36.21 ± 10.10	29.10 ± 7.98	6.021	< 0.001 ^a
RAVLT2	4.19 ± 2.47	2.91 ± 2.26	4.231	< 0.001 ^a
RAVLT3	4.31 ± 2.59	4.47 ± 2.15	-1.501	0.135 ^a
RAVLT4	51.55 ± 31.04	72.85 ± 30.45	-5.464	< 0.001 ^a
LEDLTOTAL	4.96 ± 2.36	3.41 ± 2.66	4.931	< 0.001 ^a
DIGTSCOR	40.75 ± 11.09	36.72 ± 10.96	2.883	< 0.005 ^a
TRABSCOR	109.43 ± 62.94	132.09 ± 71.36	-2.704	0.007 ^a
FAQ	1.50 ± 2.99	4.96 ± 4.79	-7.243	< 0.001 ^a
mPACCdigit	-5.376 ± 2.96	-8.06 ± 2.96	7.174	< 0.001 ^a
mPACCtrailsB	-5.47 ± 3.06	-8.22 ± 2.98	7.174	< 0.001 ^a

Table 3: **Clinical Features and Cognitive Assessment Score.** Values are shown as mean ± standard deviation or percentage. Test statistics and P-values for differences between MCI-S and MCI-C are based on (a) t-test or (b) chi- square test. MCI-S = non-progressive MCI; MCI-P = progressive MCI; APOE = apolipoprotein E; MMSE = Mini-Mental State Examination. RAVLT = The Rey Auditory Verbal Learning Test (immediate: sum of 5 trails; learning: trial 5-trial 1; Forgetting: trial 5-delayed; perc.forgetting: Present forgetting) ; DIGT = The Digit- Symbol Coding test; TRAB = Trail Making tests; CDRSB = Clinical Dementia Rating Scaled Response; FAQ = Activities of Daily living Score; ADAS = Alzheimer’s Disease Assessment Scale–Cognitive sub- scale; mPACCdigit = the Digit Symbol Substitution Test from the Preclinical Alzheimer Cognitive Composite;

Characteristics	MCI-S	MCI-C	Test statistic	P-value
HippoR	3684 ± 438	3366 ± 437	5.735	< 0.001
HippoL	3414 ± 418	3105 ± 388	5.994	< 0.001
fWMR	96720 ± 6218	96976 ± 5585	-0.338	0.73
fWML	93671 ± 5836	94238 ± 5160	-0.802	0.42
pIWML	50149 ± 3714	50038 ± 3467	0.242	0.81
tIWMR	56076 ± 3252	55934 ± 2931	0.359	0.72
ACgCR	3167 ± 756	3128 ± 641	0.438	0.66
ACgCL	4104 ± 787	4075 ± 689	0.312	0.76
EntR	2189 ± 365	1983 ± 373	4.412	< 0.001
EntL	2050 ± 399	1844 ± 356	4.240	< 0.001
MCgCR	4176 ± 547	4200 ± 541	-0.341	0.73
MCgCL	3988 ± 493	4002 ± 559	-0.213	0.83
MFCR	1581 ± 342	1505 ± 524	1.805	0.07
MFCL	1566 ± 285	1548 ± 291	0.487	0.62
OpIFGR	2575 ± 608	2425 ± 546	2.021	0.04
OpIFGL	2465 ± 550	2361 ± 579	1.466	0.14
OrIFGR	1252 ± 315	1196 ± 362	1.322	0.18
OrIFGL	1514 ± 335	1398 ± 356	2.658	< 0.001
PCgCR	3679 ± 466	3528 ± 415	2.657	< 0.001
PCgCL	3991 ± 442	3789 ± 424	3.676	< 0.001
PCuR	10129 ± 1193	9862 ± 1313	1.701	0.09
PCuL	10005 ± 1263	9759 ± 1299	1.522	0.13
SPLR	8867 ± 1140	8693 ± 1219	1.180	0.02
SPLL	8880 ± 1192	8662 ± 1313	1.390	0.17

Table 4: **Significant MRI Features.** Values are shown as mean ± standard deviation or percentage. Test statistics and P-values for differences between MCI-C and MCI-S are based on t-test. MCI-S = non-progressive MCI; MCI-C = progressive MCI. HippoR = Right Hippocampus; HippoL = Left Hippocampus; fWMR = frontal lobe WM right; fWML = frontal lobe WM left; pIWMR = parietal lobe WM right; pIWML = parietal lobe WM left; tIWMR = temporal lobe WM right; tIWML = temporal lobe WM left; ACgCR=Right ACgG anterior cingulate gyrus; ACgCL=Left ACgG anterior cingulate gyrus; EntR = Right Ent entorhinal area; EntL = Left Ent entorhinal area; MCgCR = Right MCgG middle cingulate gyrus ;MCgCL = Left MCgG middle cingulate gyrus; MFCR = Right MFC medial frontal cortex; MFCL = Left MFC medial frontal cortex; OpIFGR = Right OpIFG opercular part of the inferior frontal gyrus; OpIFGL = Left OpIFG opercular part of the inferior frontal gyrus; OrIFGR = Right OrIFG orbital part of the inferior frontal gyrus; OrIFGL = Left OrIFG orbital part of the inferior frontal gyrus; PCgCR = Right PCgG posterior cingulate gyrus ; PCgCL = Left PCgG posterior cingulate gyrus; PCuR = Right PCu precuneus; PCuL = Left PCu precuneus; SPLR = Right SPL superior parietal lobule; SPLL = Left SPL superior parietal lobule.